January 2012

contact: qualif@mercator-ocean.fr

QuO Va Dis?
Quarterly Ocean Validation Display #6

Validation bulletin for July-August-September (JAS) 2011

Edition:
Charles Desportes, Marie Drévillon, Charly Régnier
(MERCATOR OCEAN/Production Dep./Products Quality)

Contributions :
Eric Greiner (CLS)
Jean-Michel Lellouche, Olivier Le Galloudec, Bruno Levier, Coralie Perruche, Abdelali El Moussaoui (MERCATOR OCEAN/ Production Dep./R&D)
Fabien Léger (LEGOS)

Credits for validation methodology and tools:
Eric Greiner, Mounir Benkiran, Nathalie Verbrugge, Hélène Etienne (CLS)
Fabrice Hernandez, Laurence Crosnier (MERCATOR OCEAN)
Nicolas Ferry, Gilles Garric, Jean-Michel Lellouche (MERCATOR OCEAN)
Jean-Marc Molines (CNRS), Sébastien Theeten (Ifremer), the DRAKKAR and NEMO groups.
Nicolas Pene (ex-AKKA), Silvana Buarque (Météo-France), the BCG group (Météo-France, CERFACS)

Information on input data:
Christine Boone, Stéphanie Guinehut, Gaël Nicolas (CLS/ARMOR team)

Abstract

*This bulletin gives an estimate of the accuracy of MERCATOR OCEAN's analyses and forecast for the season of **July-August-September 2011**. It also provides a summary of useful information on the context of the production for this period. Diagnostics will be displayed for the global 1/12° (PSY4), global ¼° (PSY3) and the Atlantic and Mediterranean zoom at 1/12° (PSY2) monitoring and forecasting systems currently producing daily 3D temperature salinity and current products. Two new systems are operational since July 2011: **IBI** on the North East Atlantic at 1/36° horizontal resolution, and **BIOMER** a global biogeochemical model at 1° horizontal resolution forced with PSY3V3R1.The BIOMER system is introduced in this issue.*

Table of contents

I Executive summary

The Mercator Ocean global monitoring and forecasting system (MyOcean V1 global MFC) is evaluated for the **period April-May-June 2011**. The system's description of the **ocean water masses is very accurate on global average** and almost everywhere between the bottom and 200m. Between 0 and 500m departures from *in situ* observations **rarely exceed 1 °C and 0.2 psu** (mostly in high variability regions like the Gulf Stream or the Eastern Tropical Pacific). During this northern hemisphere summer season the systems display stratification weaknesses in the North Atlantic and North Pacific (resulting in cold biases in the surface layer especially in the global ¼° PSY3V3R1).

A **cold SST** (and 3DT) bias of 0.1 °C on average is observed all year long in the **high resolution global at 1/12°** (PSY4V1R3) which does not yet benefit from the bias correction scheme that is implemented in PSY3V3R1 and PSY2V4R2.

The temperature and salinity forecast have **significant skill** in many regions of the ocean in the 0-500m layer, but the signal is noisy.

The monitoring systems are generally very close to altimetric observations (global average of 6cm residual RMS error). Future updates of the Mean Dynamic Topography will correct the local biases that are currently observed for instance in the Banda Sea, and hopefully will prevent the **degradation of the subsurface currents at the Equator**. The latter are unrealistic in both global systems, especially in the warm pools in the western equatorial Pacific and Atlantic.

The **surface currents** are underestimated in the mid latitudes and overestimated at the equator with respect to *in situ* measurements of drifting buoys (drifter velocities are corrected of windage and slippage with a method developed by Mercator Océan). The underestimation ranges from 20% in strong currents up to 60% in weak currents. On the contrary the orientation of the current vectors is well represented**. The 1/12° global currents are slightly closer to drifters' observations than ¼° global currents**, especially in equatorial countercurrents.

The high resolution North East Atlantic at 1/36° (IBI36V1) with no data assimilation is accurate on average. **Tidal and residual sea surface elevations are well represented**. Zones of intense tidal mixing are less accurate. The mixed layer is too shallow in the Bay of Biscay (the thermocline is too diffusive). The upwelling along the Iberian coasts is underestimated.

The sea ice concentrations are overestimated in the Arctic all year round in the global 1/12° PSY4V1R3 (unrealistic rheology) PSY3V3R1 **global ¼° sea ice concentrations are realistic** but there is still too much accumulation of ice in the Arctic, especially in the Beaufort Sea. The sea ice concentration is underestimated in the Barents Sea. Antarctic sea ice concentration is underestimated in austral winter (including JAS 2011) due to atmospheric forcing problems in PSY3V3R1. The global 1/12° PSY4V1R3 sea ice concentration is overestimated all year round in the Antarctic because of rheology problems.

The **large scale structures corresponding to specific biogeographic regions** (double-gyres, ACC, etc…) **are well reproduced** by the global biogeochemical model at 1° BIOMER. However there are **serious discrepancies in the Tropical band** due to overestimated vertical velocities. The latter are the source of anomalous levels of nitrates in the equatorial surface layer. O2, however, is close to climatological estimations. The seasonal cycle is realistic in most parts of the ocean. However **the timing of the blooms is not yet in phase with observations**.

II Status and evolutions of the systems

II.1. Short description and current status of the systems

PSY3V3R1 and PSY2V4R1 systems have been operated at MERCATOR OCEAN since 2010 December, 15th. These systems provide the version 1 products of the MyOcean global monitoring and forecasting centre. As reminded in Table 1 the atmospheric forcing is updated daily with the latest ECMWF analysis and forecast, and a new oceanic forecast is run every day for both PSY3V3R1 and PSY2V4R1. This daily update of the forcing (referred to as PSY3QV3R1 and PSY2QV4R1) is not broadcasted by MyOcean (it will be for V2).
An updated version (or release) of PSY2 called PSY2V4R2 is operated since the end of June 2011 and replaces PSY2V4R1. The PSY2QV4R2 system also replaces the PSY2QV4R1 system. The improvements of this version have been described in *QuOVaDis?* #5 and are reminded in Table 1. The PSY2V4R1 and PSY2V4R2 systems could not be operated in parallel. In consequence no PSY2V4R1 products are available for the JAS 2011 quarter.

The latest scientific evolutions of the systems (in red in Table 1) were described in *QuOVaDis?* #2 and #5 and will not be detailed here. The PSY3V3R1 system is started in October 2006 from a 3D climatology of temperature and salinity (World Ocean Atlas Levitus 2005) while the PSY2V4R2 was started in October 2009. After a short 3-month spin up of the model and data assimilation, the performance of PSY3V3R1 has been evaluated on the 2007-2009 period (MyOcean internal calibration report, which results are synthesised in *QuOVaDis?* #2). The performance of both systems over the JAS 2011 period is now described in this issue.

System name	domain	resolution	Model version	Assimilation software version	Assimilated observations	Inter dependencies	Status of production
PSY3V3R1	global	¼° on the horizontal, 50 levels on the vertical	ORCA025 LIM2 EVP NEMO 3.1 3-hourly atmospheric forcing from ECMWF, bulk CORE	SAM2 (SEEK Kernel) + IAU and bias correction	RTG-SST, SLA from Jason 1, Jason 2 and Envisat, in situ profile from CORIOLIS		Weekly 14-days forecast Daily update of atmospheric forcings for daily 7-day forecast PSY3QV3
PSY4V1R3	global	1/12° on the	ORCA12 LIM2 NEMO	SAM2 (SEEK Kernel)	RTG-SST, SLA from Jason		Weekly 7-day forecast

		horizontal, 50 levels on the vertical	1.09 Daily atmospheric forcing from ECMWF, bulk CLIO	+ IAU	1, Jason 2 and Envisat, in situ profile from CORIOLIS		
PSY2V4R2	Tropical, North Atlantic and Mediterranean Sea region	1/12° on the horizontal, 50 levels on the vertical	NATL12 LIM2 EVP NEMO 3.1 3-hourly atmospheric forcing from ECMWF, bulk CORE	SAM2 (SEEK Kernel) + IAU and bias correction + new MDT CNES/CLS09 bias corrected + more observation error near coasts	AVHRR-AMSR Reynold ¼° SST, SLA from Jason 1, Jason 2 and Envisat, in situ profile from CORIOLIS	Open boundary conditions from PSY3V3R1	Weekly Daily update of atmospheric forcings PSY2QV4
IBI36V1	North East Atlantic and West Mediterranean Sea (Iberian, Biscay and Ireland) region	1/36° on the horizontal, 50 levels on the vertical	NEATL36 NEMO 2.3 3-hourly atmospheric forcing from ECMWF, bulk CORE, tides	none	none	Two weeks spin up initialized with PSY2V4R1 and open boundary conditions from PSY2V4R1	Weekly spin up two weeks back in time. Daily update of atmospheric forcings for daily 5-day forecast IBI36QV1 To be broadcasted starting from June 2011.
BIOMER	global	1° on the horizontal, 50 levels on the vertical	PISCES, NEMO 2.3, offline	none	none	Two weeks hindcast with IR global forcing degraded at 1°	1-week average two weeks back in time.

Table 1 : Synthetic description of the Mercator Ocean operational systems. In red, the major upgrades with respect to previous versions (when existing).

The PSY4V1R3 is delivering operational products since the beginning of 2010. It does not yet benefit from the latest scientific improvements of PSY3V3R1 and PSY2V4R2. The update of PSY4 is planned for MyOcean II, starting in April 2012. This system delivers 7-day forecast (and not 14-day like PSY3V3R1 and PSY2V4R2).

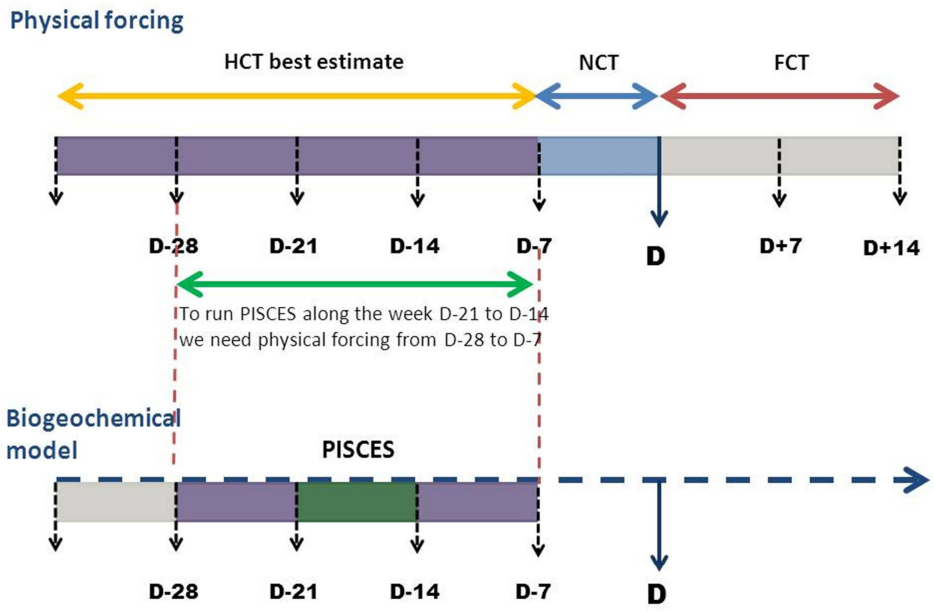

Figure 1: schematic of the operational forecast scenario for BIOMER..

The IBI36V1 system (also shortly described in Table 1) is initialized weekly and forced at the boundaries with PSY2V4R2 outputs. The operational scenario is to produce weekly a 14-day spin-up and then a 5-day forecast updated each day. This system has been "calibrated" on the year 2008 in order to begin MyOcean V1 production in June 2011. The nominal MyOcean production unit for IBI is Puertos Del Estado (Spain) while Mercator Océan produces the back up products. The Mercator Océan IBI system is officially operational since June 2011 and its results will now be routinely analysed in *Quo Va Dis?*

This *Quo Va Dis?* issue also introduces the BIOMER system (El Moussaoui et al., 2011) which is a global hindcast biogeochemical model forced by physical ocean fields. The biogeochemical model used is PISCES. It is a model of intermediate complexity designed for global ocean applications (Aumont and Bopp, 2006) and is part of NEMO modeling platform. It simulates the biogeochemical cycle of oxygen, carbon and the main nutrients controlling marine biological productivity: nitrate, ammonium, phosphate, silicic acid and iron. The model distinguishes four plankton functional types based on size: two phytoplankton groups (small = nanophytoplankton and large = diatoms) and two zooplankton groups (small = microzooplankton and large = mesozooplankton). For phytoplankton, the prognostic variables are total biomass, iron, chlorophyll and silicon (diatoms) contents. For zooplankton, total biomass is the only prognostic variable. The bacterial pool is not modeled explicitly. PISCES traces three non-living pools for organic carbon: small particulate organic carbon, big particulate organic carbon and semi-labile dissolved organic carbon, as well as biogenic silica and calcite. The model simulates dissolved inorganic carbon and total alkalinity.
Biogeochemical simulations were initialized with corresponding climatologies for nutrients (WOA 2001, Conkright et al. 2002), carbon cycle (GLODAP, Key et al. 2004) and, in the absence of corresponding data products, with model fields for dissolved iron and dissolved organic carbon.

The high demand in computing time of online global biogeochemical simulations at increased spatial resolution prompted the choice of off-line coupling between ocean physics and biogeochemistry. With focus on the long term goal of implementing biogeochemistry to the Mercator real-time physical system at 1/12° (analysis), we opted for the spatial degradation of the physical fields with the use of the tool DEGINT (Aumont et al. 1998). For the time being, BIOMER physical forcings come from PSY3V3R1. The degraded physical model is built from the original (or "parent") model by averaging fields of advection, turbulent diffusion, and tracers onto "squares" of four boxes along longitude by four boxes along latitude. The vertical resolution is not degraded. The horizontal resolution (number of grid cells) of the degraded model is only one sixteenth of that of the parent model. The degradation procedure is designed to conserve both water fluxes at the boundaries of each degraded grid cell.

The optimal forcing frequency for the biogeochemical model was tested by comparing 1, 3 and 7-day forcing frequencies. Modelled chlorophyll-a fields were not significantly different and a 7-day forcing was adopted as input of PISCES. This time period is in accordance with the time scale of physical processes considered in a simulation at ¼° ("eddy-permitting"). The operational scenario of BIOMER is described in Figure 1. A 3-week hindcast run is performed weekly starting 28 days back in time. The 7-day physical ocean forcing at 1° horizontal resolution is computed from the PSY3V3R1 hindcast.

II.2. Incidents in the course of JAS 2011

The quality of PSY3V3R1, PSY2V4R2 and PSY4V1R3 nowcast and forecast for 2011 September 21st was degraded due to the assimilation of erroneous real time SLA observations. Apart from this incident, no major technical problem was encountered with any of the systems during the JAS 2011 quarter.

III Summary of the availability and quality control of the input data

III.1. Observations available for data assimilation

III.1.1. In situ observations of T/S profiles

system	PSY3V3R1	PSY4V1R3	PSY2V4R2
Min/max number of T profiles per DA cycle	2300/3400	2300/3400	500/800
Min/max number of S profiles per DA cycle	2000/2600	2000/2600	200/500

Table 2: minimum and maximum number of observations (orders of magnitude of vertical profiles) of subsurface temperature and salinity assimilated weekly in JAS 2011 by the Mercator Ocean monitoring and forecasting systems.

As shown in Table 2 the maximum number of in situ observations is lower during this JAS season with respect to the previous AMJ season (see *QuO Va Dis?*#5)). The minimum number of profiles is reached at the beginning of July, the end of July and the end of August.

III.1.2. Sea Surface Temperature

system	PSY3V3R1	PSY4V1R3	PSY2V4R2
Min/max number (in 10^3) of SST observations	176/179	175/178	26/27

Table 3: minimum and maximum number (orders of magnitude in thousands) of SST observations (from RTG-SST) assimilated weekly in JAS 2011 by the Mercator Ocean monitoring and forecasting systems.

RTG-SST is assimilated in PSY3V3R1 and PSY4V1R3, while the AVHRR-AMSR-E Reynolds ¼° product is assimilated in PSY2V4R2 in JAS 2011.

III.1.3. Sea level anomalies along track

system	PSY3V3R1	PSY4V1R3	PSY2V4R1
Min/max number (in 10^3) of Jason 2 SLA observations	85/88	85/90	15/16
Min/max number (in 10^3) of Envisat SLA observations	67/76	72/76	13/15
Min/max number (in 10^3) of Jason 1 SLA observations	60/86	74/87	10/15

Table 4: minimum and maximum number (orders of magnitude in thousands) of SLA observations from Jason 2, Envisat and Jason 1 assimilated weekly in JAS by the Mercator Ocean monitoring and forecasting systems.

As shown in Table 4 the number of SLA observations assimilated by the system was lower than in AMJ through the whole JAS 2011 period for Jason 2. The number of Jason 1 data dropped at the end of August. The global 1/12° PSY4V1R3 assimilates a little bit more observations than PSY3V3R1 (see Jason 1 and Jason 2 figures). The products quality is not significantly altered in response to these drops in the input data number. As already mentioned an incident occurred during the September 21st run. Erroneous observations were delivered by AVISO. The resulting erroneous SLA increments were detected by Mercator Ocean (**Erreur ! Source du renvoi introuvable.**) operators and a feedback was immediately sent to AVISO. Very large innovations along isolated tracks can be seen near the coasts, for instance in Indonesia or in the Bay of Biscay. Part of this signal was taken into account by the analysis, resulting in spurious eddies in the forecast for the week 20110921 to 20110928.

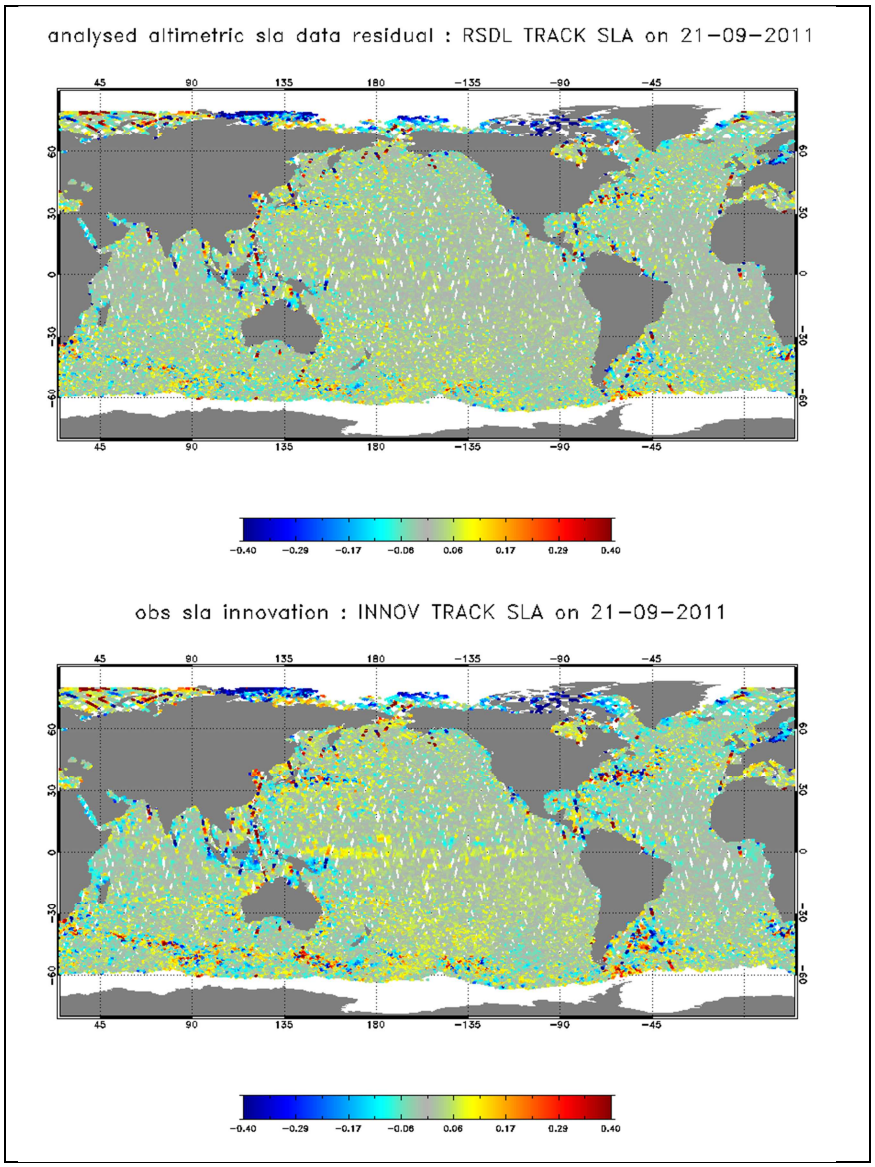

Figure 2: SLA observation minus forecast (lower panel) and observation minus analysis (upper panel) for PSY3V3R1, and the analysis performed on 20110921.

III.2. Observations available for validation

Both observational data and statistical combinations of observations are used for the real time validation of the products. All were available in real time during the JAS 2011 season:

- T/S profiles from CORIOLIS
- OSTIA SST (with one problem on July 21st) from UKMO
- Arctic sea ice concentration and drift from CERSAT
- SURCOUF surface currents from CLS
- ARMOR-3D 3D temperature and salinity fields from CLS
- Drifters velocities from Météo-France reprocessed by CLS
- Tide gauges

A recent study by Grodsky et al (GRL, May 2011) shows that drifters velocities overestimate current velocities in regions and periods of strong winds due to undetected undrogued

drifters. This information will be taken into account for comparisons with Mercator Ocean currents.

IV Information on the large scale climatic conditions

Mercator Ocean participates in the monthly seasonal forecast expertise at Météo-France. This chapter summarizes the state of the ocean and atmosphere during the JAS 2011 season, as discussed in the "Bulletin Climatique Global" of Météo-France.

This JAS 2011 season was characterized by the decay of La Niña event in the equatorial Pacific Ocean (Figure 3). Nevertheless the central Tropical Pacific Ocean is still colder than the climatology with negative temperature anomalies at depth (we show here the 0-300m layer) extending from the dateline to 90°W. A positive anomaly appears close to the South American coast but does not propagate. The spatial structure of the positive and negative anomalies in the Pacific is consistent with trade wind anomalies in the central pacific. In the atmosphere the SOI index stayed positive (while Niño boxes SST indexes are neutral) consistently with the la Niña phase of ENSO (nb: there was an error on the sign of SOI in *QuOVaDis ?*#4).

Anomalous heat content is accumulated in the Indian Ocean near the Somali current which was not the case last quarter. This is either linked with the seasonal cycle and the end of the Northeast monsoon. A negative anomaly persists near 15°S east of Madagascar. The Atlantic Ocean is still warmer than the climatology. The Atlantic Equatorial Ocean is close to the climatology or colder at the Surface in its eastern part. The western Mediterranean Sea and North African Atlantic coast are warmer than average (again in coherence with trade wind anomalies).

As can be seen in Figure 4, the sea ice extent in the Arctic Ocean is generally less than (or equivalent to) the observed minimum especially in May and June. The situation seems to be worst than the record low in 2007. Ice extend is tracking below the year 2007, we will see in the next bulletin if the September 2011 arctic minimum sea ice extend beat the 2007 record.

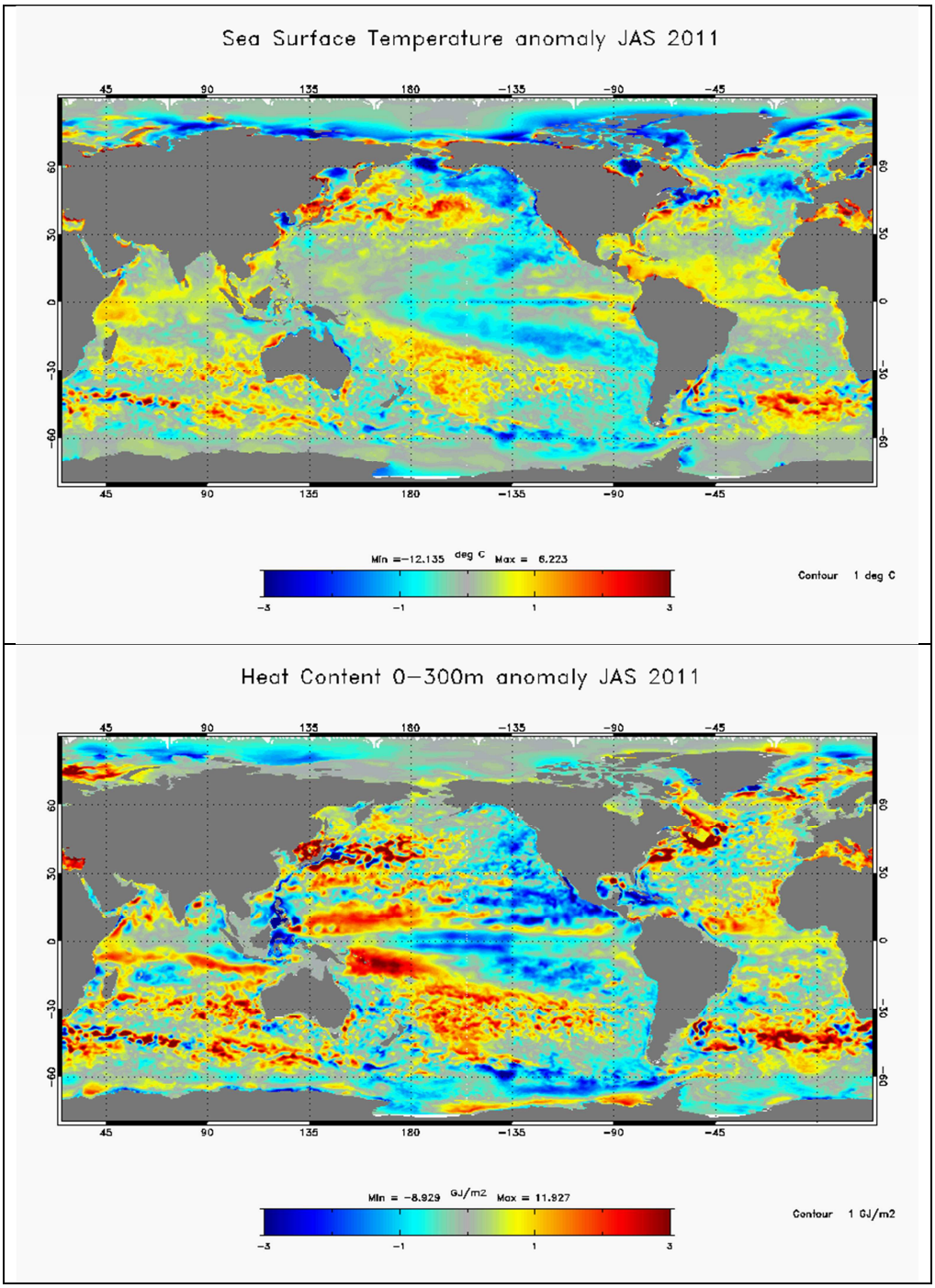

Figure 3: Seasonal JAS 2011 temperature anomalies with respect to WOA05 (World Ocean Atlas from Levitus 2005) climatology. Upper panel: SST anomaly (°C) at the global scale from the 1/4° ocean monitoring and forecasting system PSY3V3R1. Lower panel heat content anomaly ($\rho_0 C_p \Delta T$, with constant ρ_0=1020 kg/m3) from the surface to 300m.

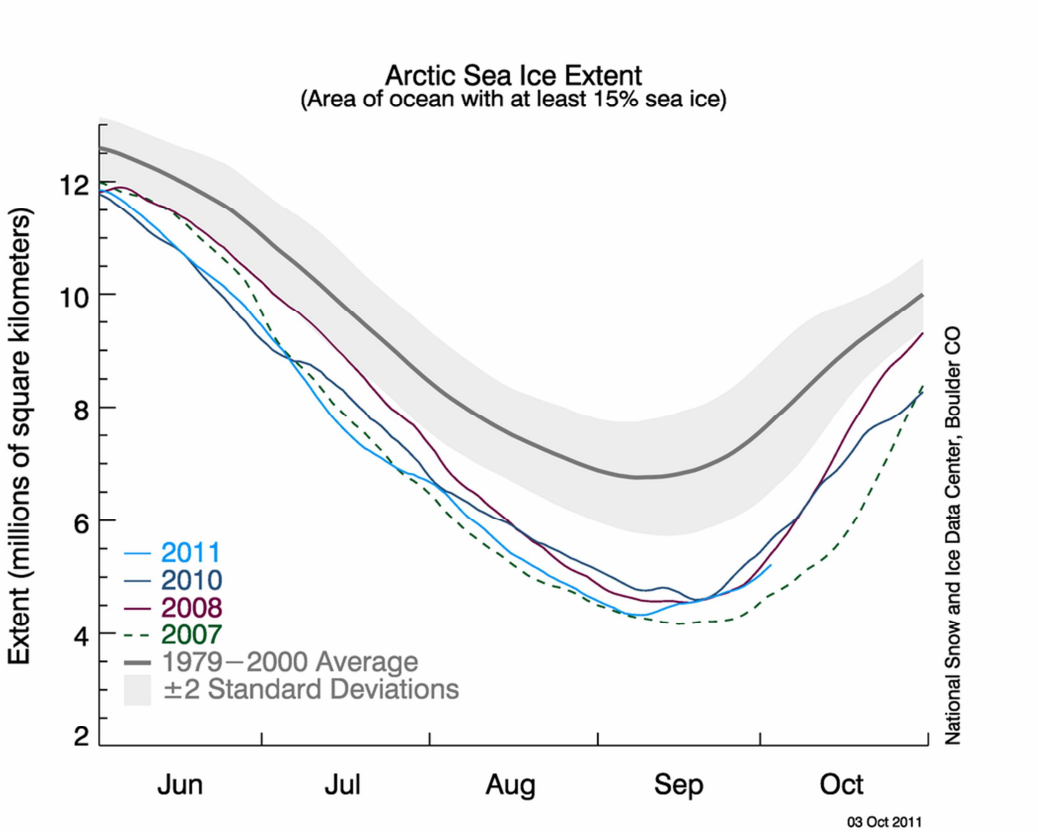

Figure 4: Arctic sea ice extent from the NSIDC:
http://nsidc.org/data/seaice_index/images/daily_images/N_stddev_timeseries.png

V Accuracy of the products

V.1. Data assimilation performance

V.1.1. Sea surface height

V.1.1.1. North Atlantic Ocean and Mediterranean Sea

The Tropical and North Atlantic Ocean SLA assimilation scores for all systems in JAS 2011 are displayed in Figure 5. The different systems (PSY4V1R3, PSY3V3R1, and PSY2V4R2) reach identical levels of performance. One can note that PSY2V4R2 is too low (by 1 or 2 cm) in most regions. The biases are generally small except in the tropical regions like SEC regions and in the Gulf Stream region (especially for 1/12° systems).The tropical biases may be in link with the fresh anomaly that can be diagnosed in the tropics (see section V.1.3). Part of the tropical biases and Gulf Stream biases can also be attributed to local errors in the current mean dynamical topography (MDT). The RMS errors are almost identical in all systems.

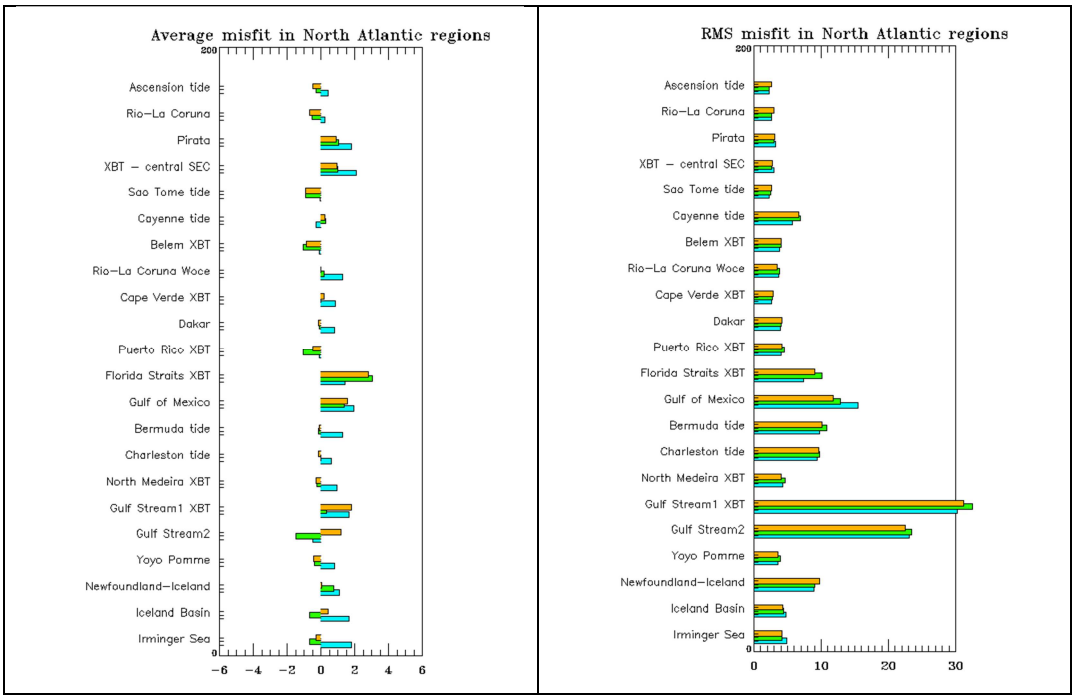

Figure 5: Comparison of SLA data assimilation scores (left: average misfit in cm, right: RMS misfit in cm) in JAS 2011. The colours refer to Mercator Ocean systems in the Tropical and North Atlantic: PSY2V4R2 (light blue), PSY3V3R1 (green), PSY4V1R3 (orange). The scores are averaged for all available satellite along track data (Jason 1, Jason 2 and Envisat). The geographical location of regions is displayed in annex A.

In the Mediterranean Sea a bias of 6 to 8 cm is present in PSY2V4R2 in the Aegean Sea, Adriatic Seas and Alboran Sea, less than 6 cm in other regions, as can be seen in Figure 6. The bias is generally lower in winter than in summer and autumn seasons. The RMS of the innovation (misfit) of PSY2V4R2 is generally less than 8 cm, reaching its maximum in regions where a bias is present.

The system still shows overall good performance as the RMS of the innovation is generally lower than the intrinsic variability of the observations (not shown).

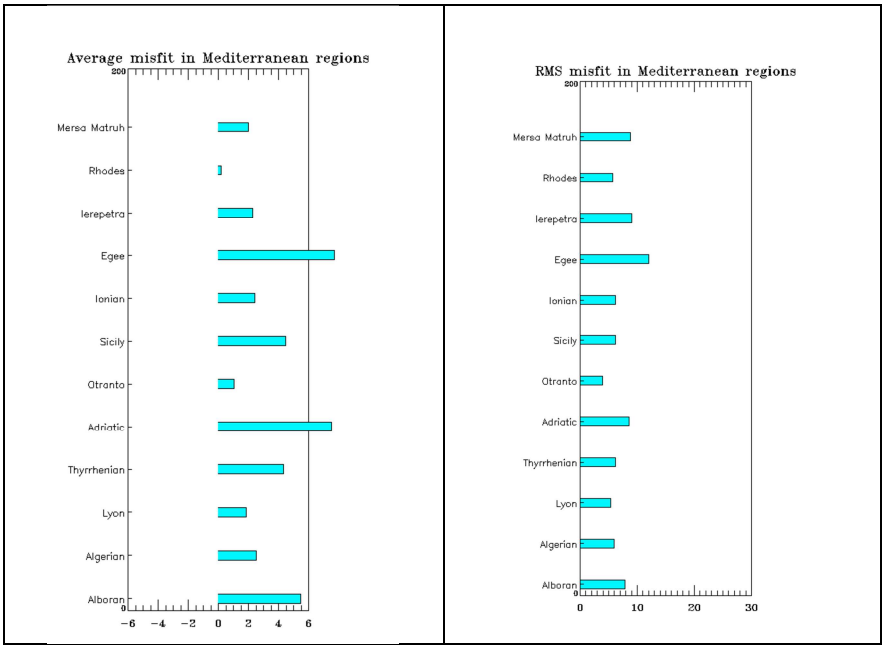

Figure 6: SLA data assimilation scores (left: average misfit in cm, right: RMS misfit in cm) in JAS 2011 for PSY2V4R2 in the Mediterranean Sea. The scores are averaged for all available satellite along track data (Jason 1, Jason 2 and Envisat). See annex B for geographical location of regions.

V.1.1.2. Performance at global scale in PSY3 (1/4°) and PSY4 (1/12°)

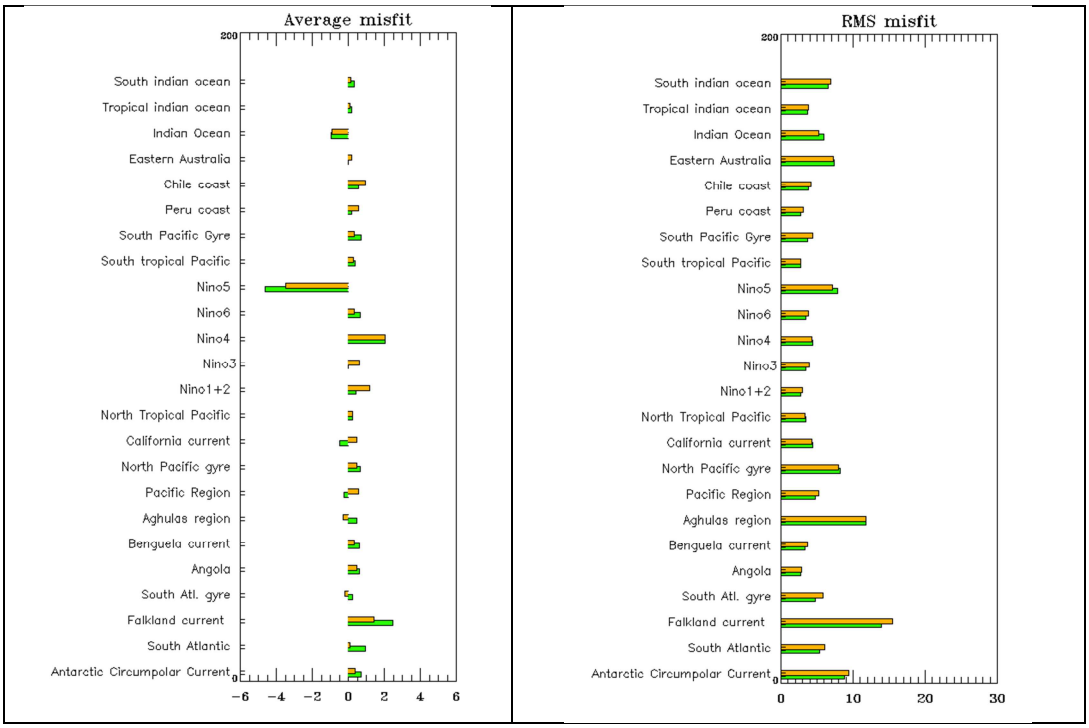

Figure 7: Comparison of SLA data assimilation scores (left: average misfit in cm, right: RMS misfit in cm) in JAS 2011. The colors represent all available global Mercator Ocean systems in all regions of the ocean except the Atlantic and Mediterranean: PSY3V3R1 (green) and PSY4V1R3 (orange). The geographical location of regions is displayed in annex B.

As can be seen on Figure 7 the performance of intermediate resolution global PSY3V3R1 and high resolution global PSY4V1R3 in terms of SLA assimilation is very comparable. The bias is small except in the "Nino 5" box centred on the Banda Sea in Indonesia which corresponds to a MDT problem. These problems disappear when using the MDT updated with GOCE and bias correction (tests made by E. Greiner, B. Tranchant, O. Le Galloudec, this MDT is used in the PSY2V4R2 release in the Atlantic and Mediterranean).

V.1.2. Sea surface temperature

V.1.2.1. North and Tropical Atlantic Ocean and Mediterranean Sea in all systems

In the Atlantic the three systems display different regional behaviours in terms of SST bias as illustrated in Figure 8. A cold bias of around 0.2 to 0.5 °C is diagnosed in most tropical regions of high resolution global PSY4V1R3, while a cold bias of the same magnitude appears in the mid and high latitudes in ¼° PSY3V3R1.

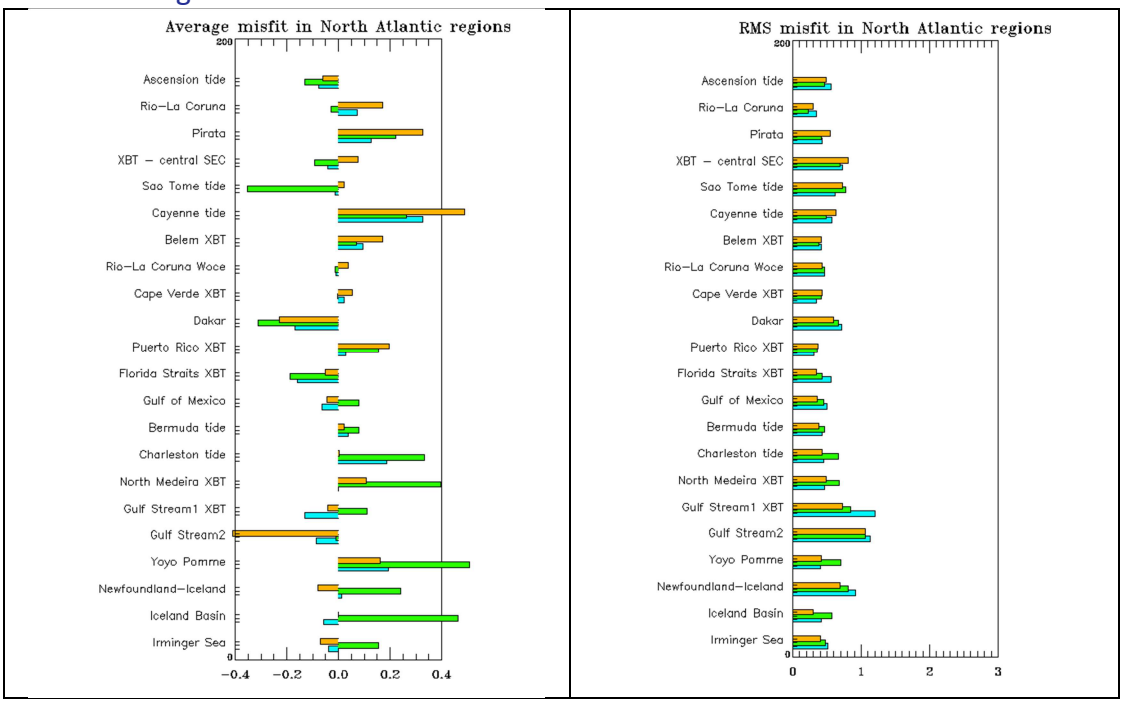

Figure 8: Comparison of RTG-SST data assimilation scores (left: average misfit in °C, right: RMS misfit in °C) in JAS 2011 and between all available Mercator Ocean systems in the Tropical and North Atlantic: PSY4V1R3 (orange), PSY3V3R1 (green). In cyan: Reynolds ¼°AVHRR-AMSR-E data assimilation scores for PSY2V4R2. The geographical location of regions is displayed in annex B.

The eastern Mediterranean Sea is too cold in most regions in PSY2V4R2 (Figure 9). The RMS error is higher where a bias is present.

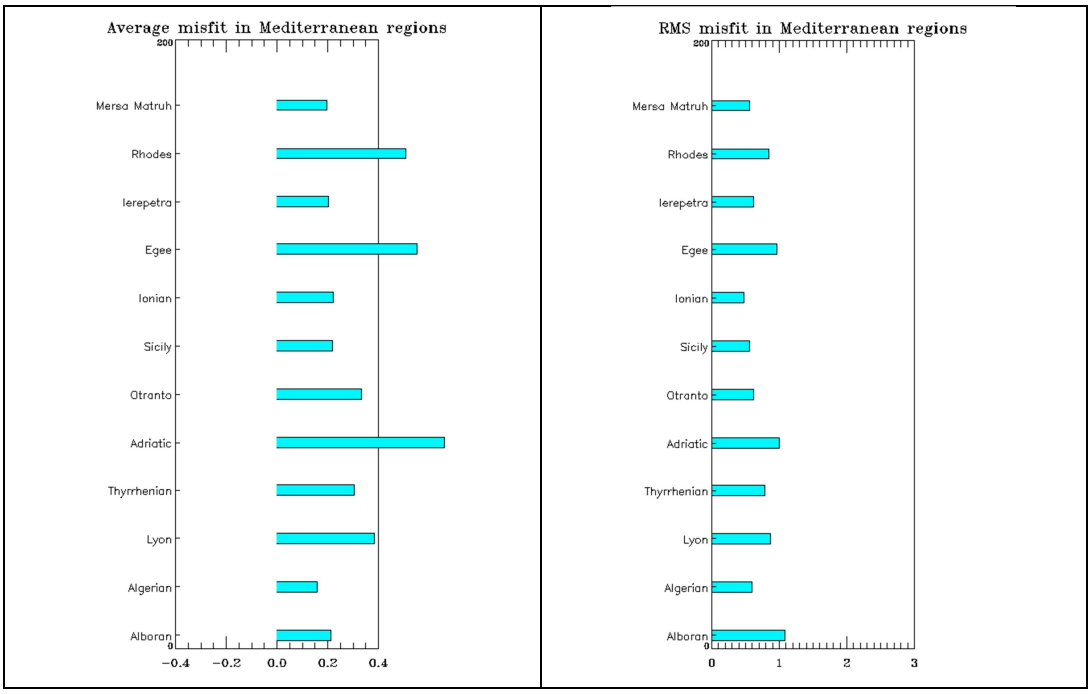

Figure 9: SST data assimilation scores (left: average misfit in °C, right: RMS misfit in °C) in JAS 2011 in the Mediterranean Sea for PSY2V4R2 (comparison with Reynolds ¼° AVHRR-AMSR). The geographical location of regions is displayed in annex B.

V.1.2.2. Performance at global scale in PSY3 (1/4°) and PSY4 (1/12°)

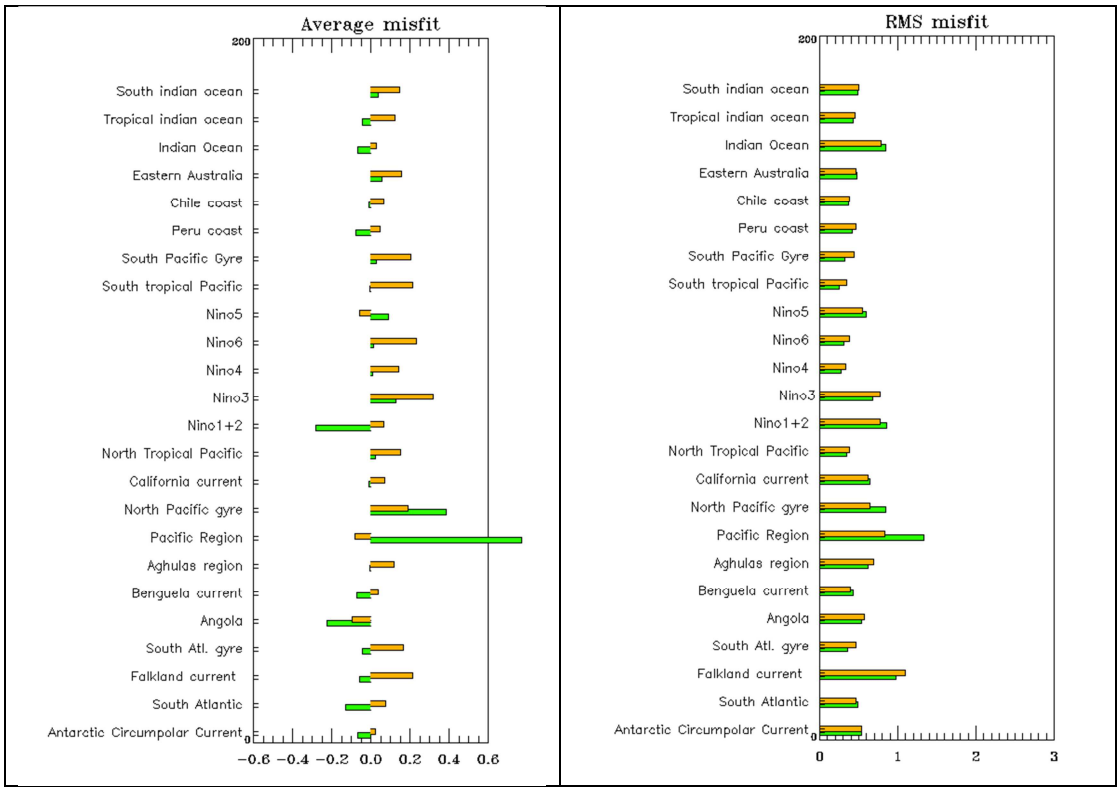

Figure 10: Comparison of RTG-SST data assimilation scores (left: average misfit in °C, right: RMS misfit in °C) in JAS 2011 in all basins except the Atlantic and Mediterranean: PSY3V3R1 (green) and PSY4V1R3 (orange). See annex B for geographical location of regions.

PSY4V1R3 exhibits a cold bias at the global scale this JAS season of about 0.1°C to 0.2°C. In general PSY3V3R1 performs better than PSY4V1R3 (Figure 10). Nevertheless PSY4V1R3 performs slightly better in the Antarctic and North Pacific.The RMS error is of the same order of magnitude for both systems. PSY3V3R1 exhibits a significant cold bias (more than 0.6 °C which is the prescribed SST error) in all the North Pacific regions (cf OSTIA comparisons Figure 30).

V.1.3. Temperature and salinity profiles

V.1.3.1. Methodology

We inter-compared the systems in all regions given in annex B and focused here on the main regions of interest for Mercator Ocean users in JAS 2011. Some more regions were selected when interesting differences take place, or when the regional statistics illustrate the large scale behaviour of the systems. The in situ data assimilation statistics on the selected regions are finally displayed in the following.

V.1.3.1.1. North Pacific gyre (global systems)

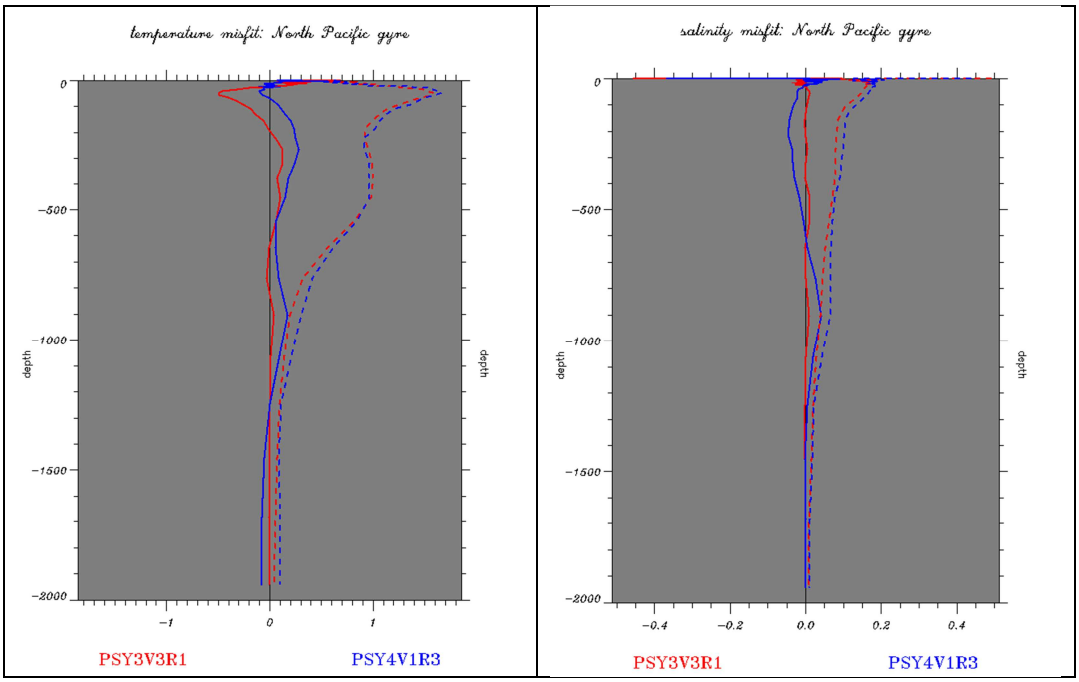

Figure 11: Profiles of JAS 2011 innovations of temperature (°C, left panel) and salinity (psu, right panel), mean (solid line) and RMS (dotted line) for PSY3V3R1 in red and PSY4V1R3 in blue in North Pacific gyre region. The geographical location of regions is displayed in annex B.

This region was of particular interest after the nuclear catastrophe that took place in Japan in March 2011. As can be seen in Figure 11, PSY3V3R1 and PSY4V1R3 RMS departures from observations are of the same order of magnitude. The ¼° global PSY3V3R1 benefits from bias

correction but it is still too cold and fresh at the surface and appears to be too warm in the 100-300 m layer this season (0.25 °C). PSY4V1R3 is generally too cold on the whole water column (0.2 °C). It is too salty at the surface and between 50-800m (0.05 psu) while it is fresher than observations under 800m.

V.1.3.1.2. South Atlantic Gyre (global systems)

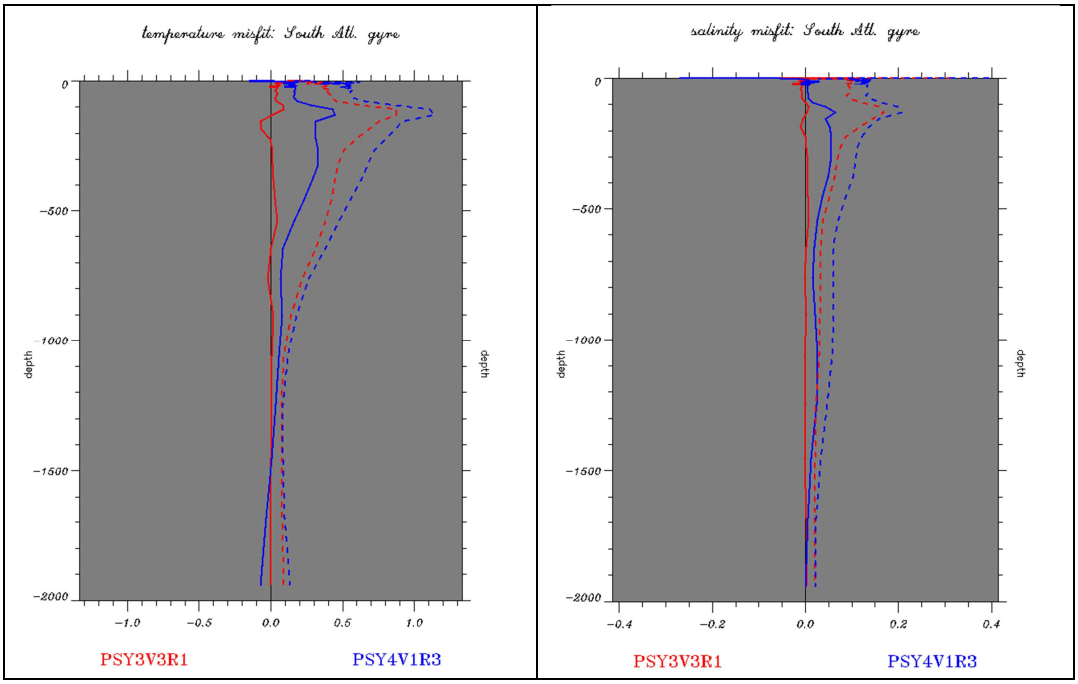

Figure 12: Profiles of JAS 2011 innovations of temperature (°C, left panel) and salinity (psu, right panel), mean (solid line) and RMS (dotted line) for PSY3V3R1 in red and PSY4V1R3 in blue in South Atlantic gyre region. The geographical location of regions is displayed in annex B.

In this region a fresh (0.05 PSU) and cold (max 0.4 °C) bias appears in PSY4V1R3 between the surface and 1500m. PSY3V3R1 has a smaller surface cold bias but becomes too warm near 200m. This region illustrates well that PSY3V3R1 is closer to the subsurface in situ observations than PSY4V1R3 thanks to bias correction.

V.1.3.1.3. Indian Ocean (global systems)

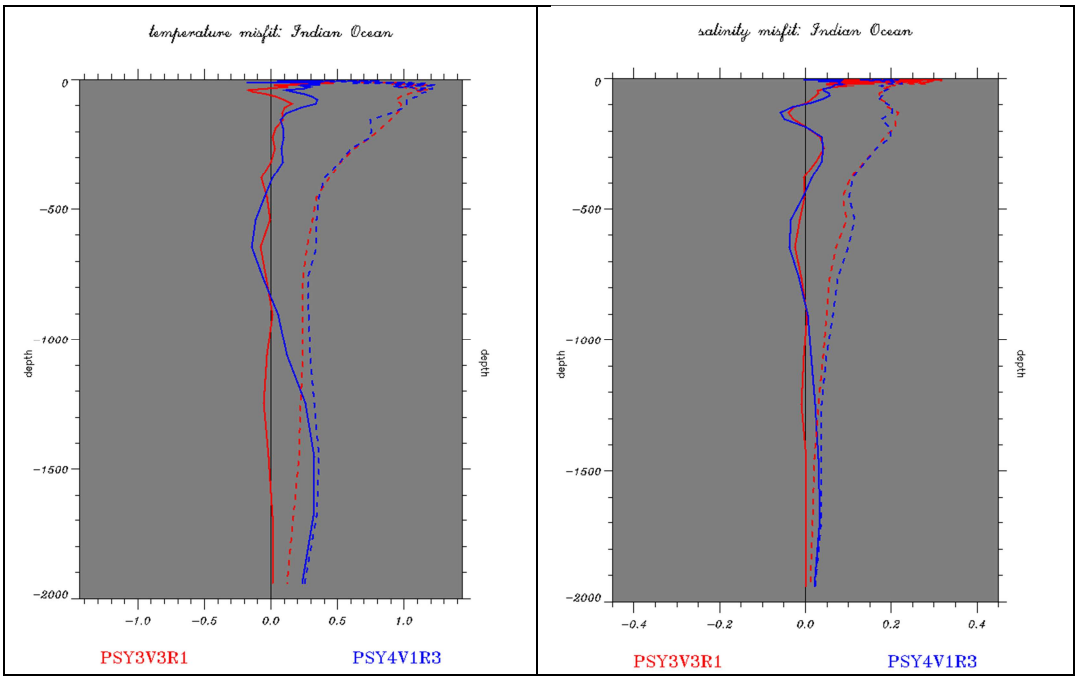

Figure 13: Profiles of JAS 2011 innovations of temperature (°C, left panel) and salinity (psu, right panel), mean (solid line) and RMS (dotted line) for PSY3V3R1 (in red) and PSY4V1R3 (in blue) in the Indian Ocean region. The geographical location of regions is displayed in annex B.

In the Indian Ocean PSY3V3R1 is clearly closer to the observations than PSY4V1R3 from 500m to 2000m in Figure 13. This is again due to the application of a bias correction in PSY3V3R1. PSY3V3R1 is nevertheless fresher (0.1 psu) and colder (0.4°C) than the observations at the surface and becomes too salty and warm at the subsurface near 200m and too cold and fresh near 300m. PSY4V1R3 has a smaller surface bias in temperature but appears too cold and salty at the subsurface between 100 and 500m. Between 500 and 800m PSY4V1R3 is too warm and salty and under 800m it is too cold and fresh. The bias correction does not compensate the underestimation of the subsurface salinity maximum in the southern gyre of the Indian Ocean. In this region the model is less stratified than the climatology between 0 and 200m (not shown).

V.1.3.2. Tropical and North Atlantic Ocean (all systems)

The regional high resolution system (PSY2V4R2) and the global ¼° PSY3V3R1 display the best performance for the North Atlantic regions and for this JAS 2011 season, as illustrated in Figure 14. The high resolution PSY2V4R2 is warmer than the observations from the surface to 1000m. Salinity biases appear mainly in PSY4V1R3 between 1000m and 1500m, at the location of the Mediterranean outflow that is still too shallow (even if far better represented in PSY2V4R2 and PSY3V3R1 than in previous systems including PSY4V1R3 cf Figure 26).

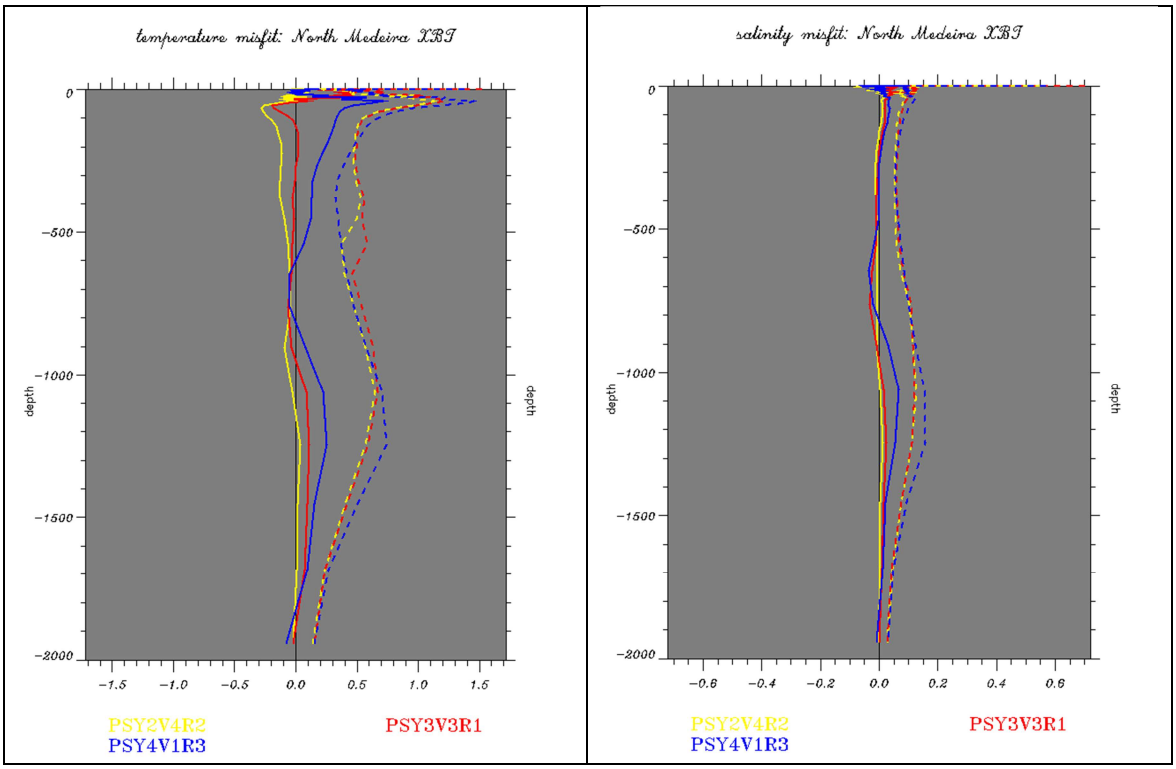

Figure 14: Profiles of JAS 2011 innovations of temperature (°C, left panel) and salinity (psu, right panel), mean (solid line) and RMS (dotted line) for PSY4V1R3 in blue, PSY3V3R1 in red, and PSY2V4R2 in yellow in North Madeira region. The geographical location of regions is displayed in annex B.

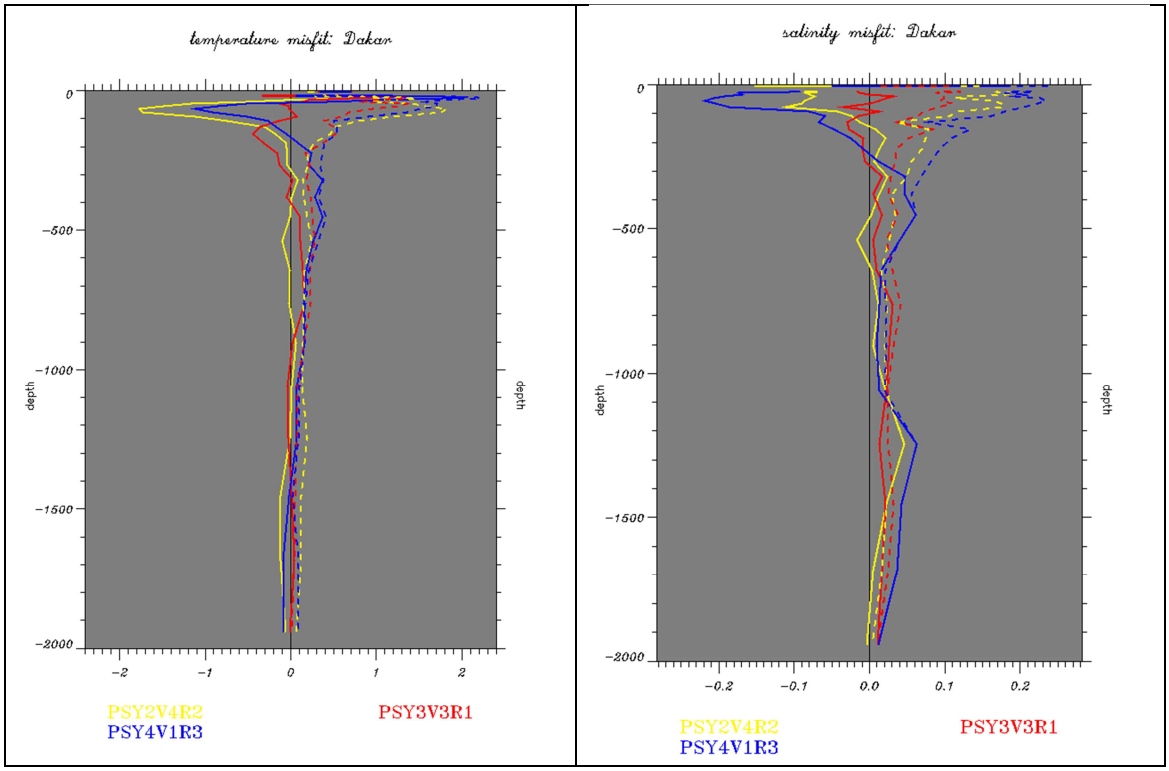

Figure 15: Profiles of JAS 2011 innovations of temperature (°C, left panel) and salinity (psu, right panel), mean (solid line) and RMS (dotted line) for PSY4V1R3 in blue, PSY3V3R1 in red, and PSY2V4R2 in yellow in Dakar region. The geographical location of regions is displayed in annex B.

The upwelling is not well represented by the systems In the Dakar region (Figure 15), and especially by high resolution systems: it is too weak for all of them, resulting in a warm bias near 50m. Between the surface and 500m the water masses too salty and warm in all the systems: the worst performance is that of PSY2V4R2 and the best is that of the global systems and especially PSY3V3R1. The regional 1/12° system has the warmest surface bias in this area.

In the Gulf Stream region (Figure 16) the PSY2V4R2 salinity RMS error is reduced with respect to all other systems. This may result from the use of the updated MDT (with GOCE and bias correction) in PSY2V4R2, which allows a better joint analysis of SLA and in situ observations in this region in particular. In this region, we note that the error is still large compared to other regions because of the high spatial and temporal variability of temperature and salinity due to eddy activity. Again, PSY2V4R2 appears warmer than the other systems.

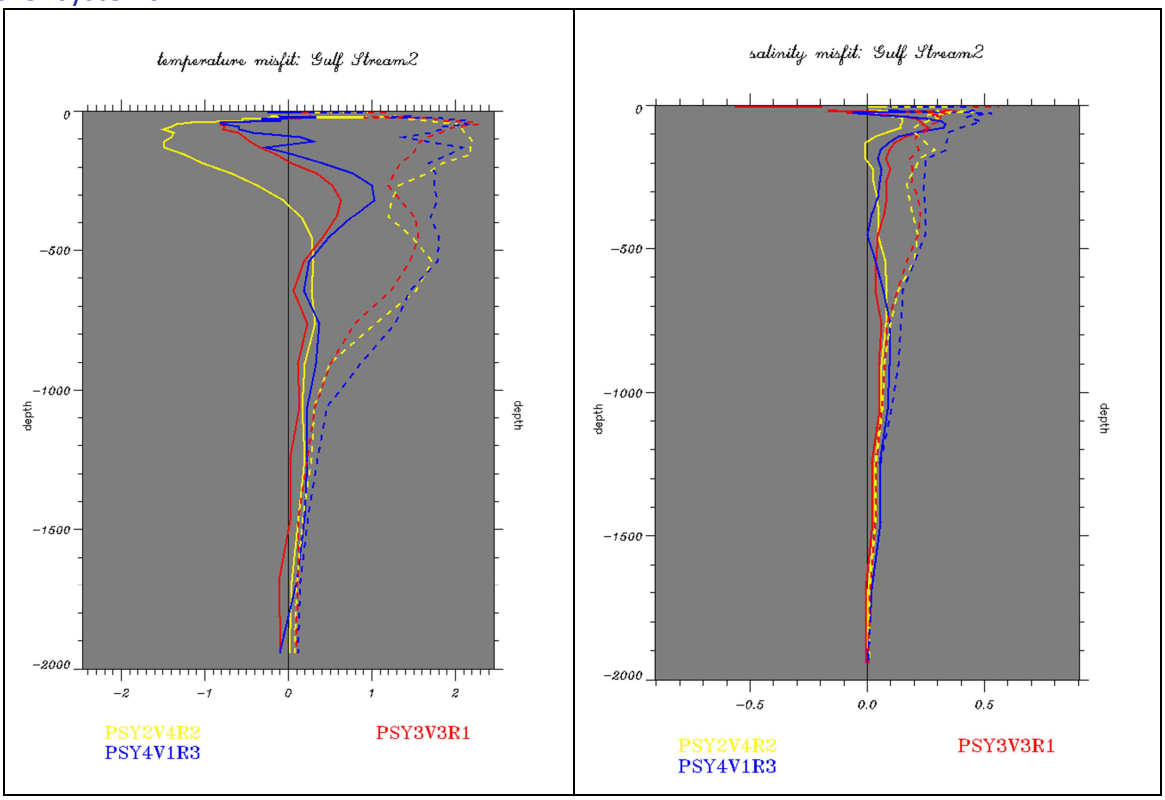

Figure 16: Profiles of JAS 2011 innovations of temperature (°C, left panel) and salinity (psu, right panel), mean (solid line) and RMS (dotted line) for PSY4V1R3 in blue, PSY3V3R1 in red, and PSY2V4R2 in yellow in Gulf Stream 2 region. The geographical location of regions is displayed in annex B.

The Cape Verde region is characteristic of the subtropical gyre in the North Atlantic where all systems stay on average close to the temperature and salinity profiles as can be seen in Figure 17. The highest errors are located near the thermocline and halocline. The global high resolution system with no bias correction PSY4V1R3 is significantly fresher than observed between 100 and 500m and too cold from the surface to 500m.
We note that the high resolution regional PSY2V4R2 is still biased near 200m (too warm again) because the bias correction is only applied under the thermocline. We can deduce that the global high resolution should reach the same performance level when it benefits from a bias correction.

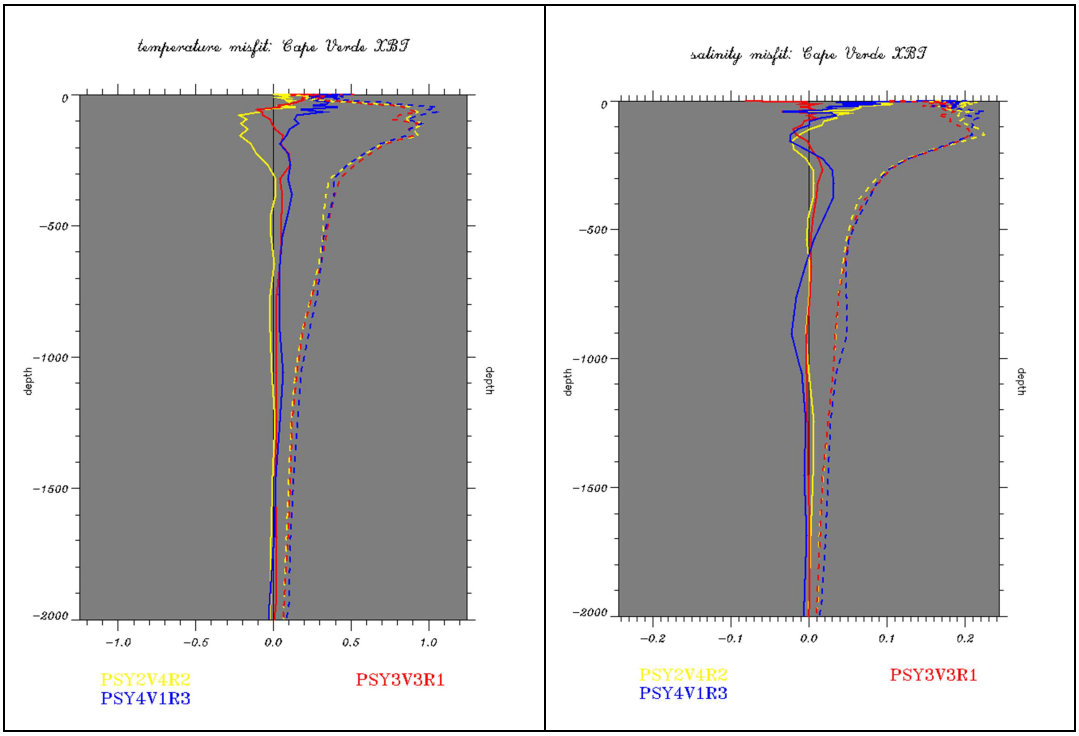

Figure 17: Profiles of JAS 2011 innovations of temperature (°C, left panel) and salinity (psu, right panel), mean (solid line) and RMS (dotted line) for PSY4V1R3 in blue, PSY3V3R1 in red, and PSY2V4R2 in yellow in Cap Verde region. The geographical location of regions is displayed in annex B.

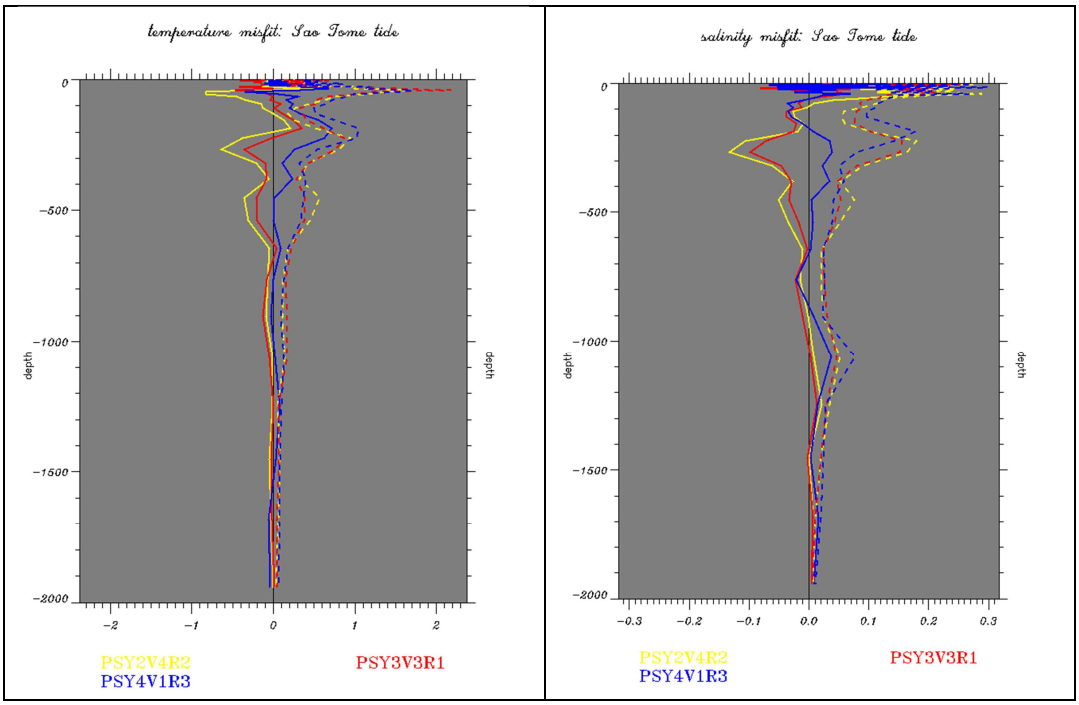

Figure 18: Profiles of JAS 2011 innovations of temperature (°C, left panel) and salinity (psu, right panel), mean (solid line) and RMS (dotted line) for PSY4V1R3 in blue, PSY3V3R1 in red, and PSY2V4R2 in yellow in Sao Tome region. The geographical location of regions is displayed in annex B.

Very few observations are assimilated in JAS 2011 in the small area of the Sao Tome tide region (between 1 and 51 profiles depending on the week). As can be seen in Figure 18 the

systems have difficulties in reproducing the undercurrents in this region as a small number of profiles are available to constrain the water masses. The fresh and cold bias present in all systems at the surface could be due to bad runoffs (Congo river)

V.1.3.1. Mediterranean Sea (high resolution regional systems at 1/12°)

In the Mediterranean Sea the high resolution is mandatory to obtain good level of performance. Only the regional high resolution zooms with bias correction is displayed as PSY2V4R2 has the best level of performance on this zone. We note in Figure 19 that the system is too cold at the surface and too warm in subsurface until 200m. The bias is consistent with a general underestimation of stratification in the systems, and with errors in the positioning of the separation between the Atlantic Inflow and the Levantine intermediate waters.

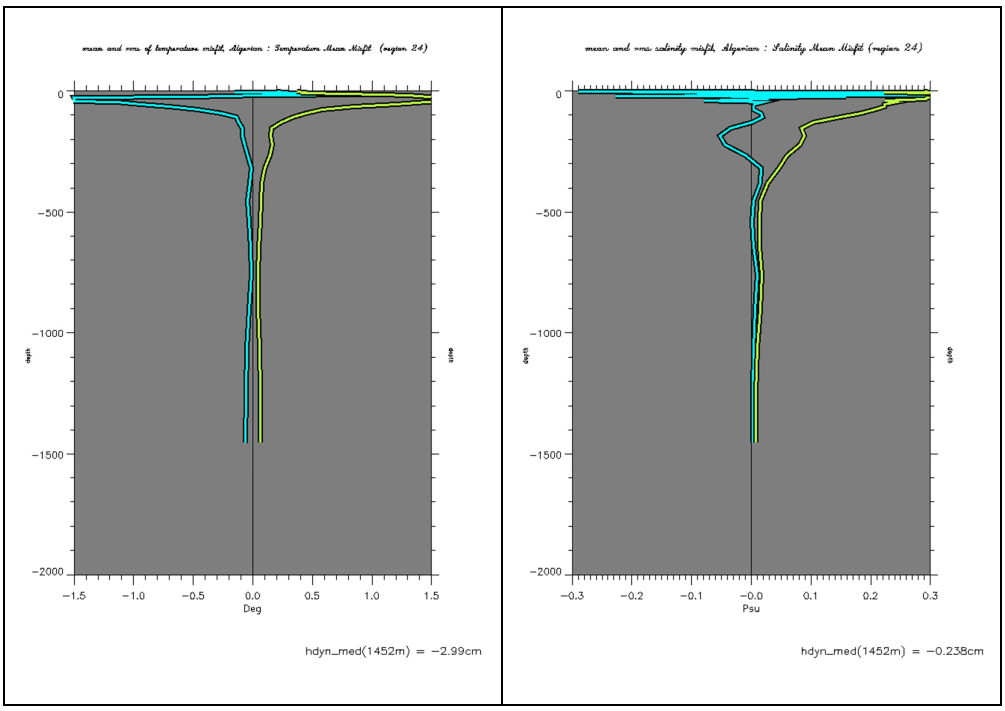

Figure 19: PSY2V4R2 results averaged in the Gulf of Lion region. Profiles of JAS 2011 average (blue) and RMS (yellow) of temperature innovations (°C, left panel) and salinity innovations (psu, rightpanel). The geographical location of regions is displayed in annex B.

Summary: While most of the deep biases disappear in the systems including bias correction, seasonal biases remain. One of the hypotheses is that the SST assimilation is not as efficient as it used to be. The Incremental Analysis Update together with the bulk formulation rejects part of the increment. There is too much mixing in the surface layer inducing a cold (and salty) bias in surface and warm (and fresh) bias in subsurface. The bias is intensifying with the summer stratification and the winter mixing episodes reduce the bias. The bias correction is not as efficient on reducing seasonal biases as it is on reducing long term systematic biases. A correction of air-sea fluxes depending on the SST increment is considered for future versions of the system. The use of Reynolds ¼° L4 SST product (AVHRR AMSR-E) for data assimilation reduce part of the surface bias in the North Atlantic and change the signal in the Mediterranean. The use of Reynolds ¼° AVHRR analyses will be extended to the other Mercator Ocean systems in 2012. The PSY2V4R2 system is different from other systems:

- Update of the MDT with GOCE and bias correction
- Assimilation of Reynolds ¼° AVHRR-AMSRE SST observations instead of ½° RTG-SST
- Increase of observation error for the assimilation of SLA near the coast and on the shelves, and for the assimilation of SST near the coast
- Modification of the correlation/influence radii for the analysis specifically near the European coast.
- Restart from October 2009 from WOA05 climatology

In PSY2V4R2:

- The products are closer to SST observations in the North Atlantic
- The products are closer to in situ observations in the Gulf Stream and in the Mediterranean. In JAS the products are warmer than the observed T profiles.
- The products are less constrained by altimetry near the coast and on the shelves but are generally closer to in situ observations and climatologies in these regions
- The quality is slightly degraded in the Eastern Mediterranean and in the Caribbean region

V.2.Accuracy of the daily average products with respect to observations

V.2.1. T/S profiles observations

V.2.1.1. Global statistics for JAS 2011

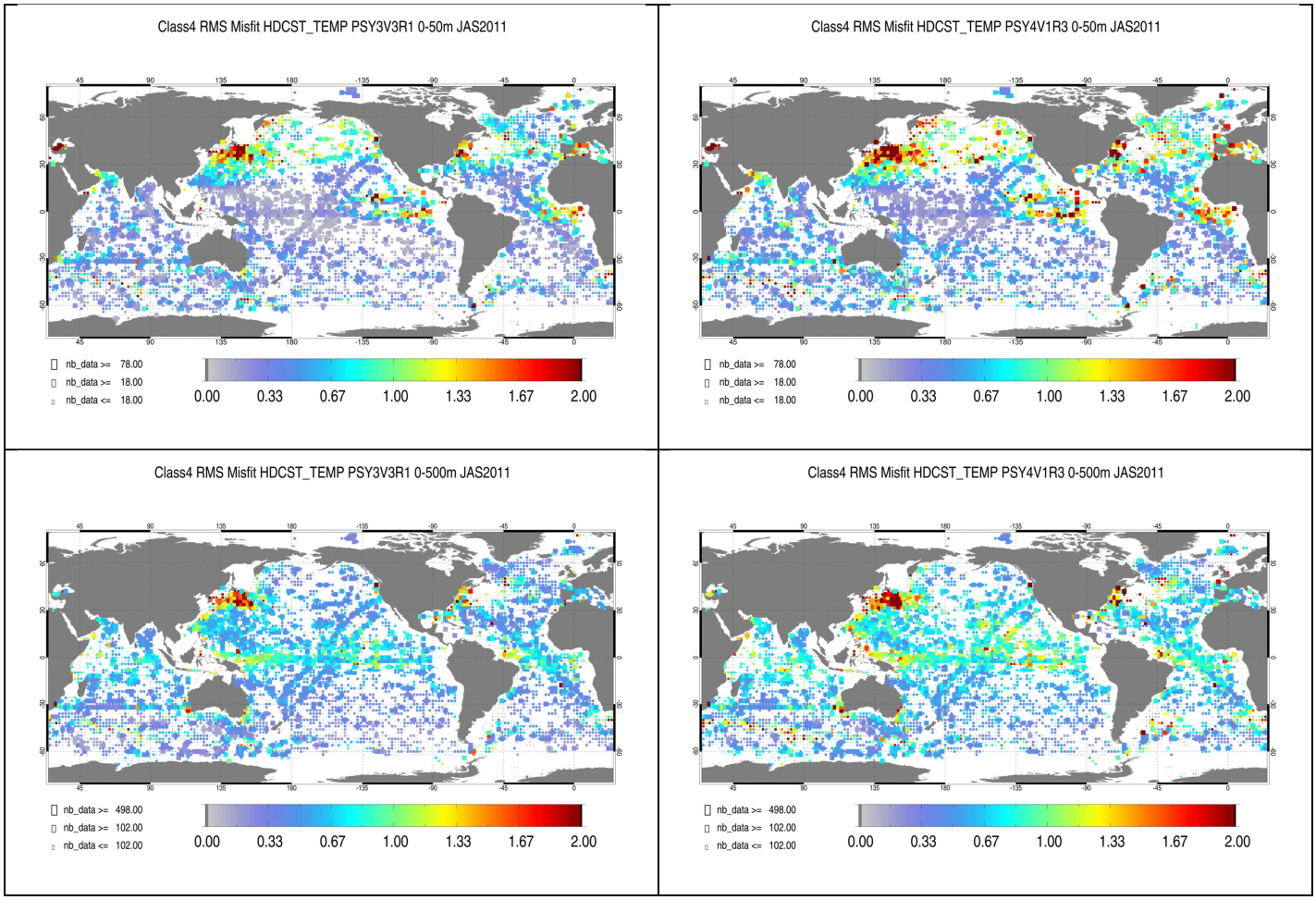

Figure 20: RMS temperature (°C) difference (model-observation) in JAS 2011 between all available T/S observations from the Coriolis database and the daily average nowcast PSY3V3R1 products on the left and nowcast PSY4V1R3 on the right column colocalised with the observations. Averages are performed in the 0-50m layer (upper panel) and in the 0-500m layer (lower panel). The size of the pixel is proportional to the number of observations used to compute the RMS in 2°x2° boxes.

As can be seen in Figure 20, temperature errors in the 0-500m layer stand between 0.5 and 1°C in most regions of the globe in both PSY3V3R1 and PSY4V1R3. Regions of high mesoscale activity (Kuroshio, Gulf Stream, Agulhas current) and regions of upwelling in the tropical Atlantic and Tropical Pacific display higher errors (up to 3°C). PSY4V1R3 has higher variability and no bias correction and thus it is less accurate than PSY3V3R1 on average in these regions. In the tropical Pacific the signature of ENSO variability can be detected in both systems in the Eastern Pacific. In general Tropical regions seem to be better represented in the global ¼ ° system. PSY3V3R1 is more accurate than PSY4V1R3 mainly due to the better MDT and bias correction in PSY3V3R1. Anyway, both systems have a bias in the western part

of the Pacific basin (warm pool). Future systems will use a new MDT (such as used in PSY2V4R2) which reduces the biases in the western tropical Pacific.

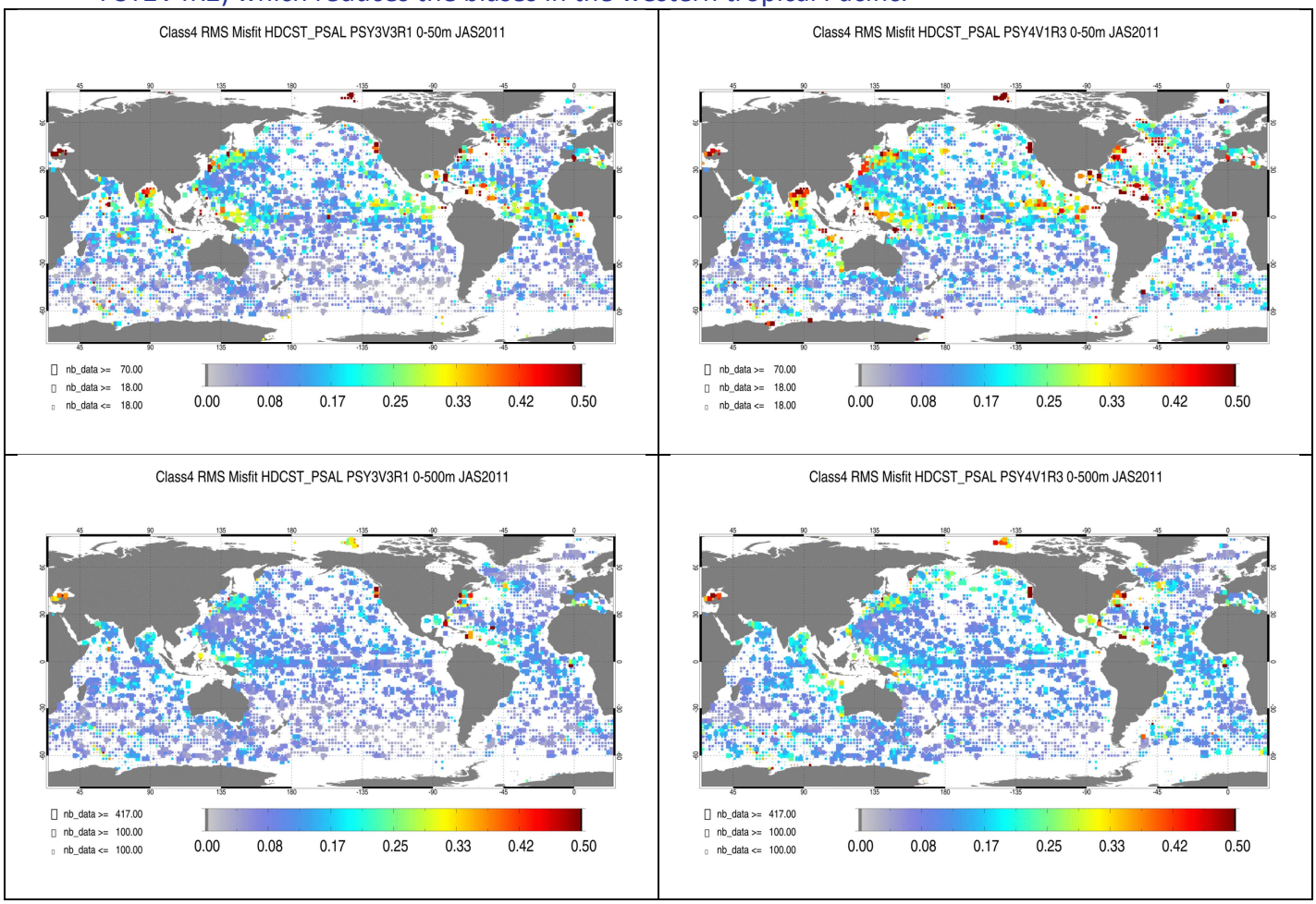

Figure 21: RMS salinity (psu) difference (model-observation) in JAS 2011 between all available T/S observations from the Coriolis database and the daily average hindcast PSY3V3R1 products on the left and hindcast PSY4V1R3 on the right column, colocalised with the observations. Averages are performed in the 0-50m layer (upper panel) and in the 0-500m layer (lower panel). The size of the pixel is proportional to the number of observations used to compute the RMS in 2°x2° boxes.

The salinity RMS errors (Figure 21) are usually less than 0.2 psu but can reach high values in regions of high runoff (Amazon, Sea Ice limit) or precipitations (SPCZ), and in regions of high mesoscale variability. The salinity error is generally smaller in PSY3V3R1 than in PSY4V1R3 for instance here in the North Pacific gyre, the Indian Ocean, the South Atlantic Ocean or the Tropical Pacific Ocean. Strong departures from the observations are also noticed in the Gulf of Guinea.

In the Beaufort sea PSY3V3R1 seems to be more accurate than PSY4V1R3 compared to what may be Sea mammals observations, in temperature and especially in salinity. In this case further investigations would be needed on the calibration of these real time observations. We note that for a given region a minimum of 90 measurements is used to compute the statistics for this three months period.

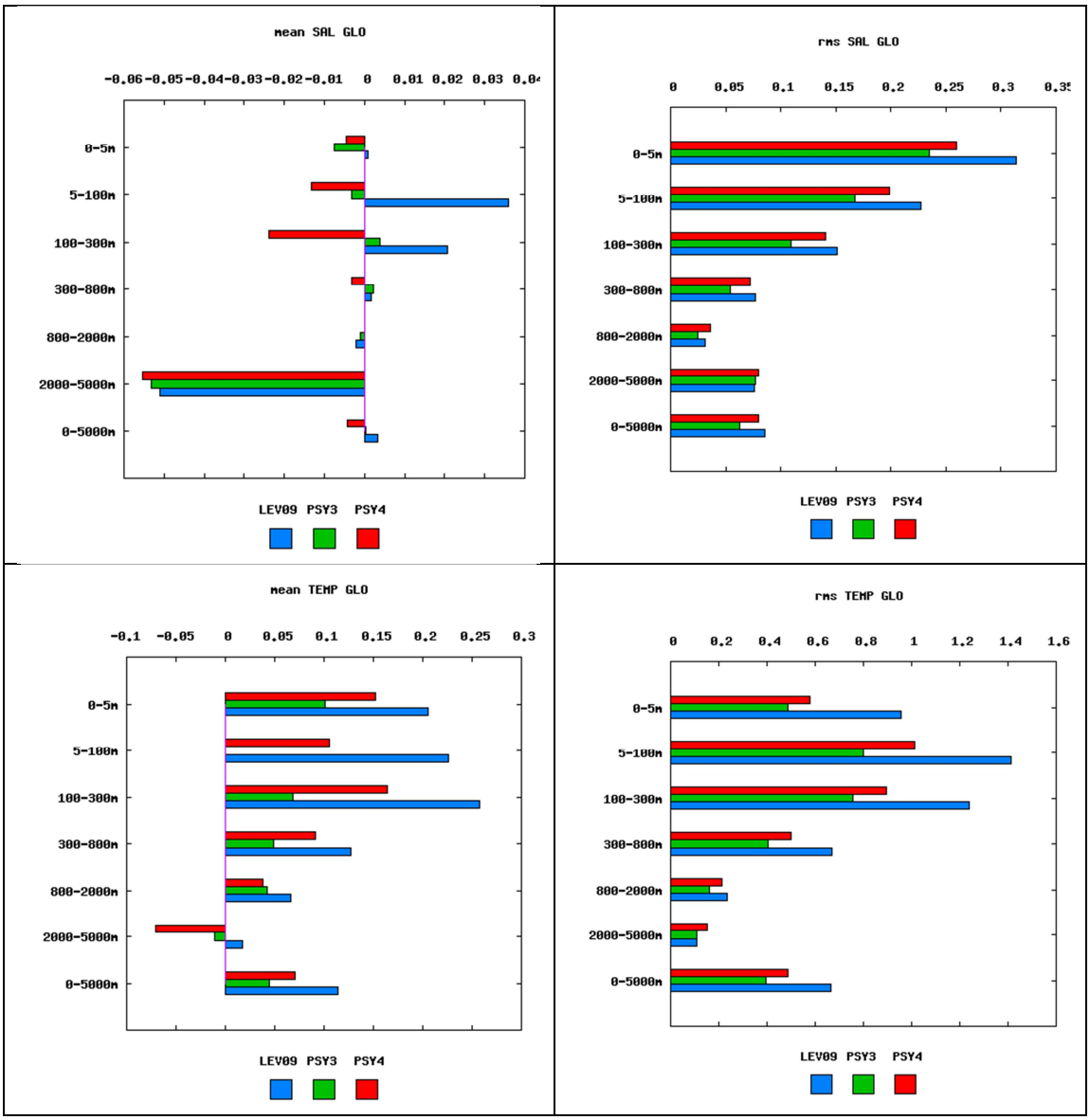

Figure 22 : Global statistics for salinity (psu, upper panel) and temperature (°C, lower panel) averaged in 6 consecutive layers from 0 to 5000m. Mean difference (observation-model, left column) and RMS difference (right column) between all available T/S observations from the Coriolis database and the daily average nowcast PSY3V3R1 products (green) , nowcast PSY4V1R3 (red) and WOA09 climatology (blue) colocalised with the observations. NB: average on model levels is performed as an intermediate step which reduces the artefacts of inhomogeneous density of observations on the vertical.

For the global region in Figure 22, the intermediate resolution model (PSY3V3R1) is more accurate than the high resolution model (PSY4V1R3) in terms of RMS and mean difference for both temperature and salinity. For the subsurface layers (5-100m, 100-300m) we can clearly see the effect of the bias correction which is applied in PSY3V3R1 and not in PSY4V1R3. Both global systems are too cold on the whole water column, PSY3V3R1 being significantly closer to the observations than PSY4V1R3. PSY4V1R3 is globally too salty in the 5-800 m layer contrary to PSY3V3R1 which becomes slightly fresh from 100 m up to 800 m depth. The two systems are clearly better than the WOA09 climatology (Levitus 2009) over the whole water column in temperature and salinity. We note that there is a salty bias in the 2000-5000m layer which is not representative of the global ocean. Indeed for the period of JAS the data in the 2000-5000m layer are very sparse and located mainly near the Drake

Passage, Gulf of Guinea, West tropical Pacific, Kuroshio, North Brazil Current, near Florida, near Canary Islands (Figure 23).

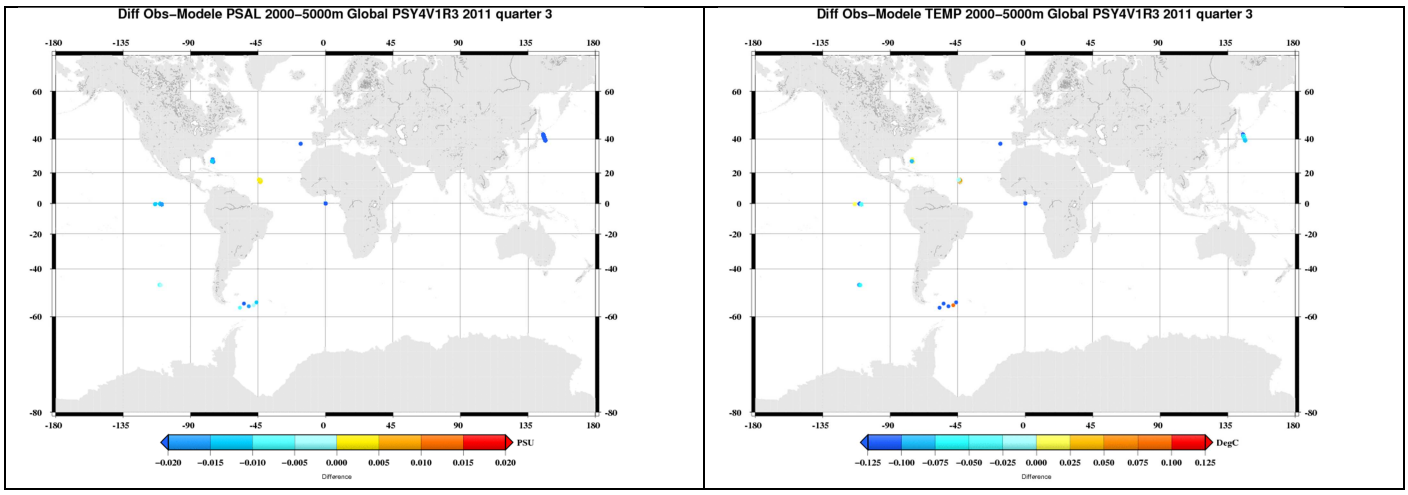

Figure 23 : Difference Observations-model PSY4V1R3 of all available TS in situ data in the 2000-5000m layer in temperature (°C, right panel) and salinity (psu, left panel).

V.2.1.2. Atlantic Ocean and Mediterranean Sea

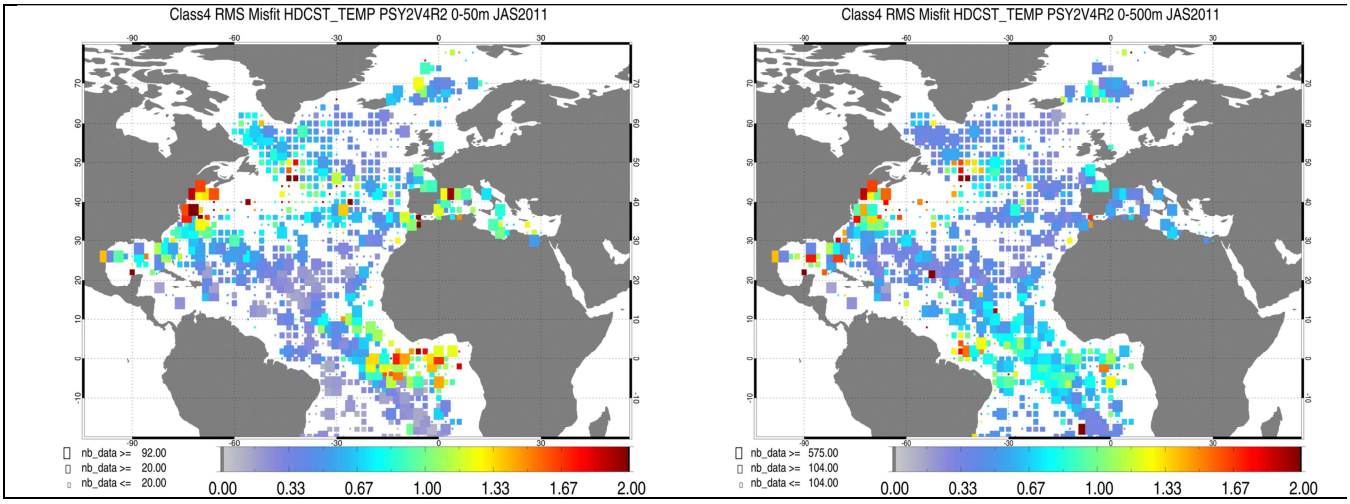

Figure 24: Upper panel: RMS difference (model-observation) of temperature (°C) in JAS 2011 between all available T/S observations from the Coriolis database and the daily average PSY2V4R2 products colocalised with the observations in the 0-50m layer (left column) and 0-500m layer (right column).

The general performance of PSY2V4R2 (departures from observations in the 0-500m layer) is less than 0.3°C and 0.05 psu in many regions of the Atlantic and Mediterranean (Figure 24 and Figure 25). Temperature and salinity biases appear in the Gulf Stream, and mainly salinity biases in the Gulf of Guinea, the North Brazil Current, the Labrador Sea, Gulf of Mexico. In the eastern tropical Atlantic biases concentrate in the 0-50m layer, while in the Western tropical Atlantic the whole 0-500m layer is biased (fresh bias). For this period, there are not many data in the central part of the Gulf Stream. The system is less accurate near the coast where it is less constrained (especially by altimetry and SST).

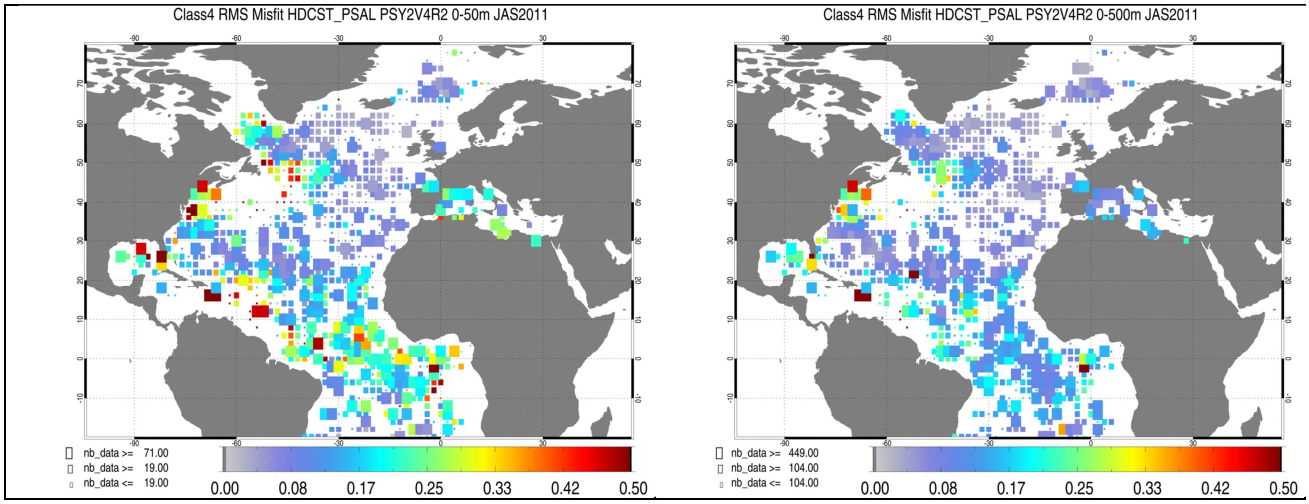

Figure 25: Upper panel: RMS difference (model-observation) of salinity (psu) in the 0-50m layer in JAS 2011 between all available T/S observations from the Coriolis database and the daily average PSY2V4R2 products colocalised with the observations observations in the 0-50m layer (left column) and 0-500m layer (right column).

V.2.1.3. Water masses diagnostics

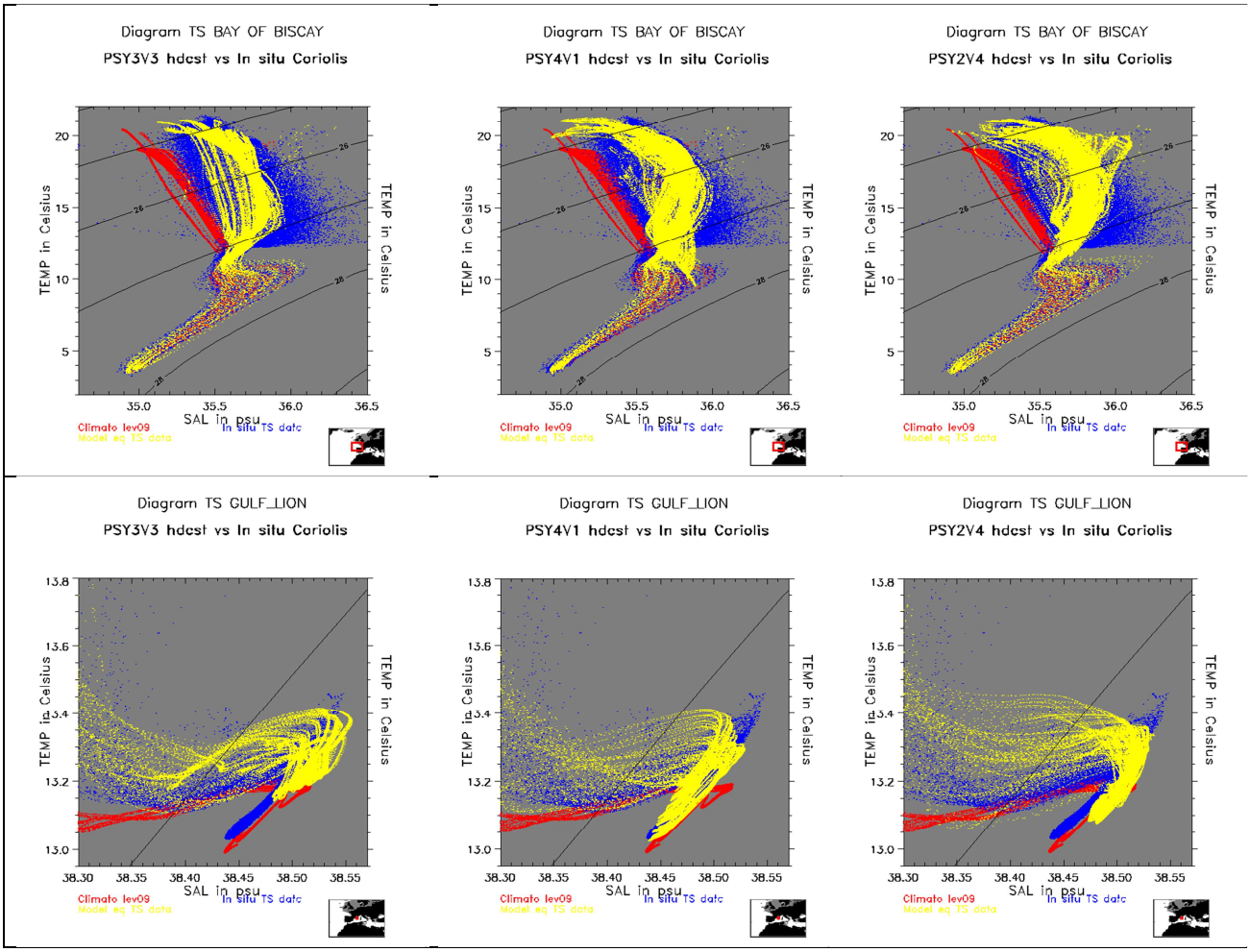

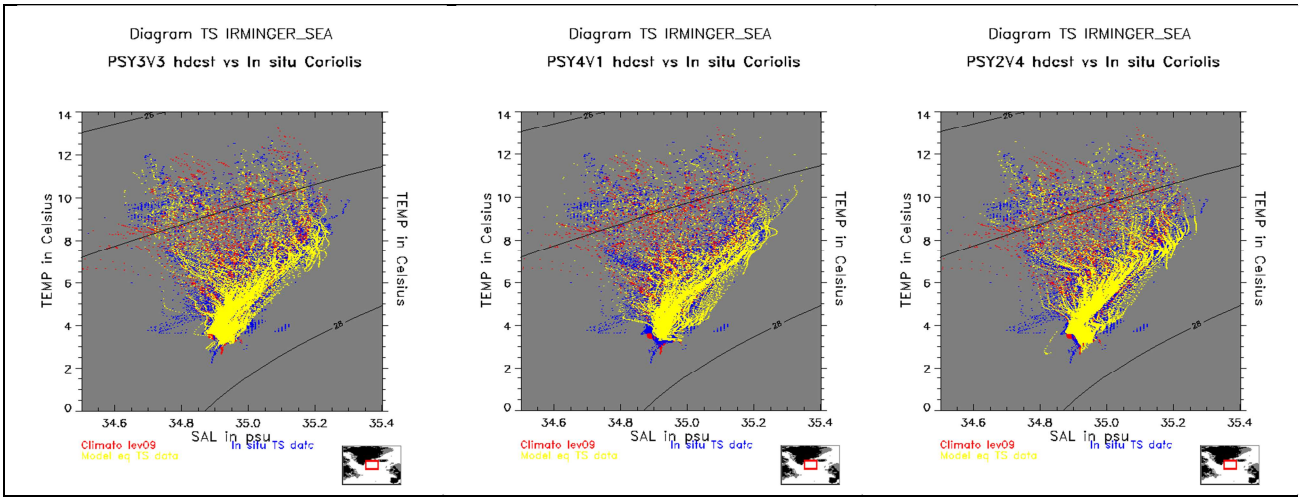

Figure 26: Water masses (Theta, S) diagrams in the Bay of Biscay (upper panel), Gulf of Lion (middle panel) and Irminger Sea (lower panel), comparison between PSY3V3R1 (left column) and PSY4V1R3 (middle column) and PSY2V4R2 (right column) in JAS 2011. PSY2, PSY3 and PSY4: yellow dots; Levitus WOA09 climatology: red dots; in situ observations: blue dots.

We use here the daily products (analyses) collocated with the T/S profiles to draw "T, S" diagrams.

In the Bay of Biscay (Figure 26) we have the main influence of the Eastern North Atlantic Central Water, Mediterranean and Labrador Sea Water.

- Between 11°C and 20°C, 35.5 and 36.5 psu, warm and relatively salty Eastern North Atlantic Central Water gets mixed with the shelf water masses. The systems water masses characteristics are not as spread as in the observations. This could be due to the absence of mixing phenomena such as the internal tides.
- The high resolution systems PSY3V3R1 and PSY2V4R2 better represents the Mediterranean Water characterized by high salinities (Salinities near 36psu) and relatively high temperatures (Temperatures near 10°C).
- Between 4°C and 7°C, 35.0 and 35.5 psu the Labrador Sea Water appears too salty for all the systems.
-

In the Gulf of Lion:

- The Levantine Intermediate Water (maximum of salinity near 38.5 psu and 13.4°C) is too cold in PSY2V4R2 and PSY4V1R3. The global ¼° PSY3V3R1 seems to be closer to the observations than the other systems for this type of water.
- The deep waters are too warm and salty in PSY3V3R1 and PSY2V4R2 whereas the global 1/12° PSY4V1R3 is very close to the observations between 38.45 and 38.5 psu and between 13 and 13.2°C. The difference could be explained by a better initialisation of the deep waters thanks to a better climatology: PSY4V1R3 uses Levitus 1998 merged with MEDATLAS in the Mediterranean Sea whereas the other systems start from Levitus 2005 everywhere.

In the Irminger Sea:

- The North Atlantic Water (T > 7°C and S > 35.1 psu) is well represented by the three systems.
- The Irminger Sea Water (≈ 4°C and 35 psu) is too cold an salty in the three systems but PSY2 and PSY3 seems to be better than the global 1/12° PSY4.

- The Labrador Sea Water (≈ 4°C and ≈ 34.8 psu) is not well represented in the three systems where it appears too salty.

In the tropical Atlantic PSY3V3R1 and PSY4V1R3 seem to display a better behaviour than PSY2V4R2 where a fresh bias is present from the '22' to the '26' isopycn (Figure 27). This bias is stronger in the Eastern part than in the Western part of the basin. Part of the observations available in the Gulf of Guinea that are coming from gliders may be erroneous see Figure 28. (in Figure 27 we only plot the data filtered from gliders). The average salinity innovations near 300m for the JAS season (Figure 28) show that a patch of negative anomalies (meaning the model is too salty) appears locally in the Gulf of Guinea while other innovations are small in the vicinity. Moreover these anomalies are not detected deeper than 1000 m. This patch may be due to glider observations in the region that measure water masses properties very far from climatological values (also Figure 28 under investigation).

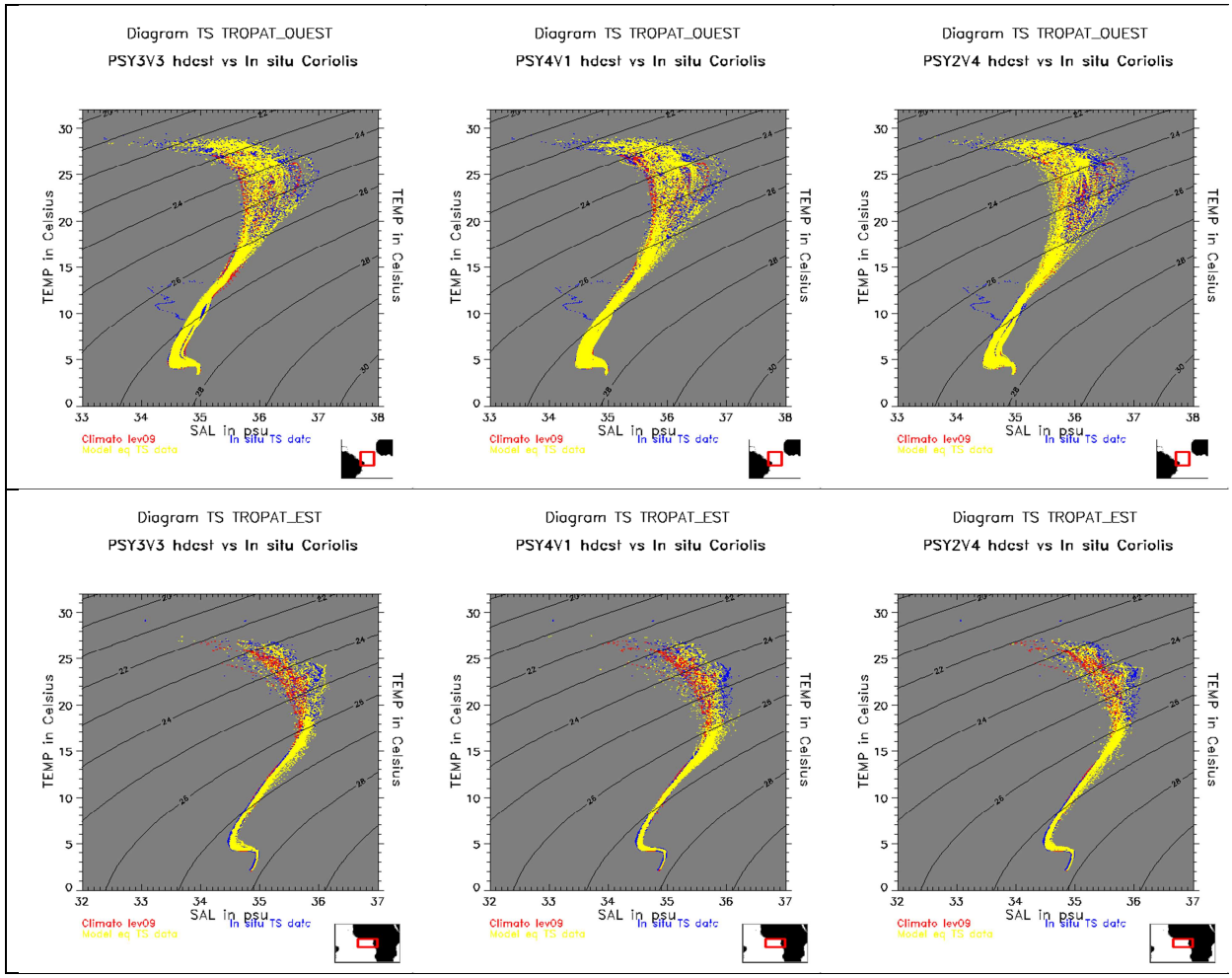

Figure 27 : Water masses (T, S) diagrams in the Western Tropical Atlantic (upper panel) and in the Eastern Tropical Atlantic (lower panel): for PSY3V3R1 (left); PSY2V4R2 (middle); and PSY4V1R3 (right) in JAS 2011. PSY2, PSY3 and PSY4: yellow dots; Levitus WOA09 climatology; red dots, in situ observations: blue dots. Gliders are roughly filtered out (Plateform number : 18956,18951,18952,EXGL0002) .

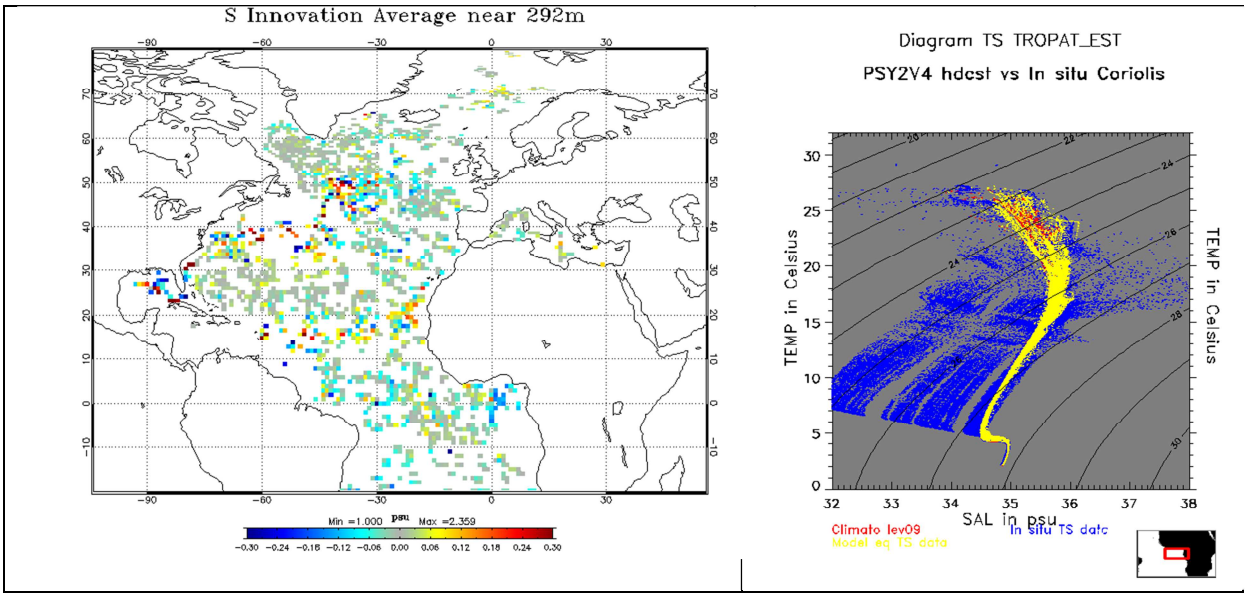

Figure 28: Average salinity (psu) PSY2V4R2 innovation on July-August-September 2011 near 300m (left panel), and T S diagram for all available observations including gliders.

In the Benguela current and Kuroshio Current (Figure 29) PSY3V3R1 and PSY4V1R3 give a realistic description of water masses. In the Benguela current, a fresh bias appears in PSY4V1R3 around the isopycn '27' at 5°C while it is not present in the PSY3V3R1 system. In the Kuroshio Current PSY4V1R3 is closer to the climatology**.** In general, the water masses characteristics display a wider spread in the high resolution 1/12° than in the ¼°, which is more consistent with T and S observations.

Regions of the North Atlantic are also displayed such as the Gulf Stream, where models are too salty from the '27' to the '28' isopycn. In this region at depth PSY3V3R1 is closer to the observations than PSY4V1R3 and the salty bias less pronounced. In the Gulf of Cadiz the signature of the Mediterranean outflow is better reproduced by PSY3V3R1 than by PSY4V1R3.

Diagram TS SOUTH_AFRICA

PSY3V3 hdcst vs In situ Coriolis

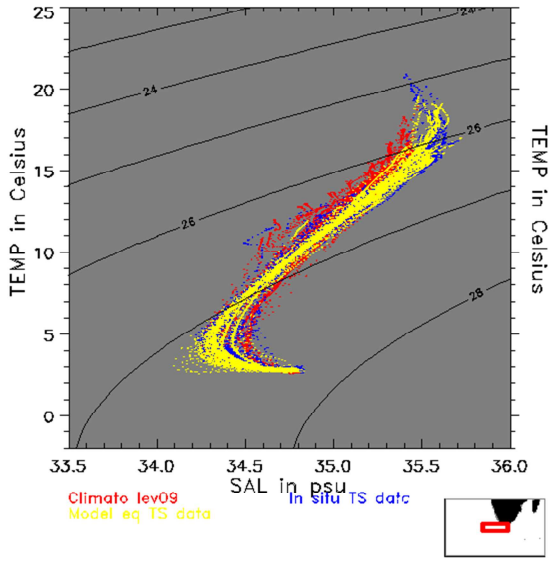

Diagram TS SOUTH_AFRICA

PSY4V1 hdcst vs In situ Coriolis

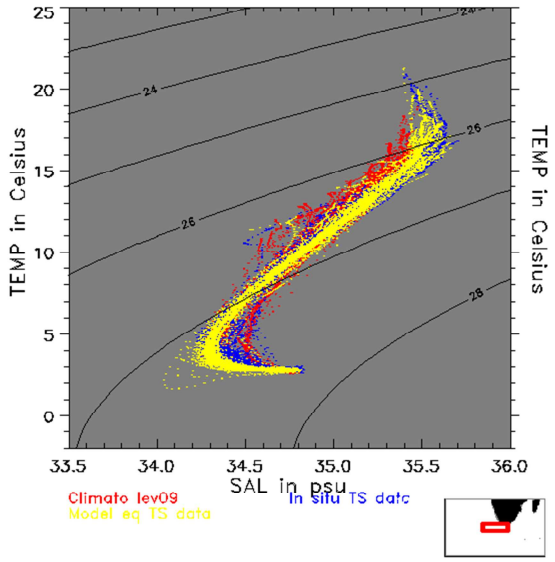

Diagram TS GS

PSY3V3 hdcst vs In situ Coriolis

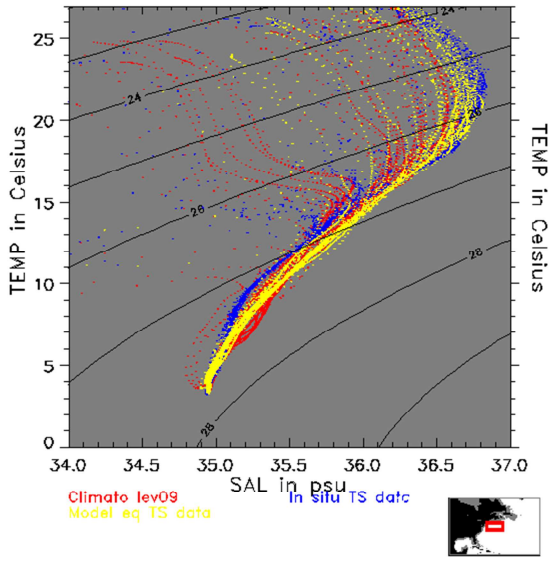

Diagram TS GS

PSY4V1 hdcst vs In situ Coriolis

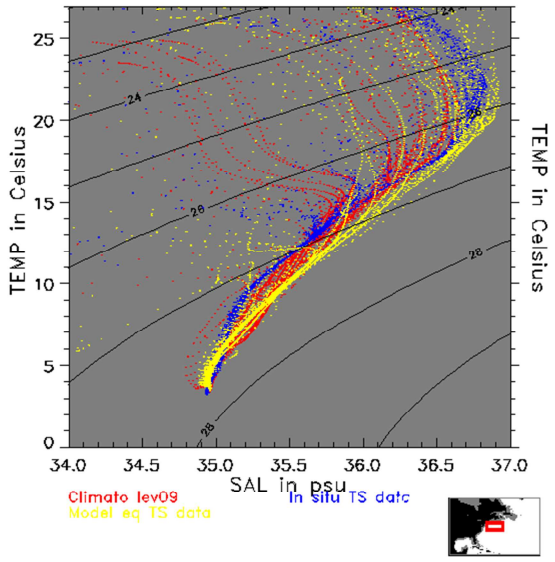

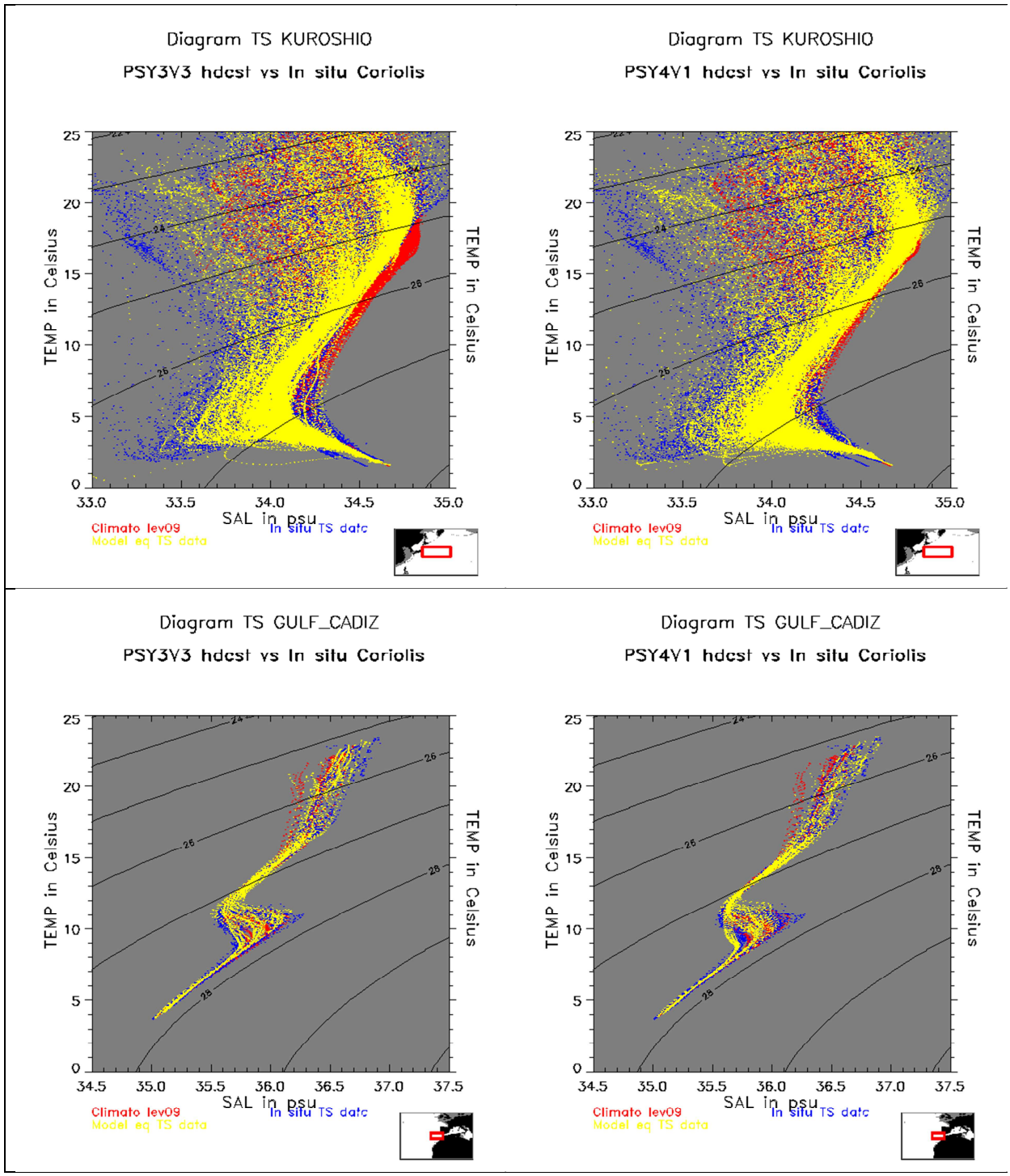

Figure 29: Water masses (T, S) diagrams in South Africa, Kuroshio, Gulf Stream region and Gulf of Cadiz (respectively from top to bottom): for PSY3V3R1 (left); PSY4V1R3 (right) in OND 2011. PSY3 and PSY4: yellow dots; Levitus WOA09 climatology: red dots; in situ observations: blue dots.

V.2.2. SST Comparisons

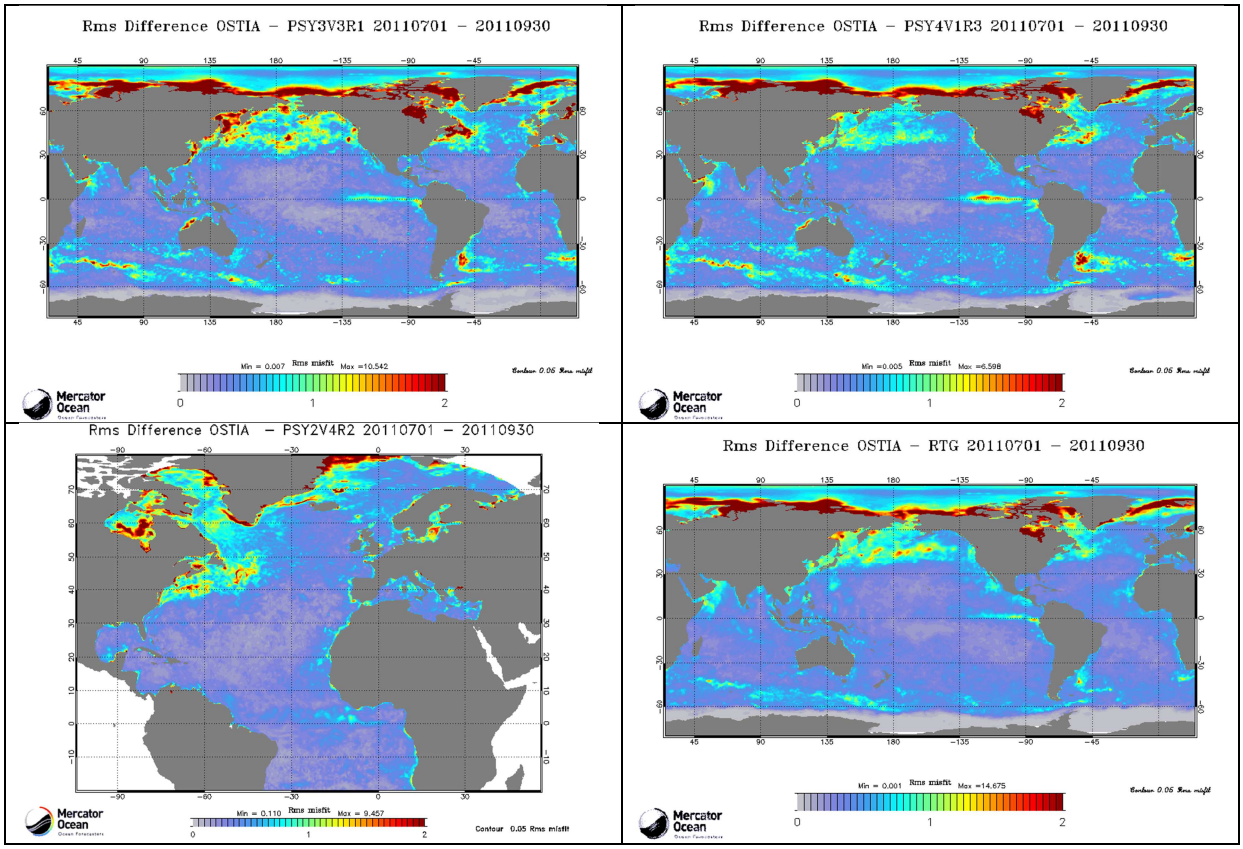

Figure 30 : RMS temperature (°C) between OSTIA daily analyses and PSY3V3R1 daily analyses (upper left), PSY4V1R3 (upper right), PSY2V4R2 (lower left) and RTG daily analyses (lower right): the systems outputs are colocalised with the observations.

Quarterly average SST differences with OSTIA analyses show that in the Antarctic, Indian, South Pacific and Atlantic basins the SST is very close to OSTIA, with difference values staying below the observation error of 0.5 °C on average. However, strong regional biases are diagnosed in the PSY3V3R1 global system at the surface in the North Pacific. For the global systems strong biases are also presents in the Arctic Ocean, the Greenland Sea and Hudson Bay while they are smaller in the high resolution regional system PSY2V4R2.

The comparison between the RTG and OSTIA products for the period JAS 2011 shows that part of these biases comes from the use of RTG SST for data assimilation in PSY3V3R1 and PSY4V1R3: the SST product RTG is known to be too cold in the high latitudes coastal regions. These biases disappear in PSY2V4R2 which assimilates the Reynolds ¼° AVHRR-AMSRE product. These products display better performance than RTG SST especially in the high latitudes.

The (cold) bias that persists in the North Pacific gyre for PSY3V3R1 is not explained by differences between OSTIA and the assimilated product Reynolds ¼°. In this period the model bias reaches its highest amplitude, it is probably linked with concurrent effects of bulk fluxes, IAU correction and unrealistic mixing (under investigation).

V.2.3. Drifting buoys velocity measurements

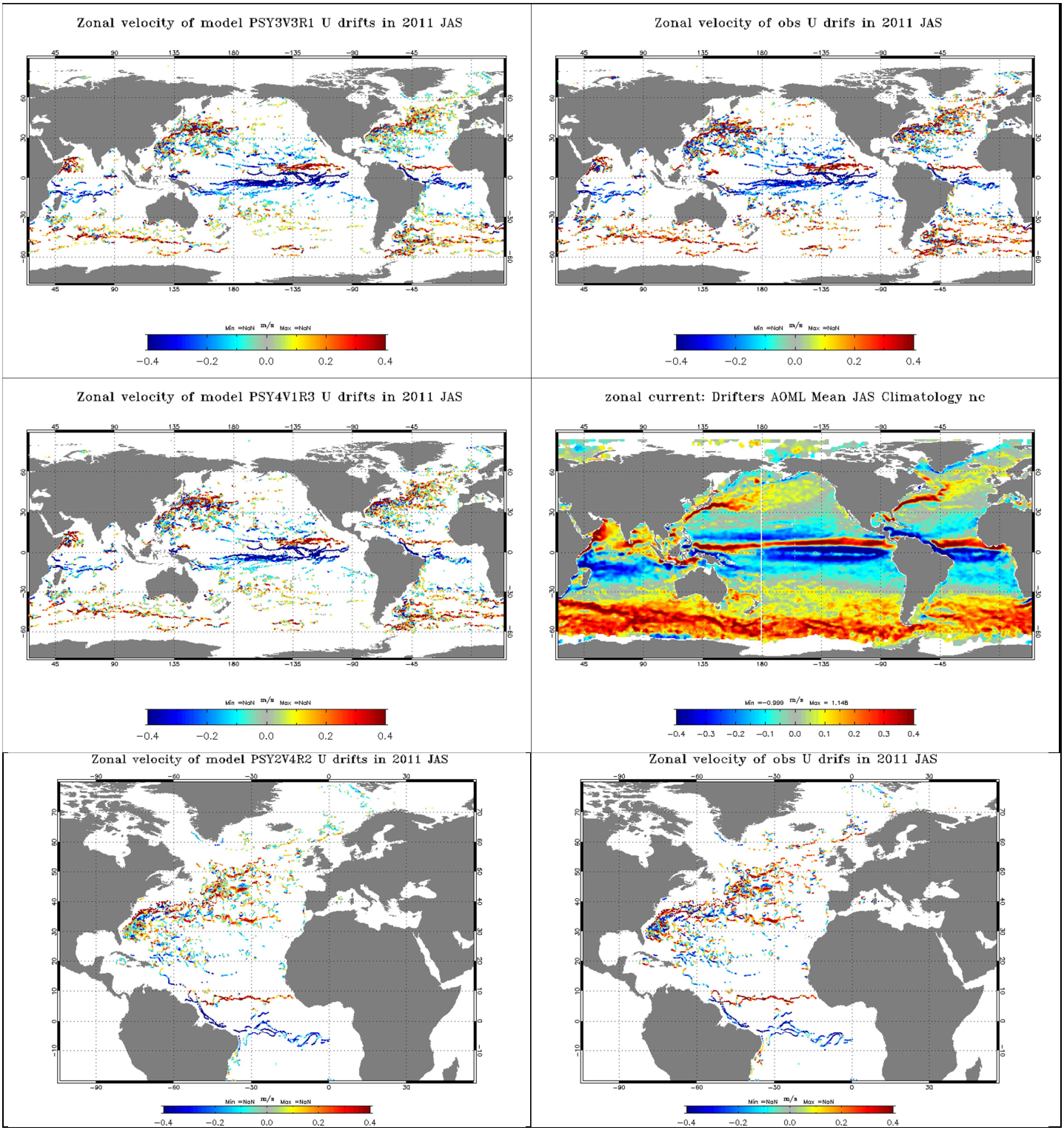

Figure 31: Comparison between modelled zonal current (left panel) and zonal current from drifters (right panel) in m/s. In the left column: velocities collocated with drifter positions in JAS 2011 for PSY3V3R1 (upper panel), PSY4V1R3 (middle panel) and PSY2V4R2 (bottom panel). In the right column, zonal current from drifters (upper) at global scale, AOML drifter climatology for JAS with 0.07 % slippage correction from Lumpkin and Garraffo 2005 (middle) and zonal current from drifters (lower) at regional scale.

In previous *QuO Va Dis?* #5 we mentioned that velocities estimated by the drifters happened to be biased towards high velocities. In JAS 2011 the Antarctic circumpolar current is less energetic in the PSY3V3R1 system than in the AOML climatology, for which only a small slippage correction is applied (Figure 31). This bias also appears in the high latitudes of the Northern Hemisphere.

Like in *QuO Va Dis?* #5 we compute comparisons with drifters velocities corrected from slippage and windage (cf *QuO Va Dis?* #5 and Annex C). Once this Mercator Océan correction is applied to the drifter observations, the zonal velocity of the model (Figure 32) at 15 m depth and the meridional velocity (not shown) seem to be more consistent with the observations for the JAS period.

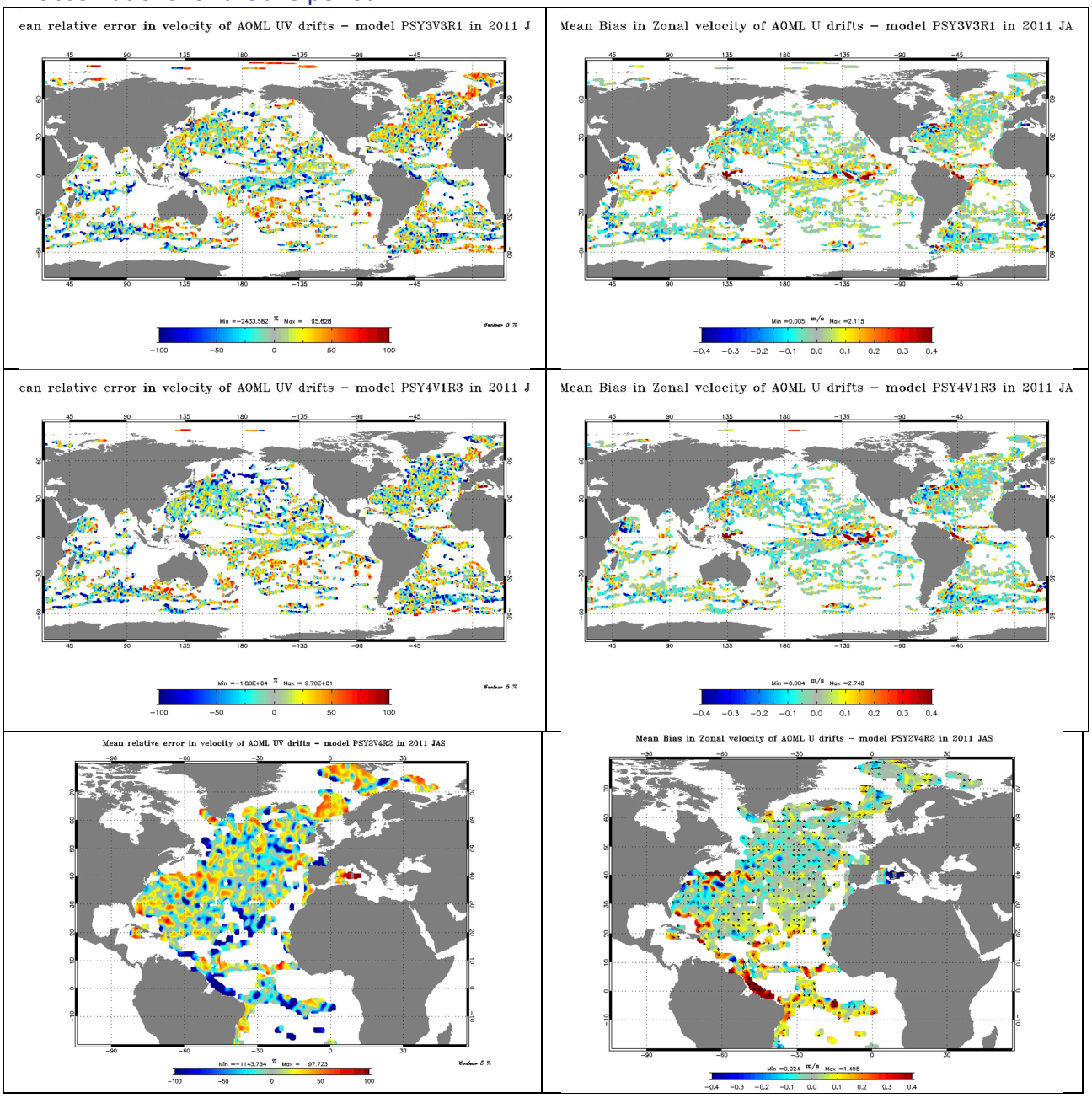

Figure 32 : Comparison of the mean relative velocity error between in situ AOML drifters and model data on the left side and mean zonal velocity bias between in situ AOML drifters with Mercator Océan correction (see text) and model data on the right side. Upper panel: PSY3V3R1, middle panel: PSY4V1R3, bottom panel : PSY2V4R2.

For the **zonal current** the two global systems are very similar, the main differences appear in the Tropical Indian Ocean and in the Tropical Pacific Ocean where PSY3V3R1 displays a weaker South and North Equatorial Current than PSY4V1R3. In this case, PSY4V1R3 is closer to observed velocities than PSY3V3R1. The zonal biases between drifters' velocities and model velocities in Figure 32 confirm that PSY4V1R3 is more realistic for the South (west part) and North Equatorial Current in the tropical Pacific.
Compared to drifters velocities, PSY4V1R3 and PSY3V3R1 underestimate the surface velocity in the mid latitudes. All systems overestimate the Equatorial currents and southern part of the North Brazil Current (NBC).
Errors appear in the Great Whirl in the Indian Ocean. This area is very active during JAS due to Summer Indian Monsoon (see also Figure 51).
For all systems the largest direction errors are local (not shown) and generally correspond to ill positioned strong current structures in high variability regions (Gulf Stream, Kurioshio, North Brazil Current, Zapiola eddy, Agulhas current, Florida current, East African Coast current, Equatorial Pacific Countercurrent).

V.2.4. Sea ice concentration

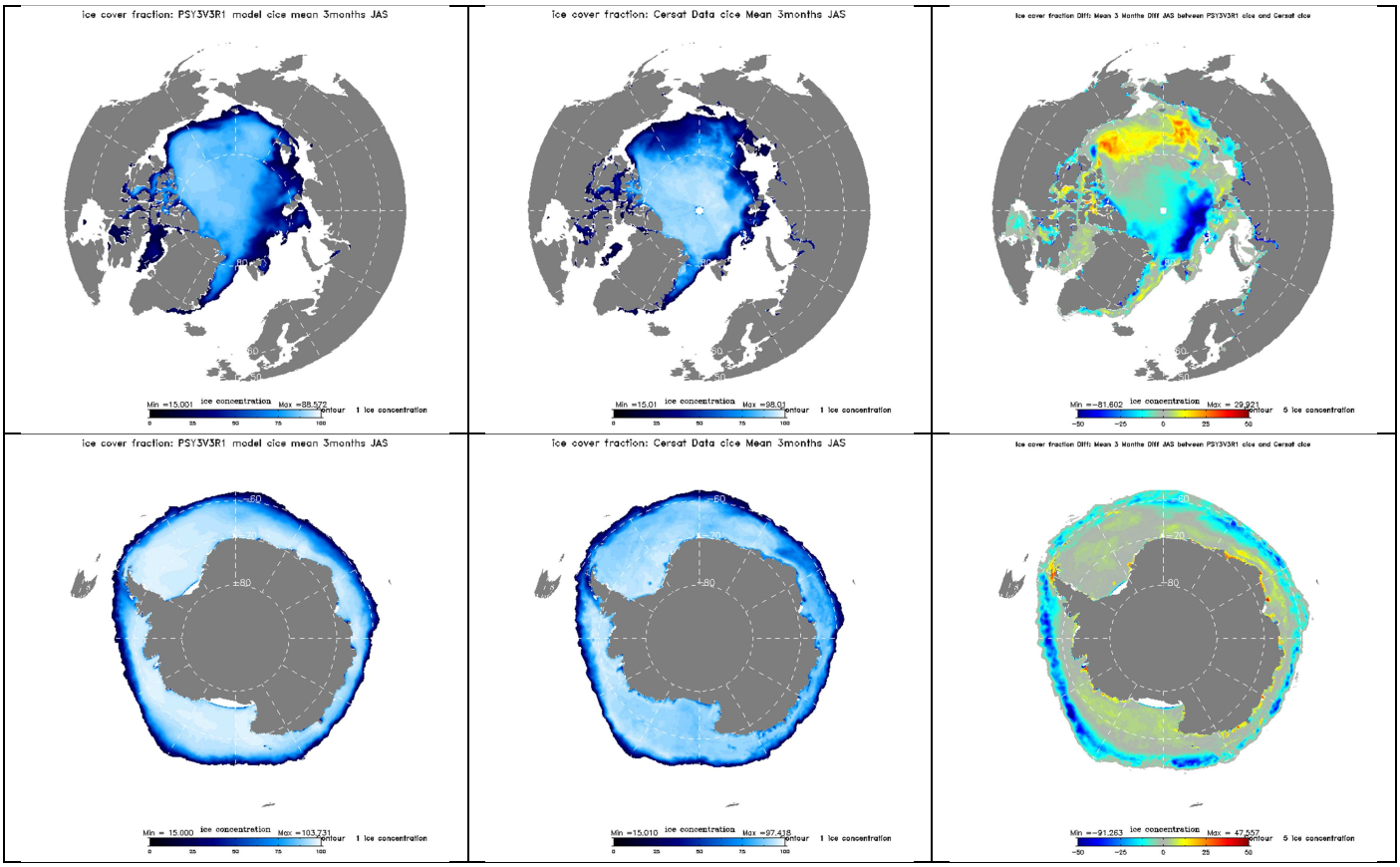

Figure 33: Comparison of the sea ice cover fraction mean for JAS 2011 for PSY3V3R1 in Arctic (upper panel) and Antarctic (lower panel), for each panel the model is on the left the mean of Cersat dataset in the middle and the difference on the right.

In JAS 2011 the PSY3V3R1 Arctic sea ice fraction is in agreement with the observations on average, it is slightly overestimated (by 15%) from the Beaufort Sea up to East Siberian Sea and underestimated (> 25%) especially in the South East of the sea ice pack. Small discrepancies inside the sea ice pack will not be considered as significant as the sea ice concentration observations over 95% are not reliable. As the model sea ice extend is in agreement with observation the strong discrepancies with observed concentration remain inside the sea ice pack. Some discrepancies are observed in the marginal seas mainly in Greenland Sea, Hudson Bay, Laptev and Siberian Seas (Figure 33).
Model studies show that the overestimation in the Canadian Archipelago is first due to badly resolved sea ice circulation (should be improved with higher horizontal resolution). The overestimation in the eastern part of the Labrador Sea is due to a weak extent of the West Greenland Current; similar behavior in the East Greenland Current.
The calibration of PSY3V3R1 on years 2007 to 2009 has shown that the sea ice extent is generally realistic. The system tends to melt too much ice during the summer, while there is still too much ice accumulating in the beaufort gyre. See Figure 53 for monthly averages time series over the last 12 months.

On the contrary PSY4V1R3 sea ice cover is unrealistic (overestimation throughout the year, not shown) due to the use of a previous version of LIM2 and daily atmospheric forcings.As expected in the Antarctic during the austral winter the sea ice concentration is underestimated in the model, especially at the south of the Admundsen and Ross Seas along the sea ice pack.
Figure 34 illustrates the fact that sea ice cover in JAS 2011 is less than the past years climatology, especially in the Barents Sea, Laptev Sea and Baffin Bay, even with a slight overestimation in PSY3V3R1 in the Arctic. In the Antarctic the signal is explained by a model bias (underestimation) and an observed climatic signal: contrary to the Artic sea ice pack the Antarctic sea ice pack tends to increase.
(cf http://nsidc.org/images/arcticseaicenews/20110105_Figure6.png)

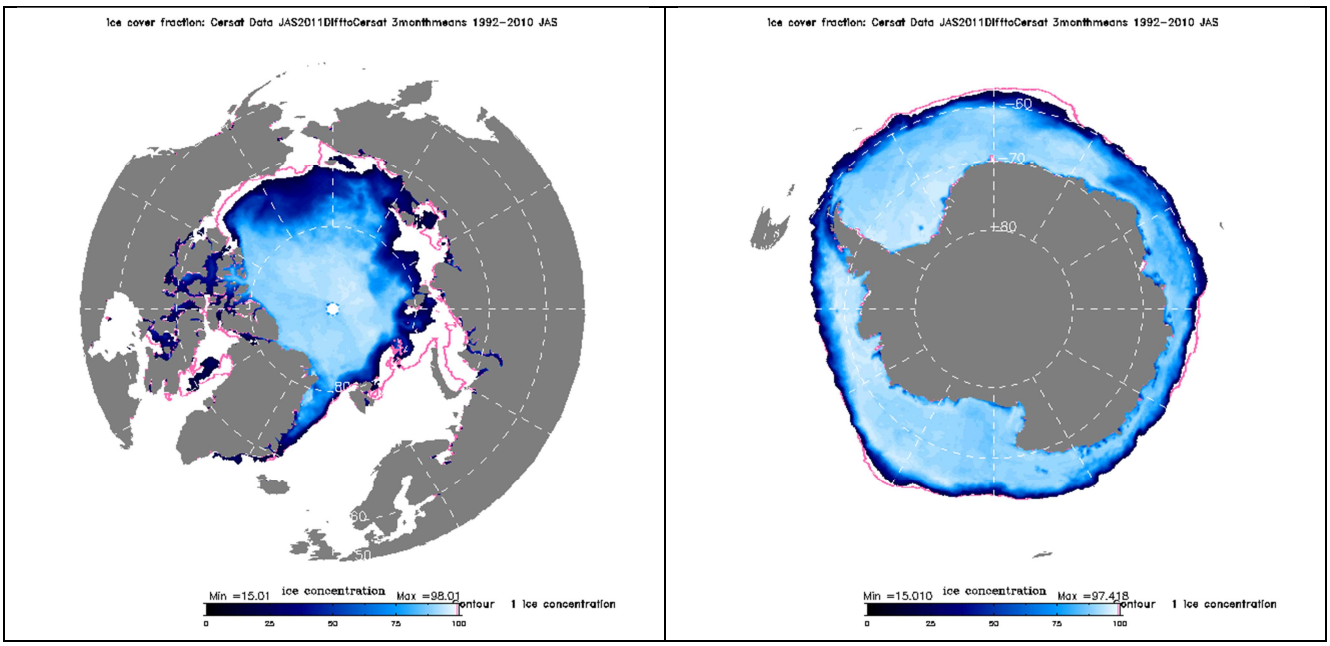

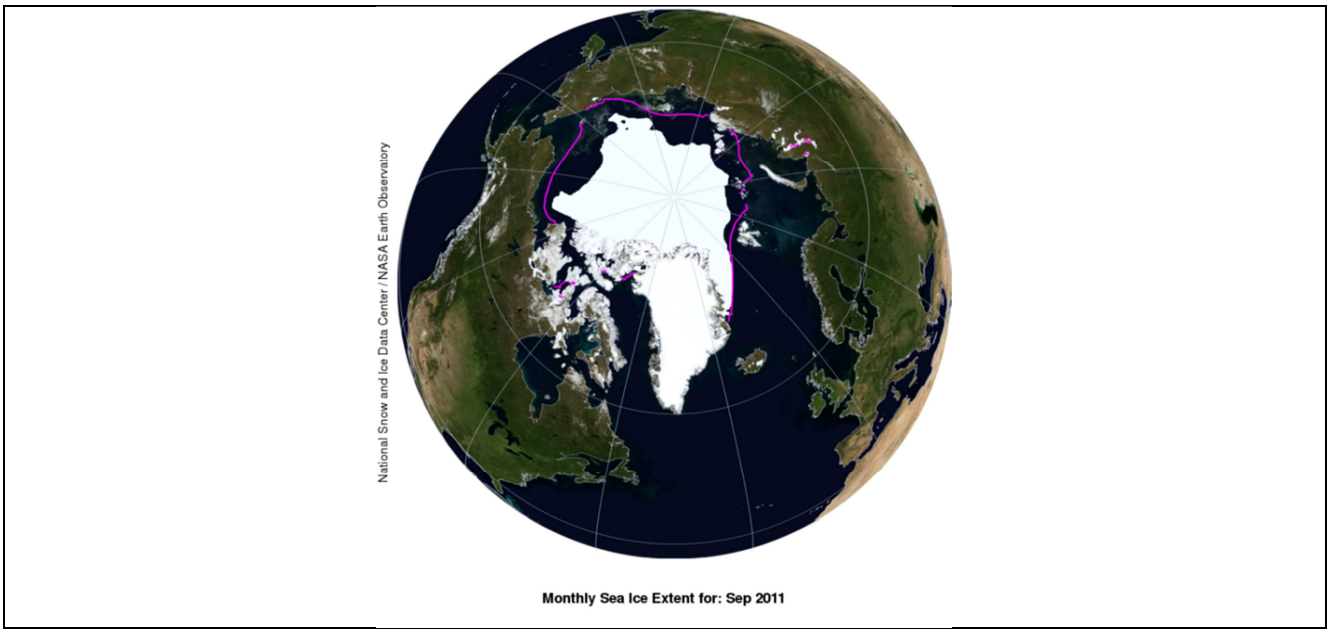

Figure 34: Upper panel: JAS 2011 sea ice extend in PSY3V3R1 with overimposed climatological JAS 1992-2010 sea ice fraction (grey line, > 15% ice concentration) for the Arctic (left) and Antarctic (right) areas.Lower panel: NSIDC map of the sea ice extend in the Arctic for September 2011 in comparison with a 1979-2000 median extend (magenta line).

V.2.5. Closer to the coast with the IBI system: multiple comparisons

V.2.5.1. Comparisons with SST from CMS

Figure 35 displays bias, RMS error and correlation calculated from comparisons with SST measured by satellite. Summer is generally the period where the biases are maximum. The maximum biases are located on the shelf. Along the Moroccan and Iberian coasts where upwellings occur; it is still a challenge to correctly model the filaments produced during the upwellings events. In the English Channel and Celtic sea: these biases are linked to the mixing induce by the tides. In the Mediterranean Sea, biases are associated to the Alboran gyre and the Algerian current. One can also notice an area with more bias between the Gulf of Lion and Corsica. Apart of the shelf, the RMS error is small (less than 0.5°C), except between 45 and 50°N; but this area is poor in observations.

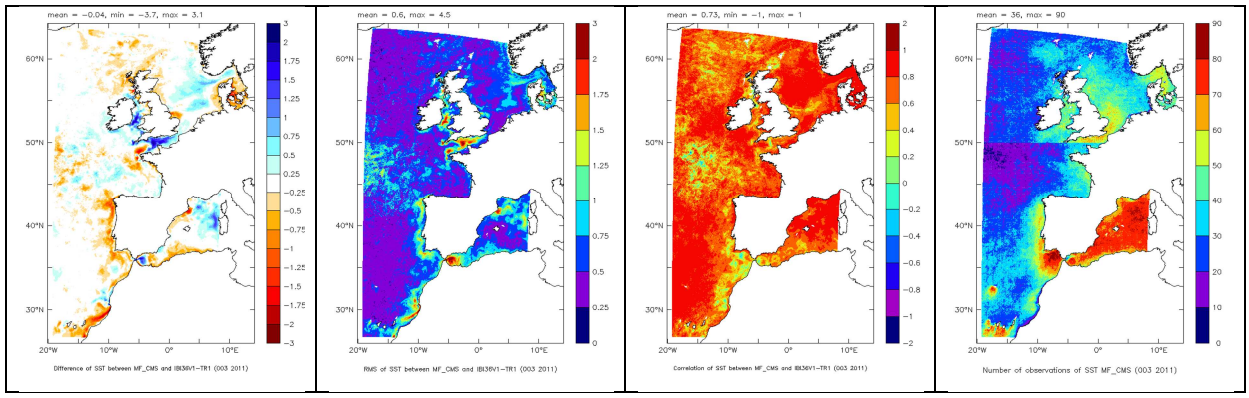

Figure 35 : Comparisons to SST (model – observation) from MF_CMS for JAS 2011 period. From the left to the right: mean bias, RMS error, correlation, number of observations

V.2.5.2. Comparisons with in situ data from EN3/ENSEMBLE for JAS 2011

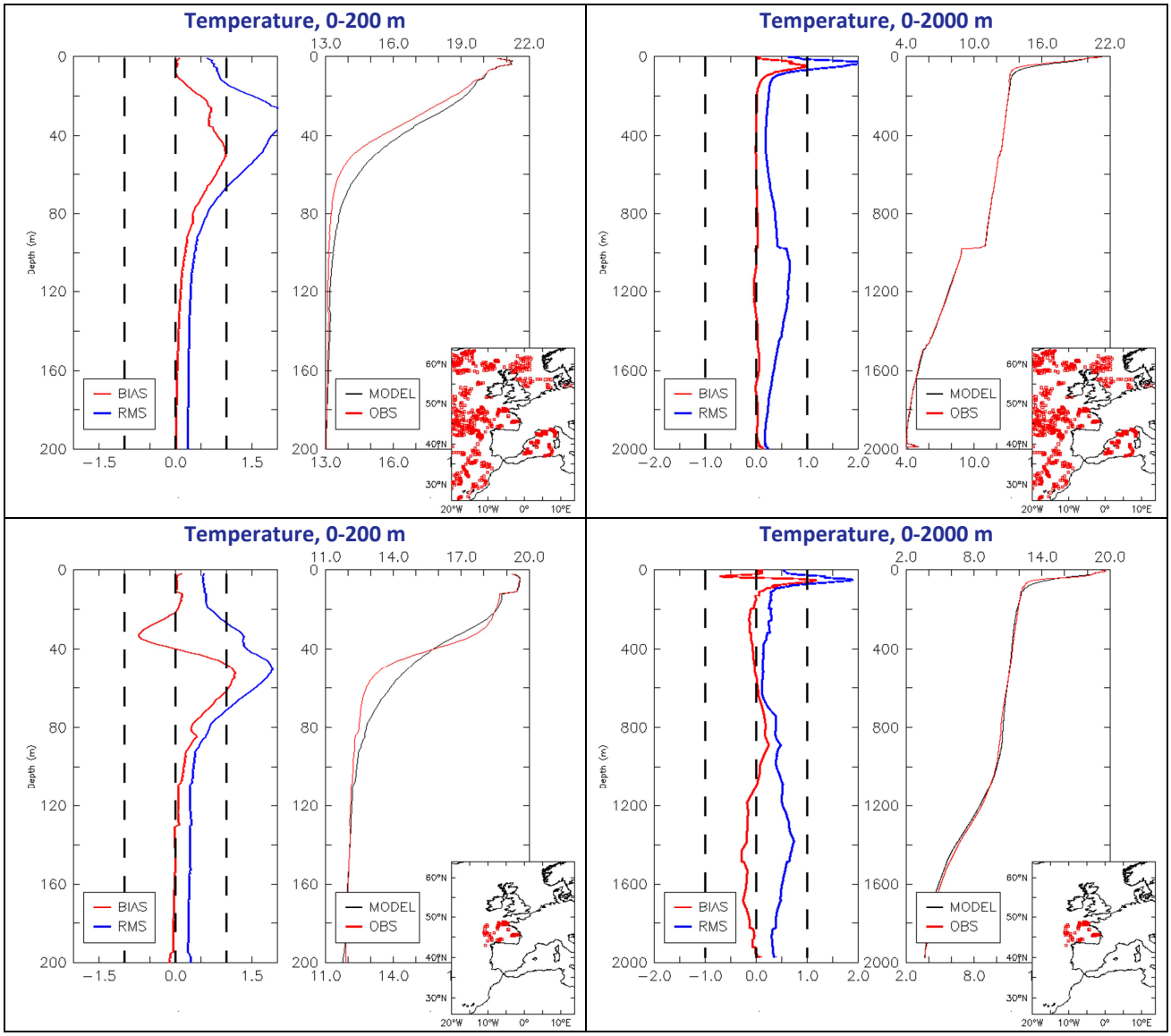

Figure 36 : On the left:mean "observation – model" temperature(°C) bias (red curve) and RMS error (blue curve), On the right: mean profile of the model (black curve) and of the observations (red curve). In the lower right corner : position of the profiles. Top panel: the whole domain; bottom panel: the Bay of Biscay region.

Averaged profiles of temperature (Figure 36) show that the mean bias and the RMS error are maximum between 20 and 80 m depth, in the thermocline. The model is too warm compared to the observations. Below the thermocline, the mean bias is almost zero, and the RMS is maximum at the Mediterranean Sea Water level. In the Bay of Biscay, the mean bias is not zero below the thermocline: the model is too warm between 600 and 1000 m depth, and too cold between 1100 and 2000 m. It can be explained by the fact that the Mediterranean water is not at the right depth (too shallow) in the model.

The mean bias and RMS error of salinity (Figure 37) are maximum near the surface. Below 100 m depth, the bias is almost zero. The RMS error is maximum at the Mediterranean Sea Water level (as for temperature). In the Bay of Biscay the model is too salty between 600 and 1000 m depth, and not salty enough between 1100 and 2000 m depth.
Note: averaged profiles are discontinuous because the number of observations differs depending of the depth.

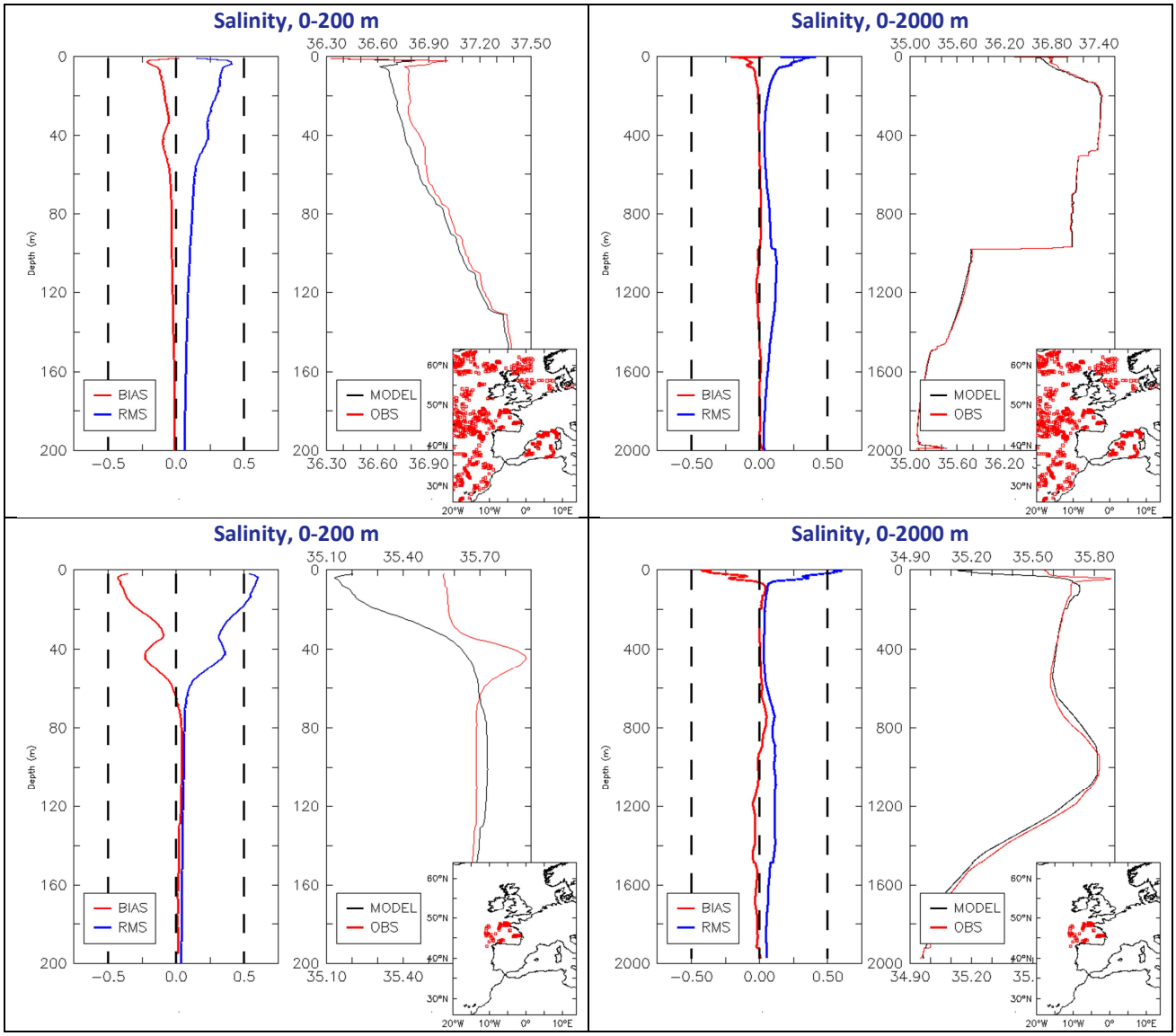

Figure 37: On the left:mean "observation – model" salinity (psu) bias (red curve) and RMS error (blue curve), On the right: mean profile of the model (black curve) and of the observations (red curve). In the lower right corner : position of the profiles. Top panel: the whole domain; bottom panel: the Bay of Biscay region.

.

V.2.5.3. MLD Comparisons with in situ data

Figure 38 shows that smallest values of the mixed layer depth are overestimated in the model, compared to the observations, especially in the bay of Biscay.

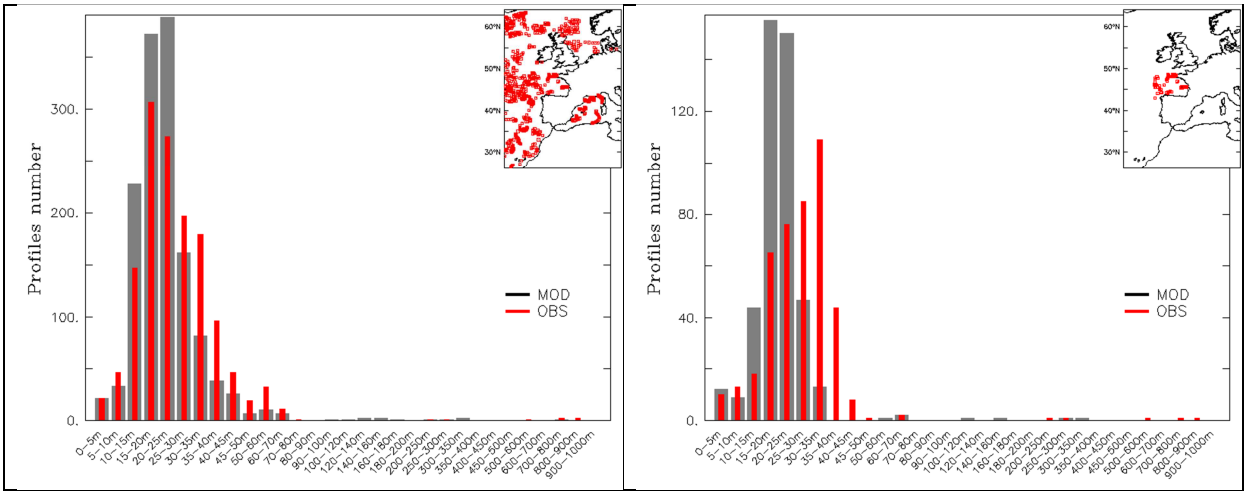

Figure 38 : Mixed Layer Depth distribution calculated from profiles with the temperature criteria (difference of 0.2 0C with the surface); the model is in grey, the observations in red. Left panel: whole domain; right panel: Bay of Biscay.

V.2.5.4. Comparisons with moorings and tide gauges

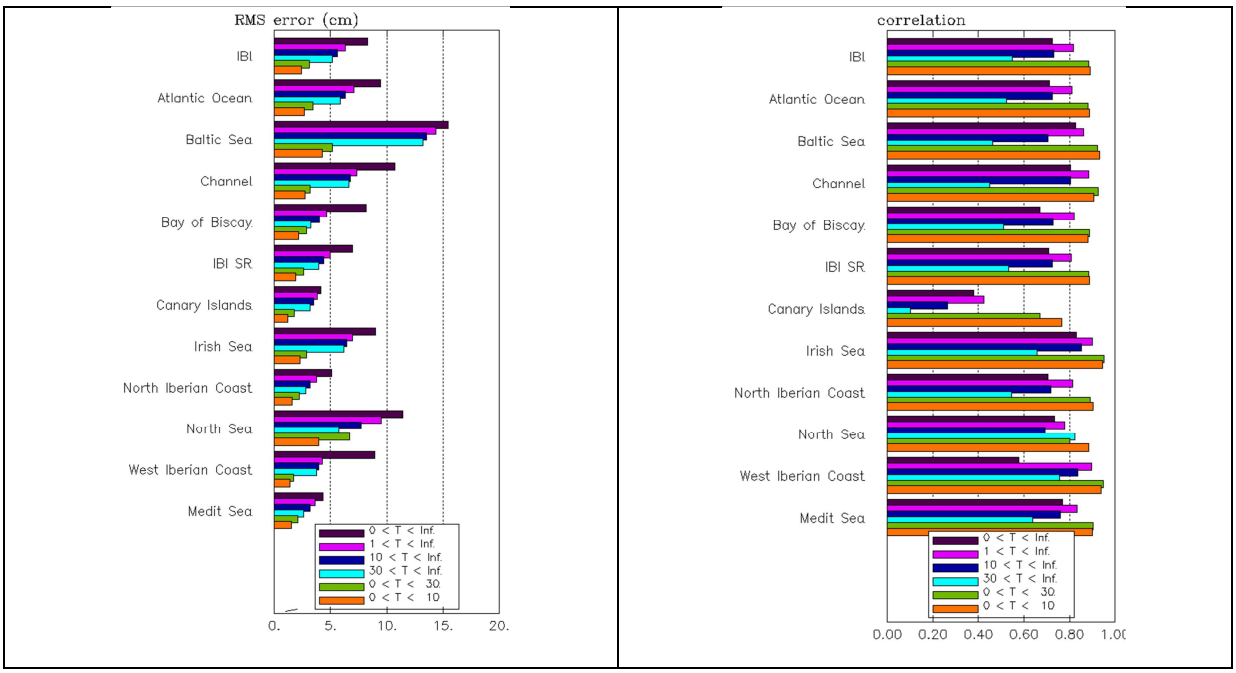

Figure 39 : RMS error (cm) and correlation for the Sea Surface Elevation at tide gauges, for different regions and frequencies.

The RMS error of the residual elevation of sea surface (Figure 39) computed with an harmonic decomposition method (Foreman 1977) and a Loess low-pass filtering, is comprised between 5 and 10 cm, except in the Baltic Sea where it reaches 15 cm. It is less

than 5 cm in the Canary Islands (but with weak correlation) and in the Mediterranean Sea. The RMS decreases for some frequencies band, and is minimum in the 0-10-day band. The correlation is weaker for frequencies greater than 30 days.

In Figure 40 (beware of inverse colobar: red means negative) we can see that the correlations between tide gauges and the IBI model are very high for the three months in the whole domain. The only exceptions are in July and August in the Channel Sea, Celtic Sea and Galician coast. For the Rms error the largest errors are located in the Gulf of Lyon because of a bad position of Liguro-Provençal current, near the Galician Coast and in the Channel Sea. The largest biases are present in the Channel and Celtic Sea, regions characterized by an important tidal mixing, and Galician Coast probably due to a bad representation of an upwelling system very active in this period.

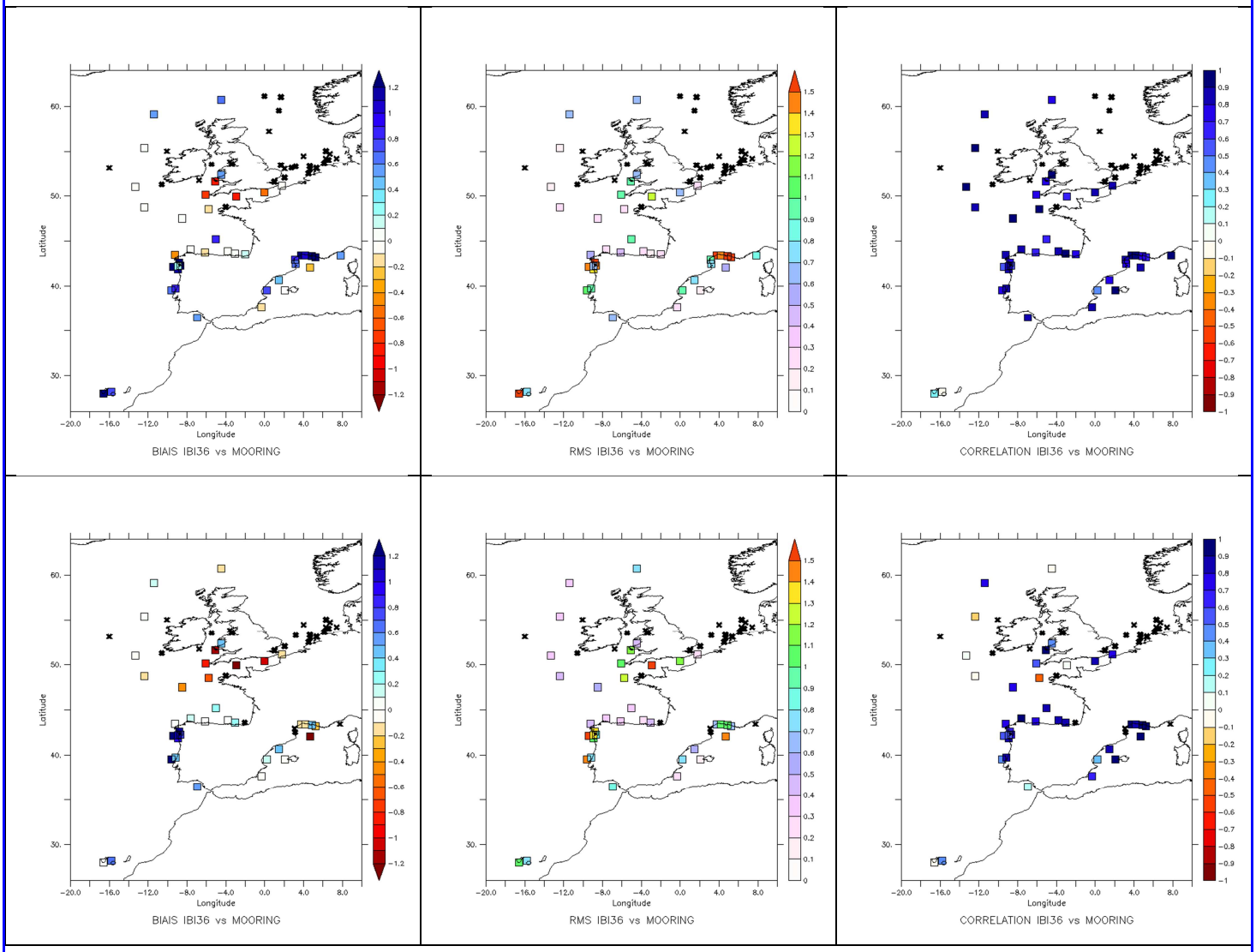

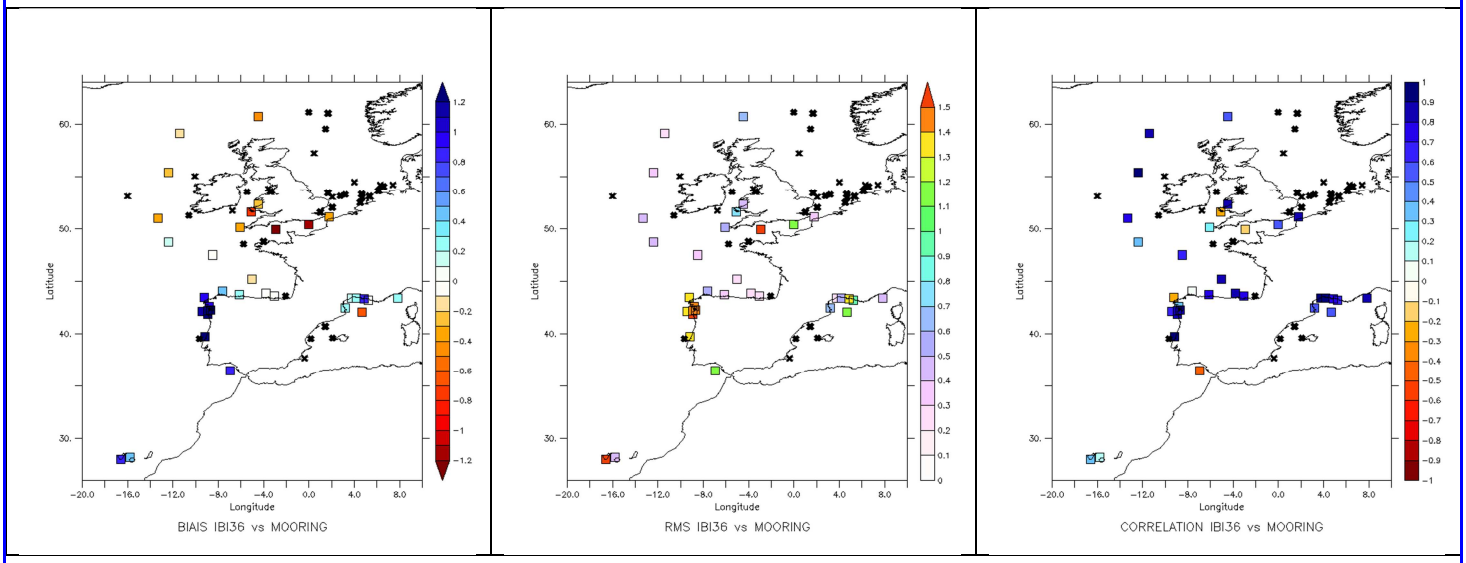

Figure 40 : Bias (Model–Observation), RMS error and correlation for the Sea Surface Elevation between IBI model and tide gauges, each panel represent a month : upper panel July, middle panel August and lower panel September.

V.2.5.5. Comparisons with hydrological section

The comparisons of temperature and salinity with in-situ measurements in the bay of Biscay cf Figure 41 (ASPEX 2011, L. Marié, IFREMER) show that the systems IBI36 and PSY2 are too diffusive with a large thermocline. They also are too fresh at the surface, but this bias is more important in PSY2 whereas IBI36 is closer to the observations.

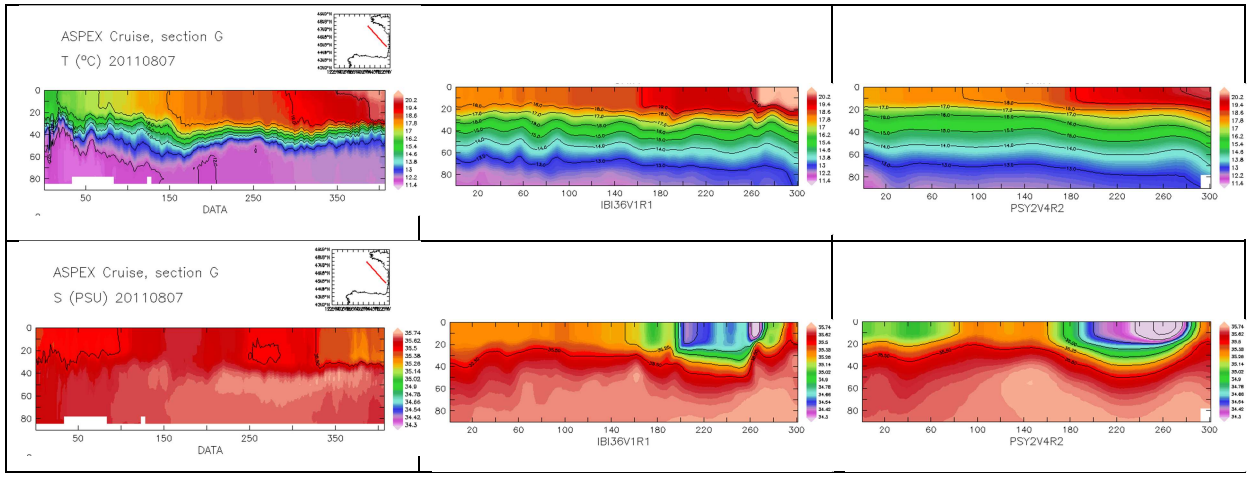

Figure 41 : Temperature (top panels) and salinity (bottom panels) sections along the Bay of Biscay shelf in August (the 7th). Left: observations (ASPEX cruise); middle: IBI36V1R1; right: PSY2V4R2.

V.2.6. Biogeochemistry validation: ocean colour maps

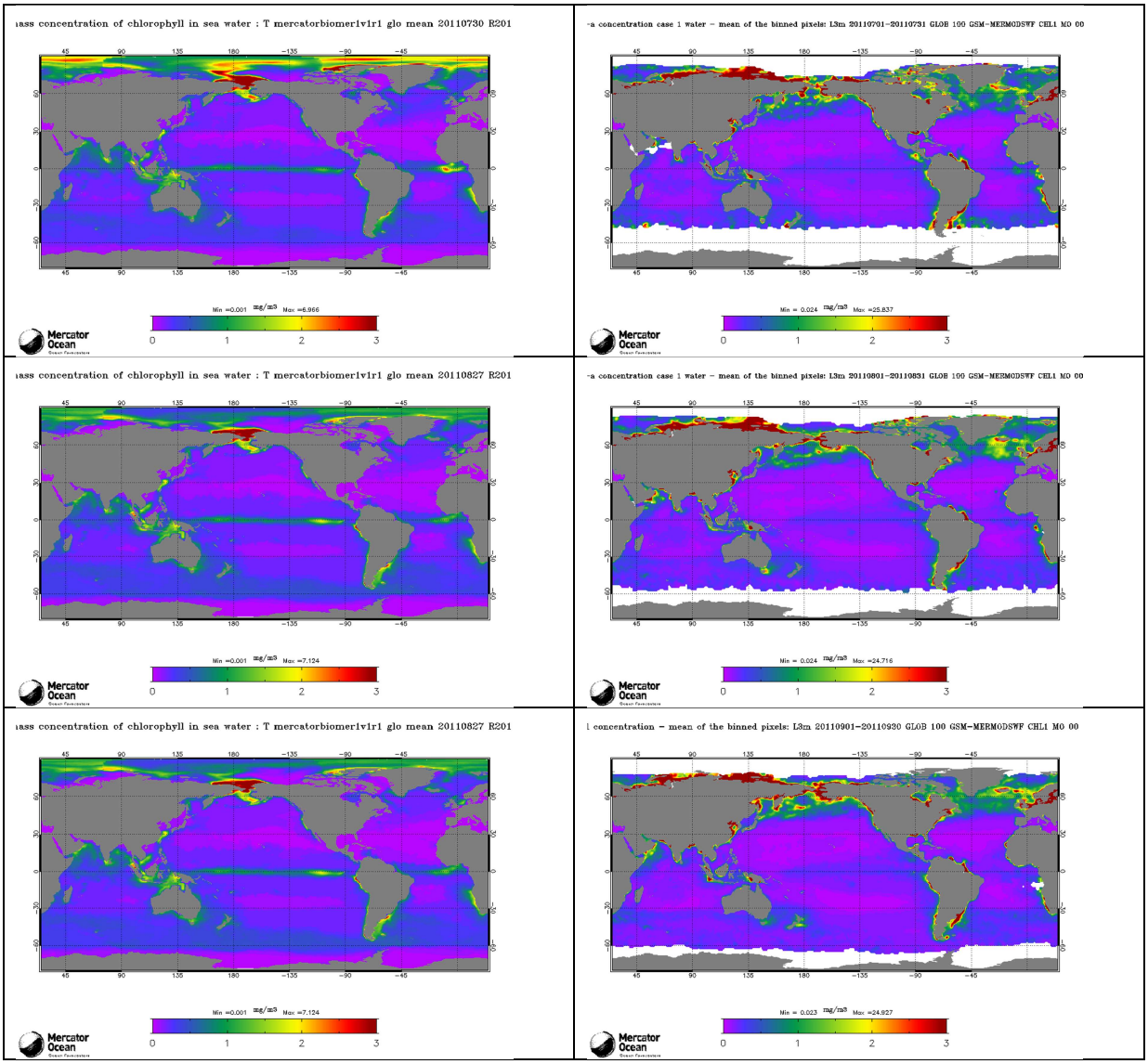

Figure 42 : Chlorophyll concentration for the Mercator system BIOMER (left panels) and Chlorophyll concentration from globcolor (right panels). The upper panel is for June, the medium panel is for August and the bottom panel is for September

Globally, there is a good agreement between BIOMER system and Globcolor ocean color maps except at the equator where the upwelling is too strong in the model. Inside Pacific and Atlantic gyres the Chlorophyll concentration seems to be realistic but strong differences appears in the Arctic Ocean and in the Greenland Sea.

VI Forecast error statistics

VI.1. General considerations

The daily forecasts (with updated atmospheric forcings) are validated in collaboration with SHOM/CFUD. This collaboration has been leading us to observe the actual degradation of the forecast quality depending on the forecast range. When the forecast range increases the quality of the ocean forecast decreases as the initialization errors propagate and the quality of the atmospheric forcing decreases. Additionally the atmospheric forcing frequency also changes (see Figure 43). The 5-day forecast quality is optimal; starting from the 6th day a drop in quality can be observed which is linked with the use of 6-hourly atmospheric fields instead of 3-hourly; and starting from the 10th day the quality is strongly degraded due to the use of persisting atmospheric forcings (but not constant from the 10th to the 14th day as they are relaxed towards a 10-day running mean).

Figure 43: Schematic of the change in atmospheric forcings applied along the 14-day ocean forecast.

VI.2. Forecast accuracy: comparisons with observations when and where available

VI.2.1. North Atlantic region

As can be seen in Figure 44 the PSY2V4R2 products have a better accuracy than the climatology in the North Atlantic region in JAS 2011 except for the 2000-5000m layer which is not representative of the whole domain (cf Figure 23).
The temperature and salinity forecast have the same biases than the analyses. The forecast are too warm between 5 and 300 m in the North Atlantic. They are too fresh at the surface. As expected the analysis RMS error is smaller than the 3-day and 6-day forecast RMS error for both temperature and salinity. This JAS season the RMS error is similar for 6-day or 3-day forecast. The surface salinity forecast do not beat the climatology at the surface and below 2000m depth.

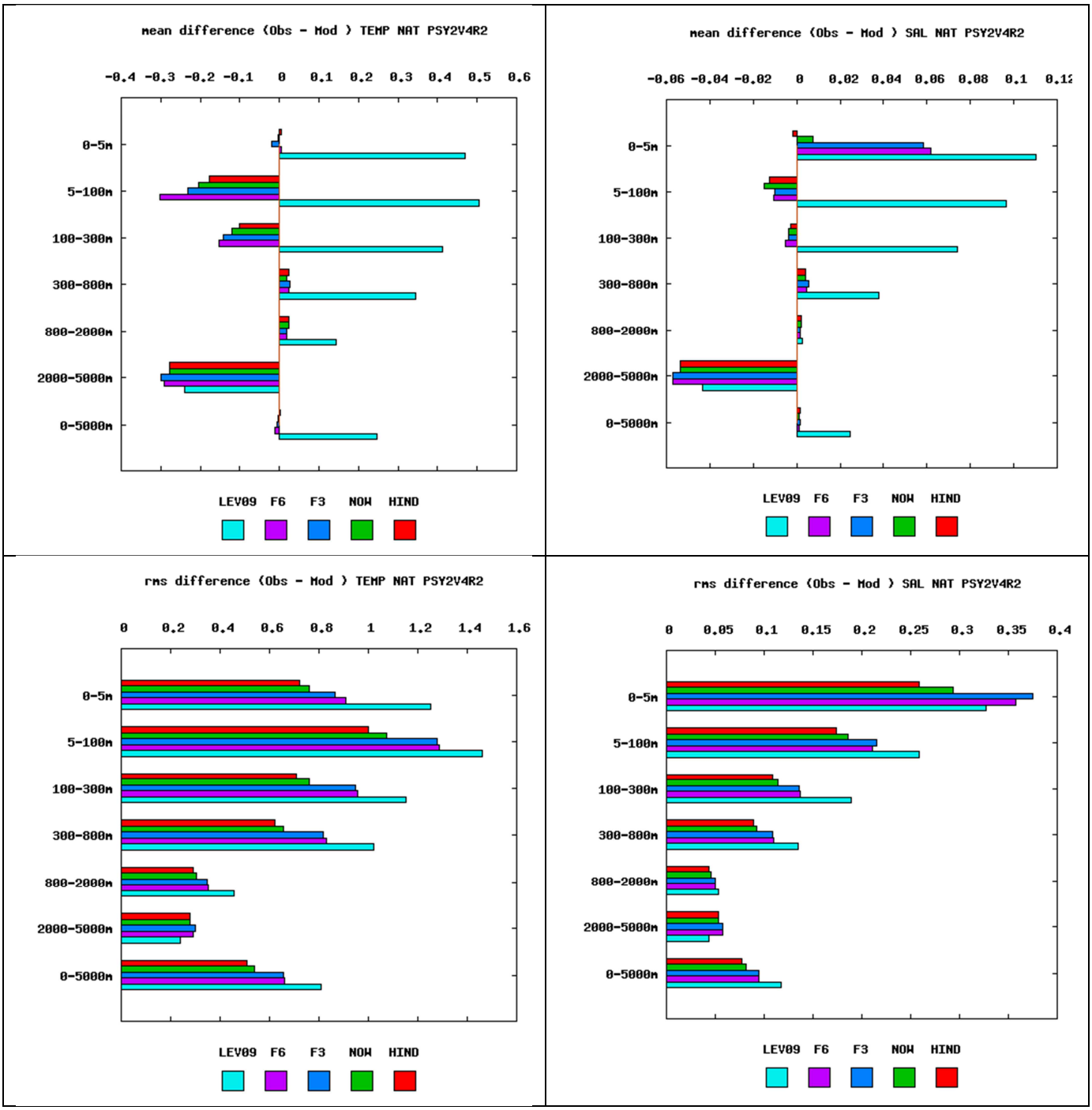

Figure 44: Accuracy intercomparison in the North Atlantic region for PSY2V4R2 in temperature (left panel) and salinity (right panel) between hindcast, nowcast, 3-day and 6-day forecast and WO09 climatology. Accuracy is measured by a mean difference (upper panel) and by a rms difference (lower panel) of temperatue and salinity with respect to all available observations from the CORIOLIS database averaged in 6 consecutive layers from 0 to 5000m. All statistics are performed for the JAS 2011 period. NB: average on model levels is performed as an intermediate step which reduces the artefacts of inhomogeneous density of observations on the vertical.

VI.2.2. Mediterranean Sea

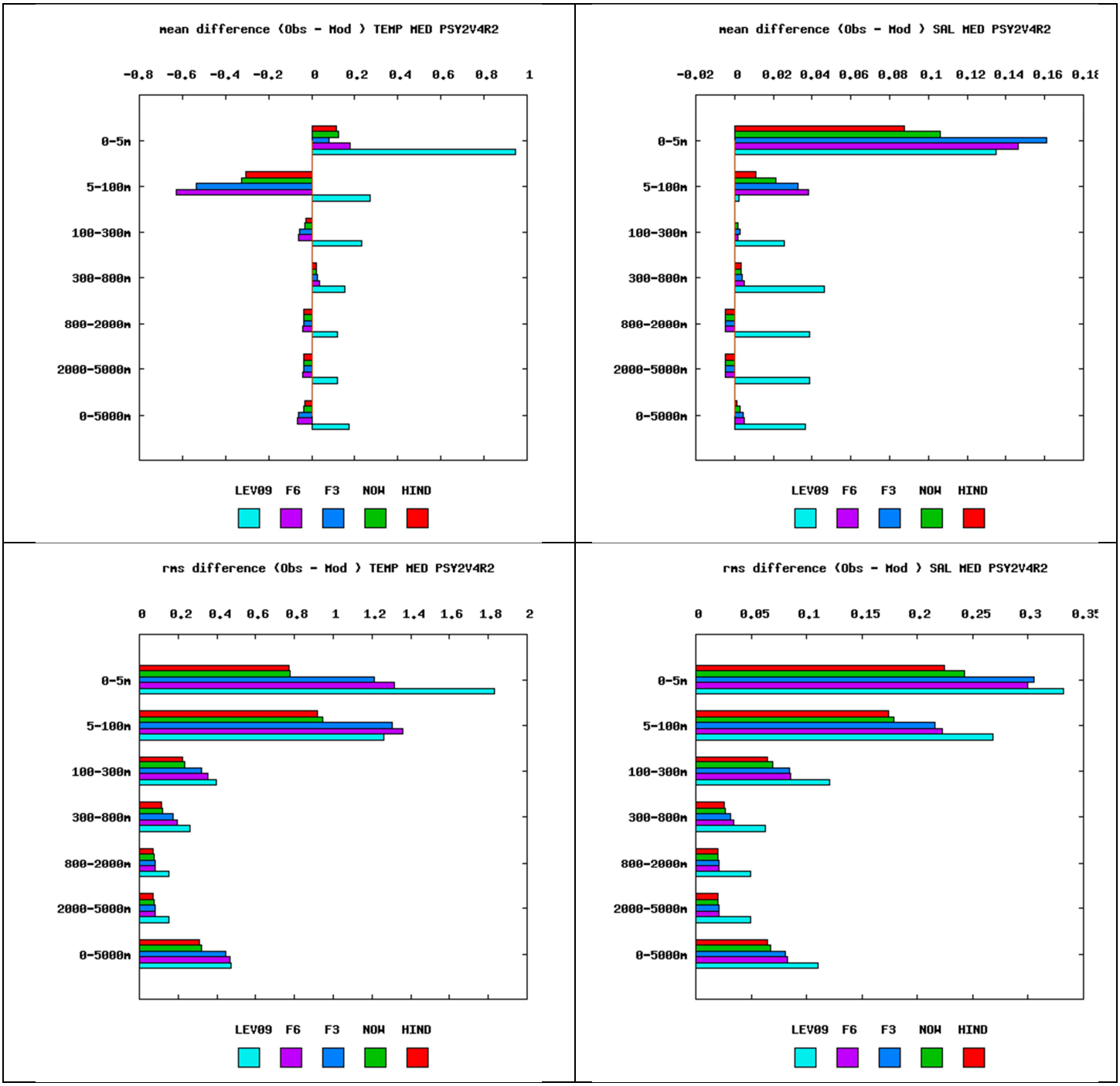

Figure 45: Accuracy intercomparison in the Mediterranean Sea region for PSY2V4R2 in temperature (°C, left column) and salinity (psu, right column) between hindcast, nowcast, 3-day and 6-day forecast and WO09 climatology. Accuracy is measured by a rms difference (lower panel) and by a mean difference (upper panel) with respect to all available observations from the CORIOLIS database averaged in 6 consecutive layers from 0 to 5000m. All statistics are performed for the JAS 2011 period. NB: average on model levels is performed as an intermediate step which reduces the artefacts of inhomogeneous density of observations on the vertical.

In the Mediterranean Sea (Figure 45) for mean differences, the PSY2V4R2 salinity and temperature forecast beat the climatology in the entire water column except in the 5-100m

layer for temperature and in the 0-100m layer for salinity. The temperature forecast in the Mediterranean is slightly more accurate at the 3-day range than at the 6-day range.

VI.2.3. Tropical Oceans, Indian, Global: what system do we choose in JAS 2011?

The best performing system in JAS 2011 in terms of water masses is PSY3V3R1 (and PSY2V4R2), even in the Tropical Atlantic as can be seen in Figure 46. This is not surprising when comparing to relatively sparse in situ measurements in very large ocean basin regions, and when we take into account that PSY4V1R3 has no bias correction for the moment. Nevertheless, the high resolution global PSY4V1R3 beats the climatology and is very promising in many regions, for instance in the Atlantic, the Indian ocean or the North Pacific. We also note that at all depth the error increases with forecast range, as could be expected, and that the 6-day forecast still beats the climatology.

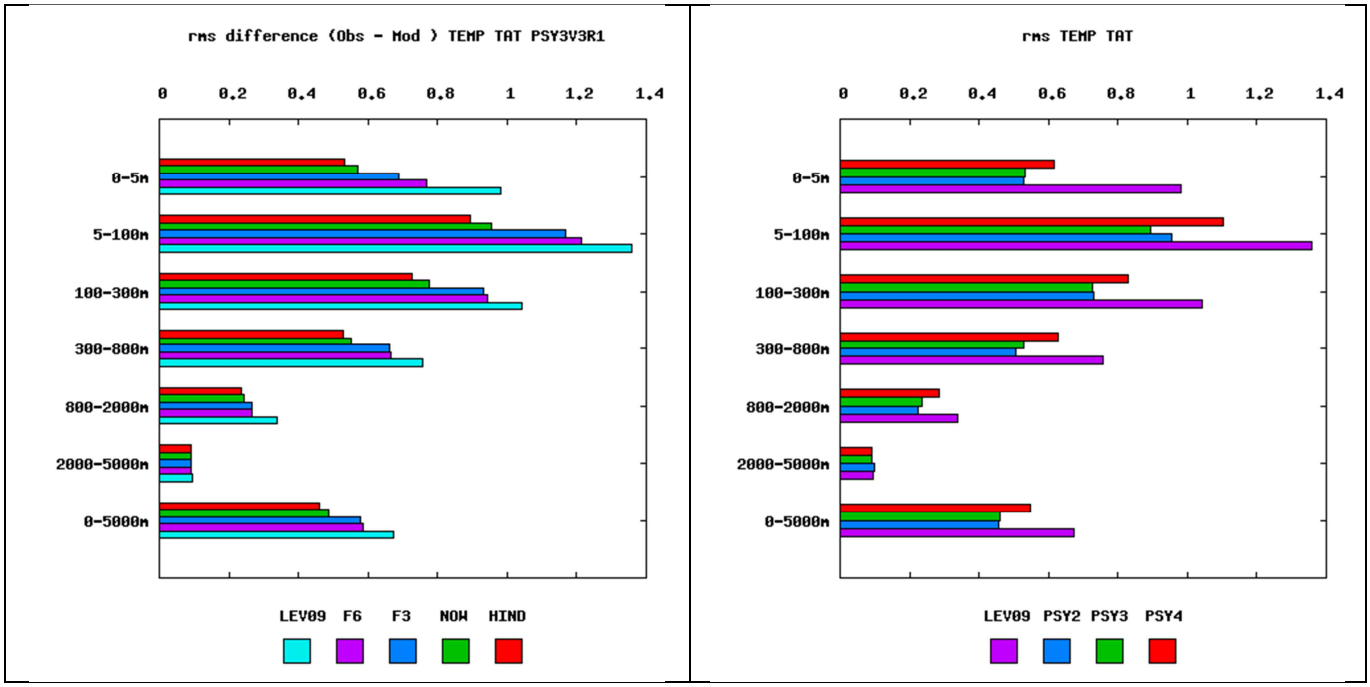

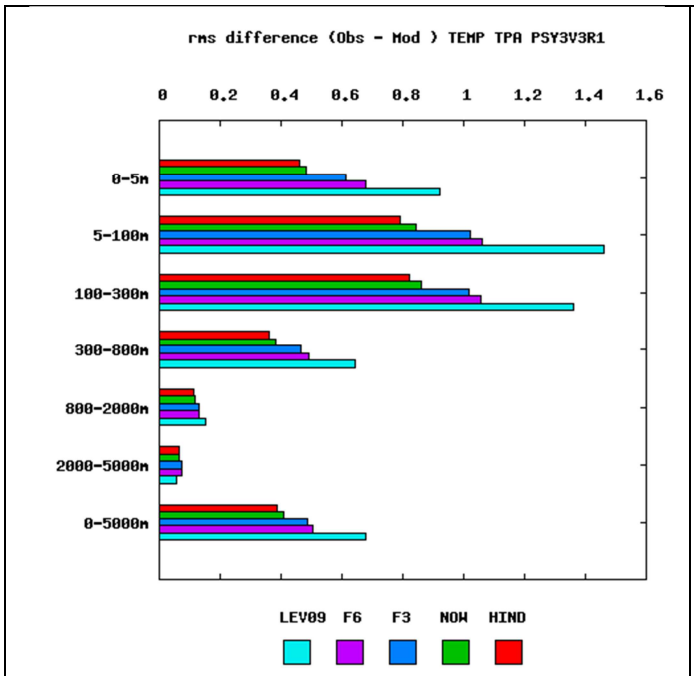
rms difference (Obs - Mod) TEMP TPA PSY3V3R1
0 0.2 0.4 0.6 0.8 1 1.2 1.4 1.6
0-5m
5-100m
100-300m
300-800m
800-2000m
2000-5000m
0-5000m
LEV09 F6 F3 NOW HIND

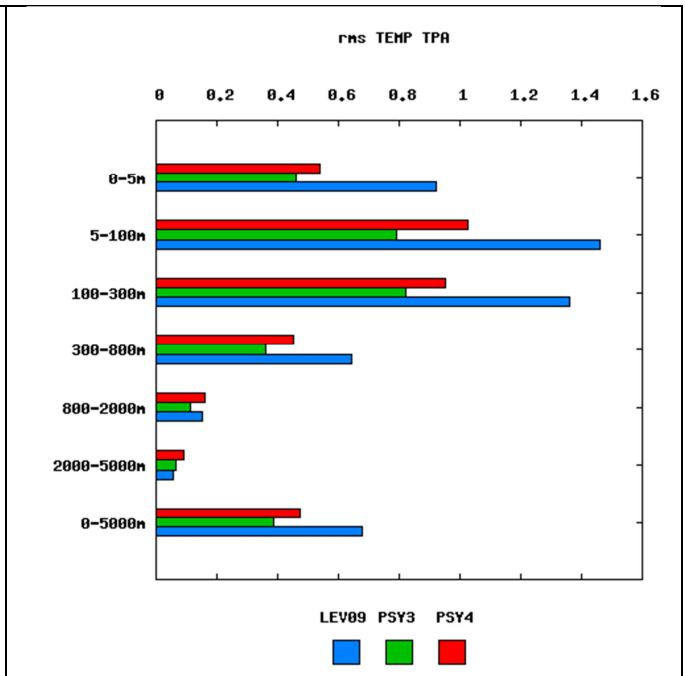
rms TEMP TPA
0 0.2 0.4 0.6 0.8 1 1.2 1.4 1.6
0-5m
5-100m
100-300m
300-800m
800-2000m
2000-5000m
0-5000m
LEV09 PSY3 PSY4

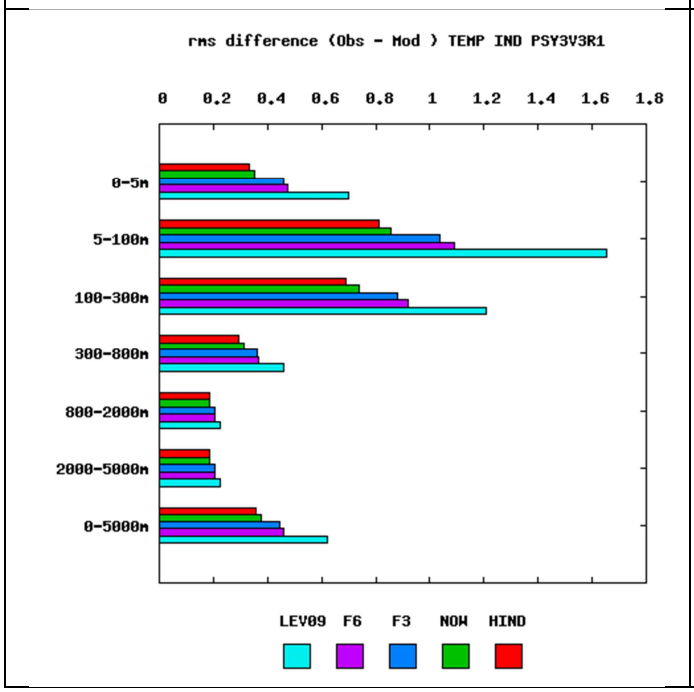
rms difference (Obs - Mod) TEMP IND PSY3V3R1
0 0.2 0.4 0.6 0.8 1 1.2 1.4 1.6 1.8
0-5m
5-100m
100-300m
300-800m
800-2000m
2000-5000m
0-5000m
LEV09 F6 F3 NOW HIND

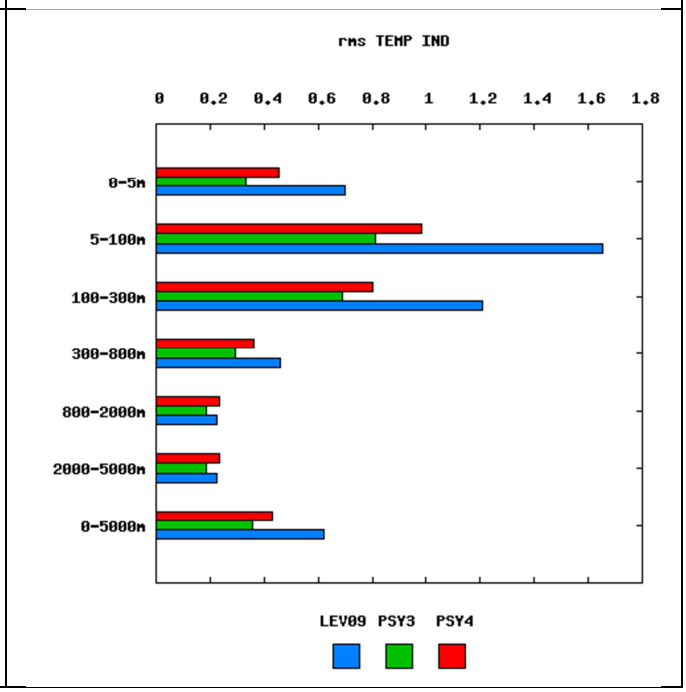
rms TEMP IND
0 0.2 0.4 0.6 0.8 1 1.2 1.4 1.6 1.8
0-5m
5-100m
100-300m
300-800m
800-2000m
2000-5000m
0-5000m
LEV09 PSY3 PSY4

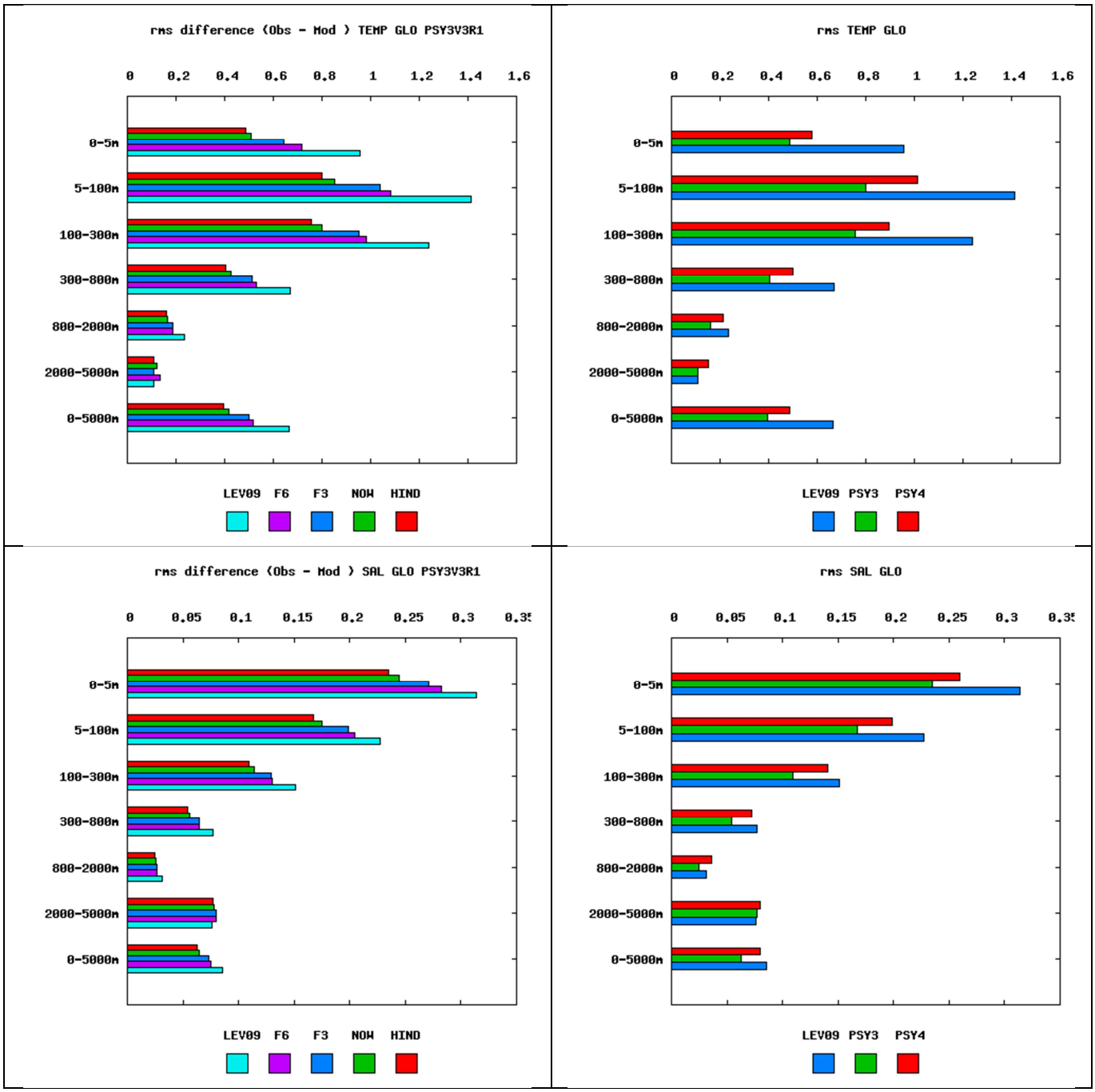

Figure 46: same as Figure 44 but for RMS statistics and for temperature (°C), PSY3V3R1 and PSY4V1R3 systems and the Tropical Atlantic (TAT), the Tropical Pacific (TPA) and the Indian Ocean (IND). The global statistics (GLO) are also shown for temperature and salinity (psu). The right column compares the analysis of the global ¼° PSY3 with the analysis of the global 1/12° PSY4 available at the end of June 2011.

I.1.1. Forecast skill scores

The Murphy Skill Score (see Equation 1) is described by Wilks, *Statistical Methods in the Atmospheric Sciences*, Academic Press, 2006. This score is close to 0 if the forecast is

equivalent to the reference. It is positive and aims towards 1 if the forecast is more accurate than the reference.

$$SS = 1 - \frac{\sum_{k=1}^{n}\left[\frac{1}{M}\sum_{m=1}^{M}\left(Forecast_m - Obs_m\right)^2\right]}{\sum_{k=1}^{n}\left[\frac{1}{M}\sum_{m=1}^{M}\left(Ref_m - Obs_m\right)^2\right]}$$

Equation 1

The Skill Score displayed on Figure 47 shows the added value of PSY3V3R1 forecast with respect to the climatology. All Mercator Ocean systems have a very good level of performance with respect to the climatology (see previous section).

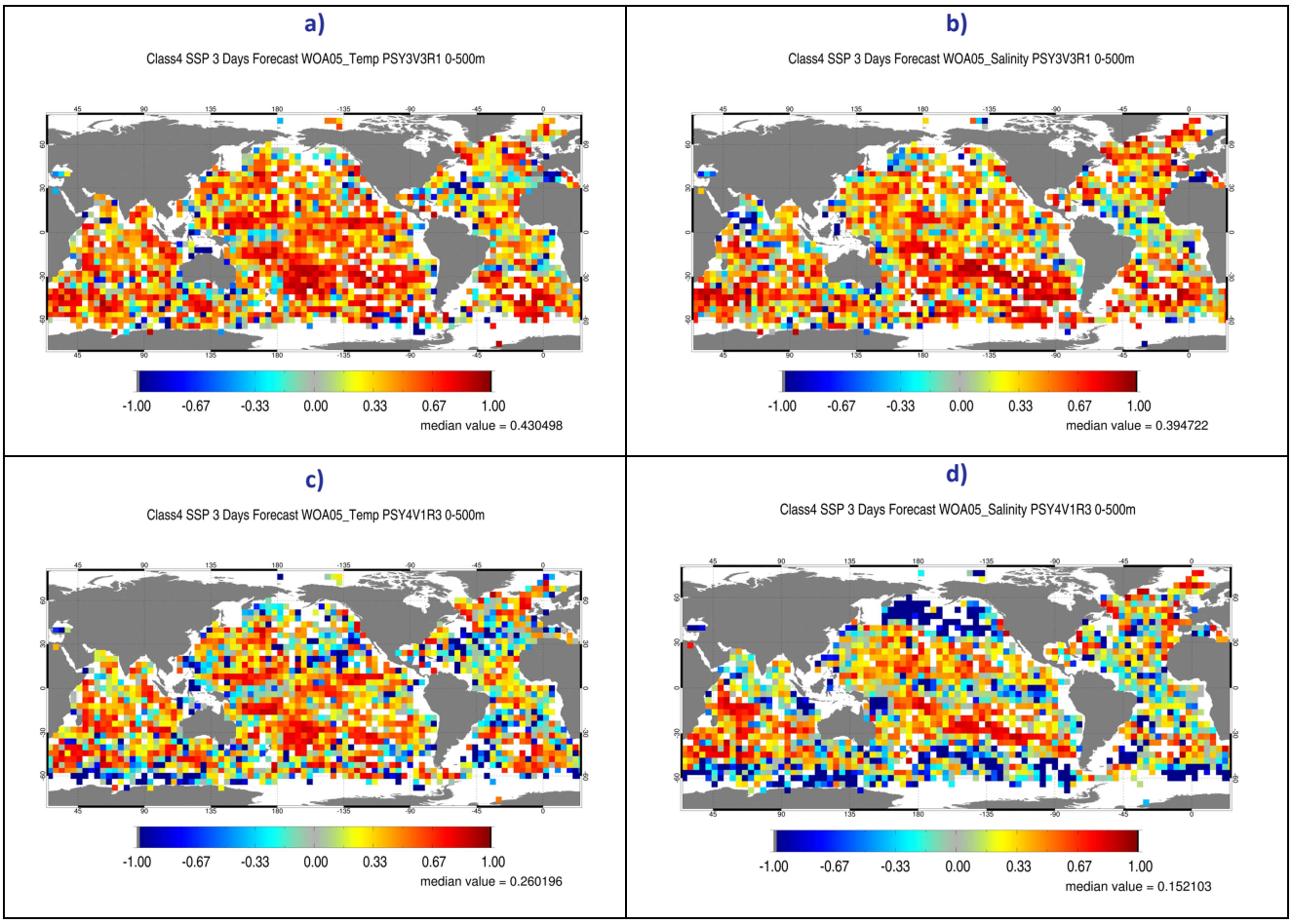

Figure 47 : Skill score in 4°x4° bins and in the 0-500m layer for temperature (left column) and salinity (right column). Yellow to red values indicate that the forecast is more accurate than the climatology. a), b) : PSY3V3R1; c), d) : PSY4V1R3.

When the reference is the persistence of the last analysis (Figure 48), the result is noisier and the model 3-day forecast seems to have skill at large scales in some regions in particular. In JAS 2011 these regions are essentially the Tropics, and the North Atlantic. When comparing forecast and persistence, PSY4V1R3 seems to have more skill in temperature than PSY3V3R1

this season. However, we notice that PSY3V3R1 is better than the climatology almost everywhere, whereas PSY4V1R3 is less accurate, especially near the poles in salinity.
This means that PSY3V3R1 is accurate on average, and the forecast is only locally more accurate than the persistence of the last analysis. On the contrary PSY4V1R3 accuracy has to be improved (in future versions it will benefit from bias correction and other updates). The ORCA12 model skill itself already displays encouraging results.

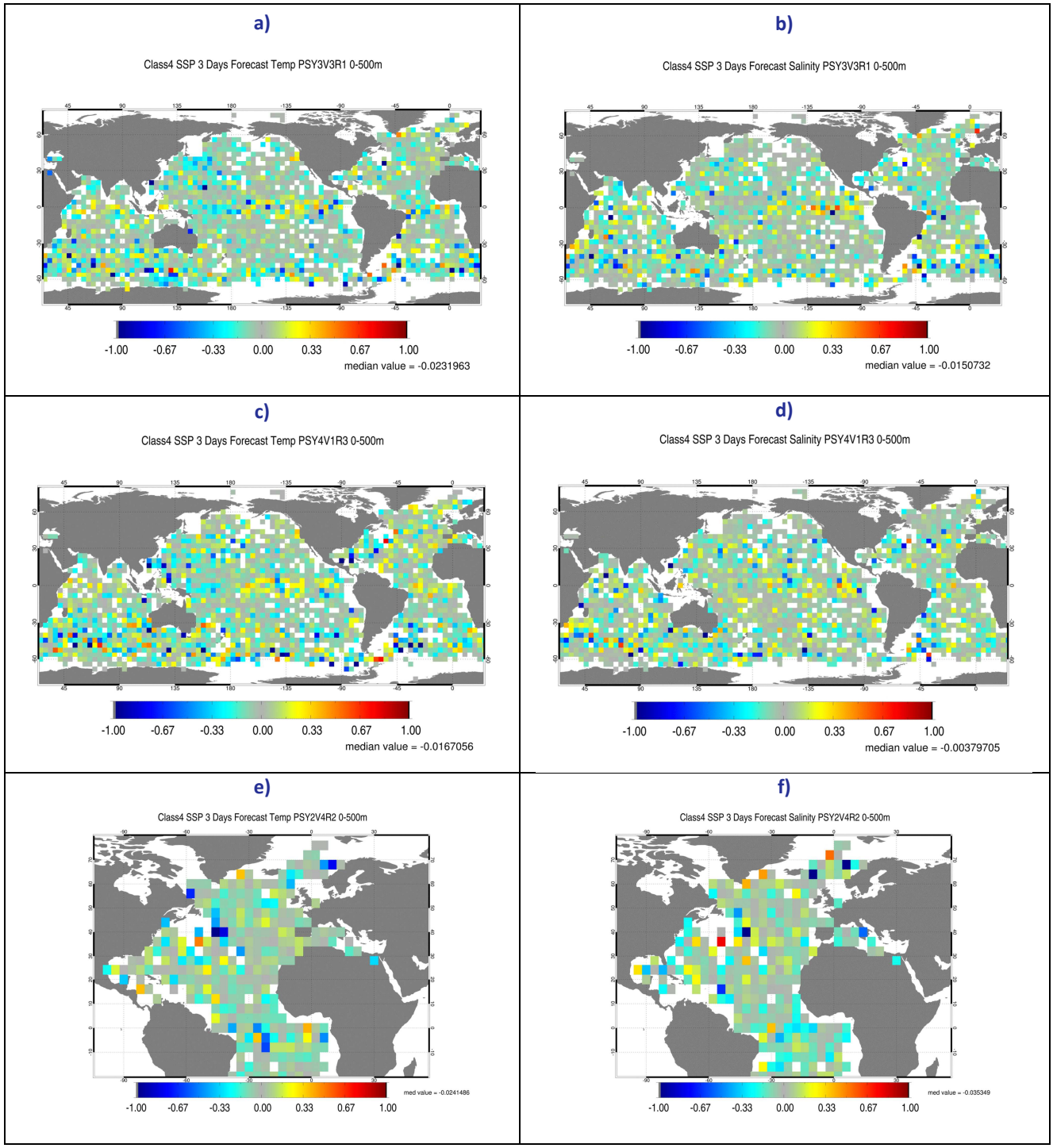

Figure 48: Skill score in 4°x4° bins and in the 0-500m layer for temperature (left column) and salinity (right column). Yellow to red values indicate that the forecast is more accurate than the persistence of the last analysis. a), b) : PSY3V3R1; c), d) : PSY4V1R3; e), f) : PSY2V4R2.

VI.3. Forecast verification: comparison with analysis everywhere

The PSY3V3R1 "forecast errors" illustrated by the sea surface temperature and salinity RMS difference between the forecast and the hindcast for all given dates of July-August-September 2011 are displayed in Figure 49. The values on most of the global domain do not exceed 1°C and 0.2 PSU. In regions of high variability like the western boundary currents, the Circumpolar current, Zapiola eddy, Agulhas current, Gulf Stream, Japan Sea and Kuroshio region the errors reach around 3°C or 0.5 PSU. The red spot visible on the SST map off California corresponds to an unrealistic local maximum of SST on July 20th, maybe due to an erroneous observation (under investigation). For SSS there is also a red spot in the Oman Sea due to erroneous data. For salinity, the error can exceed 1 PSU in regions of high runoff (Gulf of Guinea, Bay of Bengal, Amazon, Sea Ice limit) or precipitations (ITCZ, SPCZ).

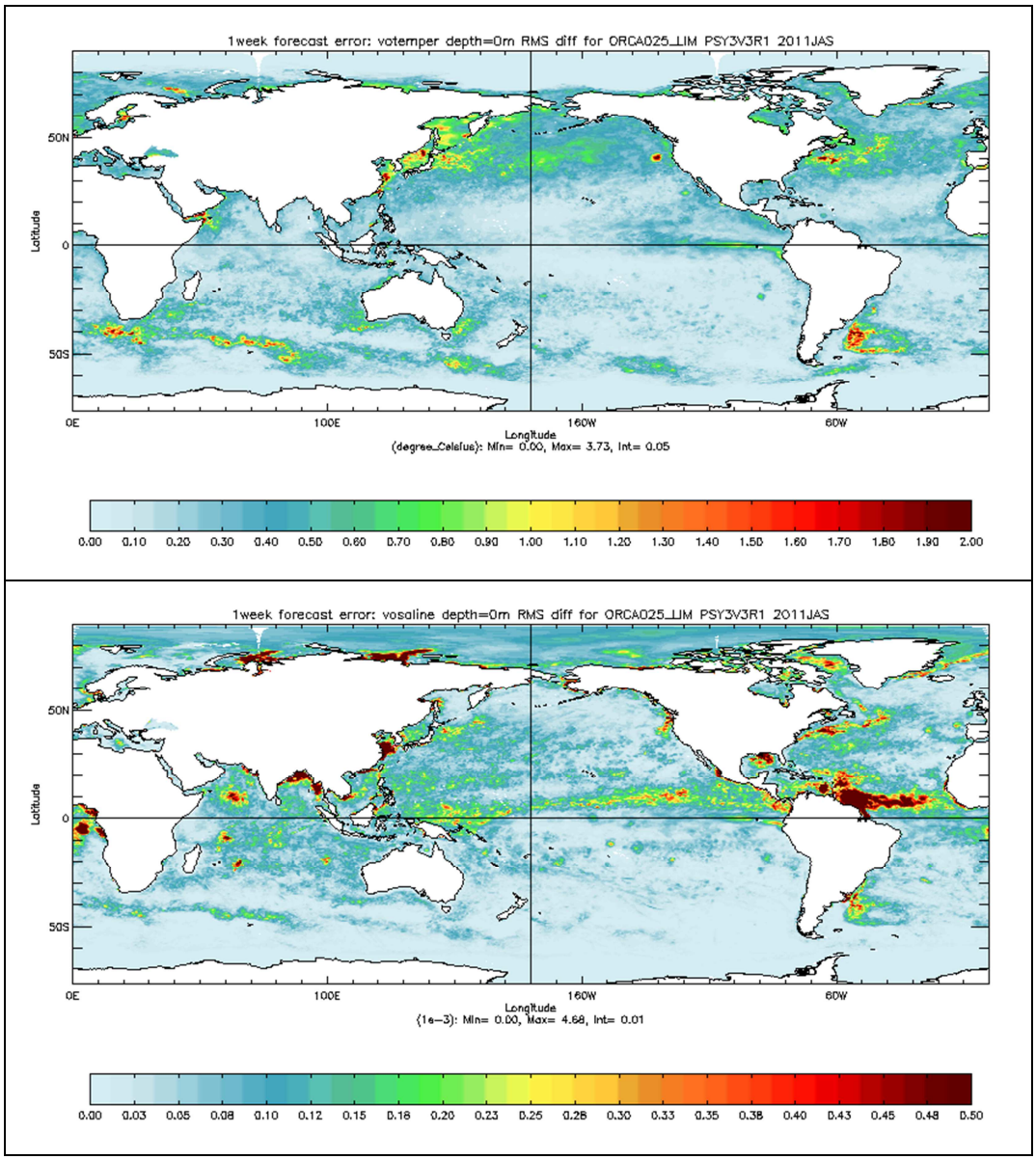

Figure 49: comparison of the sea surface temperature (°C, upper panel) and salinity (PSU, lower panel) forecast – hindcast RMS differences for the 1 week range for the PSY3V3R1 system.

II Monitoring of ocean and sea ice physics

II.1. Global mean SST and SSS

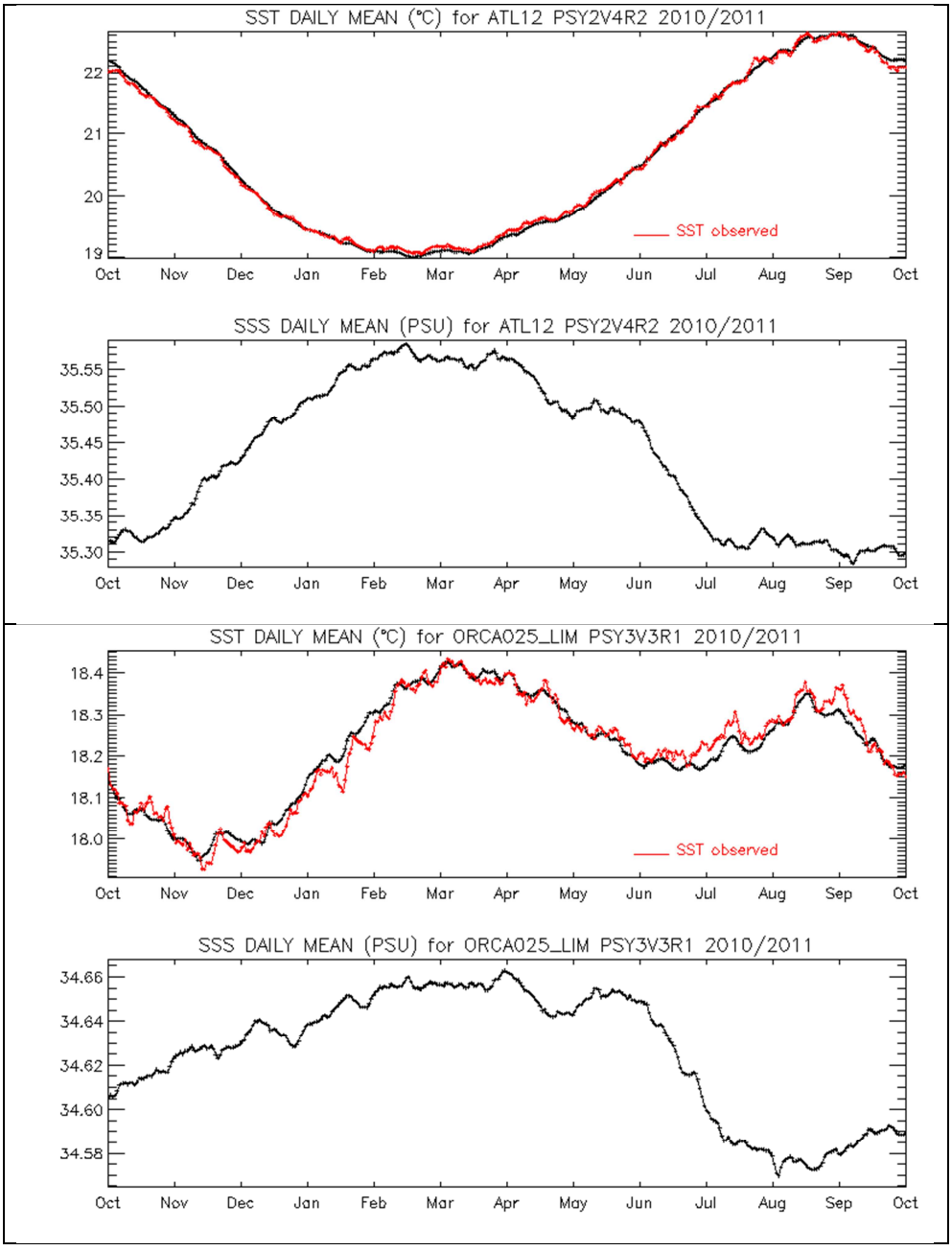

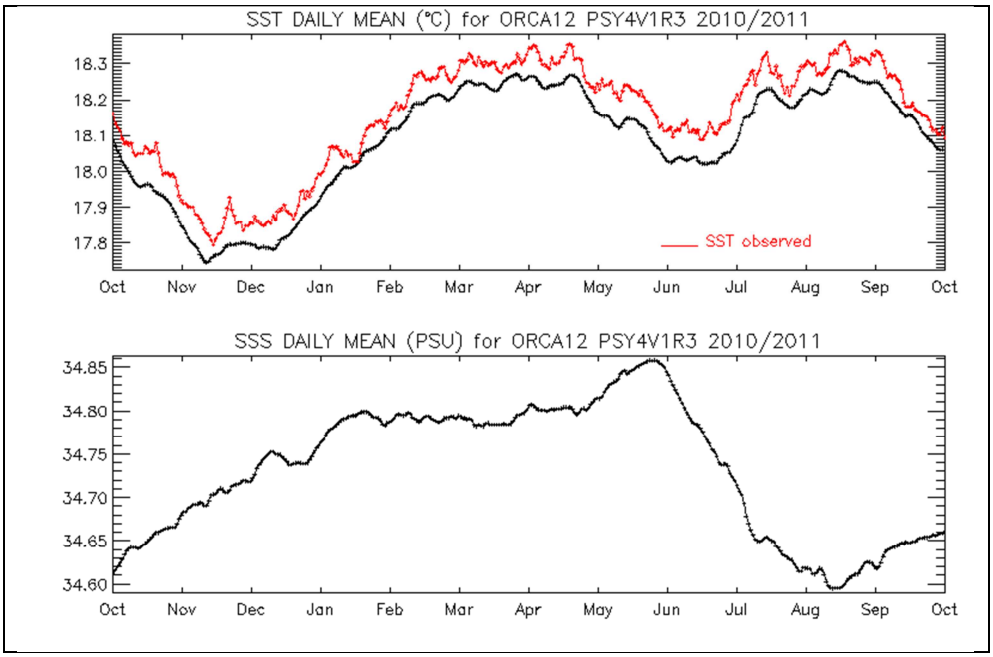

Figure 50: daily SST (°C) and salinity (psu) spatial mean for a one year period ending in JAS 2011, for Mercator Ocean systems (in black) and RTG-SST observations (in red). Upper: PSY2V4R2, middle: PSY3V3R1, lower: PSY4V1R3.

The spatial means of SST and SSS are computed for each day of the year, for PSY2V4R2, PSY3V3R1 and PSY4V1R3 systems. The mean SST is compared to the mean of RTG-SST on the same domain (Figure 50).
The biases visible during summer and autumn tend to disappear during winter and reappear in July 2011. The global mean of PSY4V1R3 SST is biased of about 0.1°C all year long, consistently with data assimilation scores of section V.1.2. This bias is mainly located in the tropics which are too cold on average. Paradoxically, local departures from RTG-SST are much stronger in PSY3V3R1 (more than 2°C at the peak of the seasonal bias) than in PSY4V1R3 (not shown).

II.2. Surface EKE

Regions of high mesoscale activity are diagnosed in Figure 51: Kuroshio, Gulf Stream, Niño 3 and 4 boxes in the central Equatorial pacific, Indian South Equatorial current, Zapiola eddy, Agulhas current, East Australian current, and Madagascar channel. PSY3V3R1 at ¼° and PSY4V1R3 at 1/12° are in very good agreement. EKE is generally higher in the high resolution PSY4V1R3 system, for instance in the Antarctic Circumpolar current and in the North West Pacific Ocean. Cyclonic activity is particularly intense in this season in West Indian Ocean, which contributes to form the great whirl visible in Figure 51 off Somalia. Drifters velocities measured in this area (see Figure 31) confirm this activity.

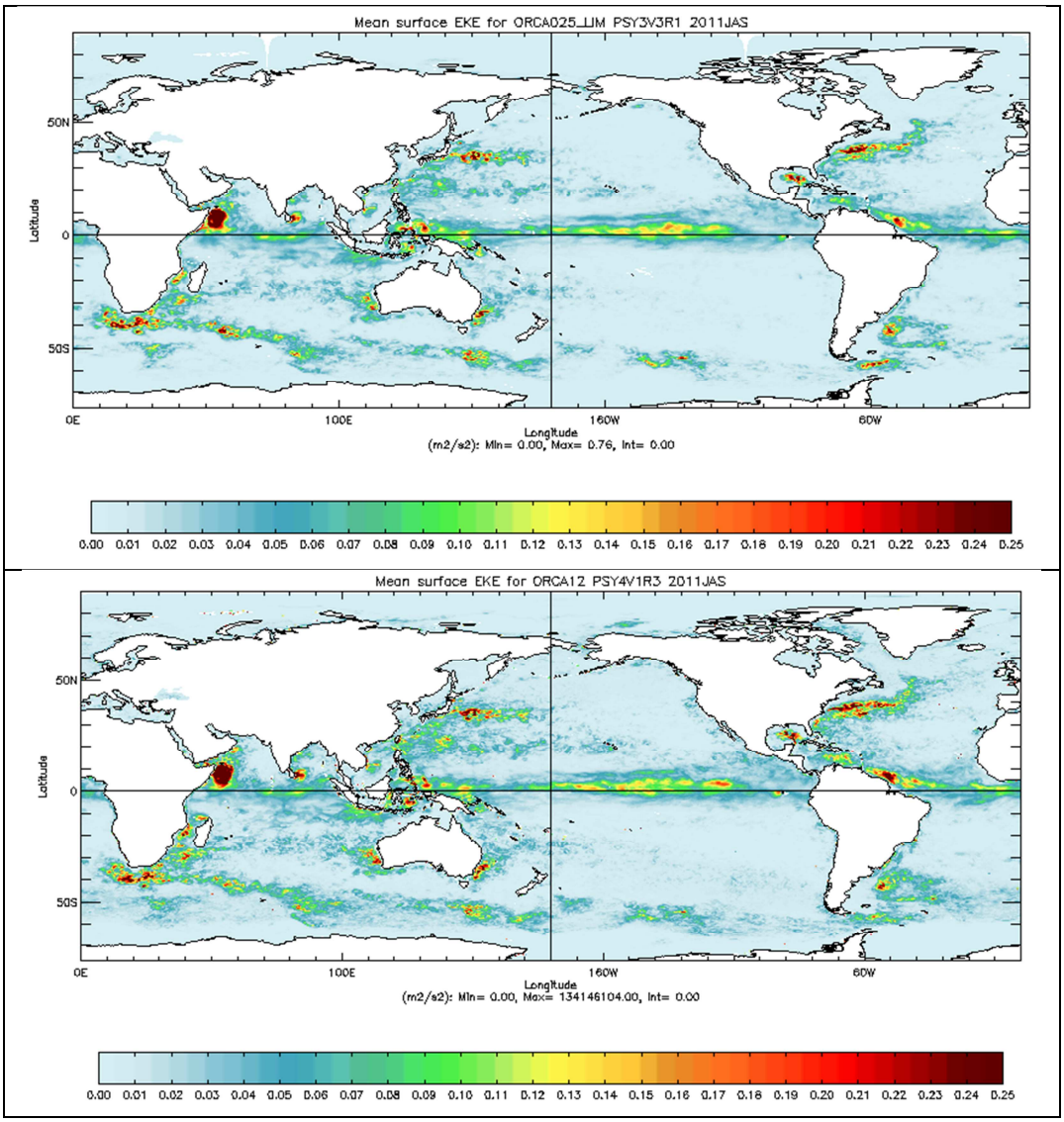

Figure 51: surface eddy kinetic energy EKE (m^2/s^2) for PSY3V3R1 (upper panel) and PSY4V1R3 (lower panel) for JAS 2011.

II.3. Mediterranean outflow

We notice in Figure52 a salty surface bias in PSY2V4R2 that may be an interannual signal, as no bias has been diagnosed comparing PSY2V4R2 to insitu observations (not shown). Sea surface temperature and salinity are less biased in PSY3V3R1 but vertical diffusion seems too strong looking at salinity. In PSY2V4R2 the Mediterranean outflow is too shallow. Consistently with Figure 29, the outflow is better reproduced by PSY3V3R1 than by PSY4V1R3.

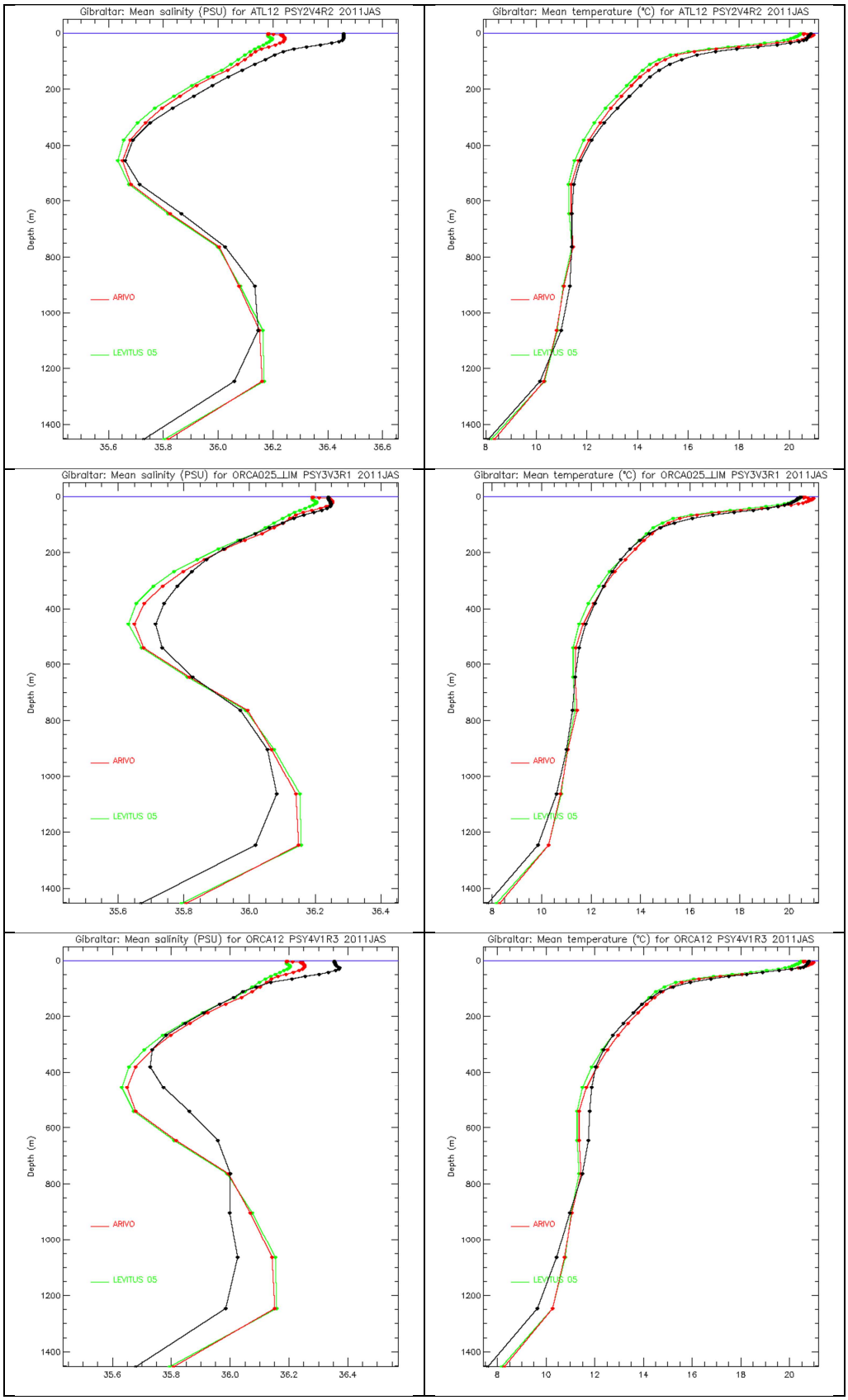

Figure52: Comparisons between mean salinity (left panel) and temperature (right panel) profiles in PSY2V4R2, PSY3V3R1 and PSY4V1R3 (from top to bottom, in black), and in the Levitus WOA05 (green) and ARIVO (red) climatologies.

II.4. Sea Ice extent and area

The time series of monthly means of ice area and ice extent (area of ocean with at least 15% sea ice) are displayed in Figure 53 and compared to SSM/I microwave observations. Both ice extent and area include the area near the pole not imaged by the sensor. NSIDC web site specifies that it is assumed to be entirely ice covered with at least 15% concentration. This area is 0.31 million square kilometres for SSM/I.

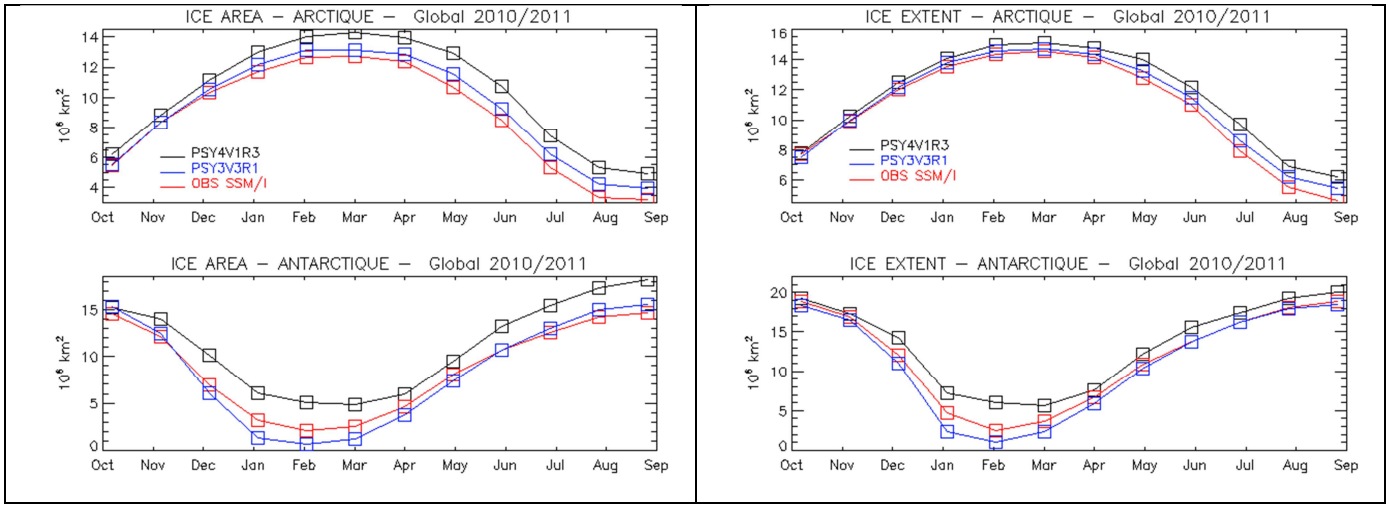

Figure 53: Sea ice area (left panel, 10^6 km2) and extent (right panel, 10^6 km2) in PSY3V3R1(blue line), PSY4V1R3 (black line) and SSM/I observations (red line) for a one year period ending in JAS 2011, in the Arctic (upper panel) and Antarctic (lower panel).

These time series indicate that sea ice products from PSY4V1R3 are generally less realistic than PSY3V3R1 products. This is partly due to the use of two different dynamics in the two models. PSY4V1R3 sea ice cover is overestimated throughout the year. The accumulation of multiannual Sea Ice in the Central arctic is overestimated by the models and especially by PSY4V1R3 all year long (see Figure 33). PSY3V3R1 ice area and extent are slightly underestimated in Antarctic and overestimated in Arctic, especially in summer. In boreal winter, PSY3V3R1 performs quite well, with respect to observations.

III R&D study: validation summary of the BIOMER system

A spin-up of three years (year 2002 repeated 3 times) is performed before beginning the PISCES simulation. The ocean physical forcing used is GLORYS1v1. It is based on the NEMO modelling platform with the general circulation model OPA on the horizontal ORCA025 grid (1/4°) and 50 vertical levels coupled with the LIM sea ice model. Daily ECMWF operational analyses with CLIO bulk formulation are used as atmospheric forcings. Assimilation of data is performed(Ferry et al. 2010): temperature, salinity and sea level data are assimilated with the SAM2v1 tool (Tranchant et al. 2008) which is an extended Kalman filter based on the SEEK approach (Brasseur and Verron, 2006). The Incremental Analysis Update (Bloom et al. 1996; Ourmières et al. 2006) is used to produce a shock-free simulation.

Biogeochemical simulation:

- Biogeochemical model: PISCES (Aumont, 2005) from NEMO 2.3
- Location: global ocean
- Period of hindcast: 2002 – 2008 with a spin-up of 3 years
- Resolution: 1°, 50 vertical levels
- Offline mode
- Initial conditions:
    - NO3, 02, PO4, Si: WOA 2001
    - DIC and Alkalinity: GLODAP climatology (preindustrial part)
    - Iron and DOC : no climatology available yet so we use a restart from a simulation of 3000 years
- Forcings:
    - River inputs: NO3, 02, PO4, Si and DIC
    - Dust deposition of Iron
    - Sediment mobilization of Iron

Physical simulation: reanalysis GLORYS1v1

- NEMO 1.09
- Data assimilation method: SAM2v1
- Resolution: ¼° (eddy-permitting), degraded to 1°
- 7-day averages
- Atmospheric forcings: ECMWF operational analysis (1-day averages) with the CLIO bulk formula used to calculate the atmospheric forcing function
- Ocean-sea ice model: LIM2
- Initial conditions for temperature and salinity: ARIVO climatologies
- Data assimilation method:
    - Extended Kalman filter based on the SEEK approach (Singular Evolutive Extended Kalman)
    - An Incremental Analysis Update (IAU) is used to reduce the spin-up effects after the analysis time
    - Assimilated observations: Sea Surface Temperature maps (daily NCEP RTG product at ½°), along track Sea Level Anomaly (provided by AVISO) associated with a Mean Dynamic Topography (RIOv5) and in situ temperature and salinity profiles (CORA-02 data base from the Coriolis data centre)

Modelled mean annual chlorophyll-a field (Figure 54a) shows a good agreement with satellite derived estimates at the global scale (Figure 54b). The large scale structures are well reproduced (e.g. double-gyres, Antarctic Circumpolar Current). The concentrations of

modelled chlorophyll are slightly too high. In the northern hemisphere, the double-gyres are correctly modelled, both in terms of chlorophyll-a magnitude and of latitudinal position of the transition zone between high productive waters to the North and oligotrophic waters to the South. This transition zone corresponds to the position of the Gulf Stream in the Atlantic Ocean and of the Kurushio in the Pacific Ocean. In the southern hemisphere, the subtropical gyres and the Antarctic Circumpolar Current are also well reproduced. At the equator, however, there are significant differences, with BIOMER_GLORYS1V1_BIO1 overestimating observed chlorophyll-a levels. Moreover, the tropical productive zone stretches too much over the subtropical gyres, and in particular east of the basins.

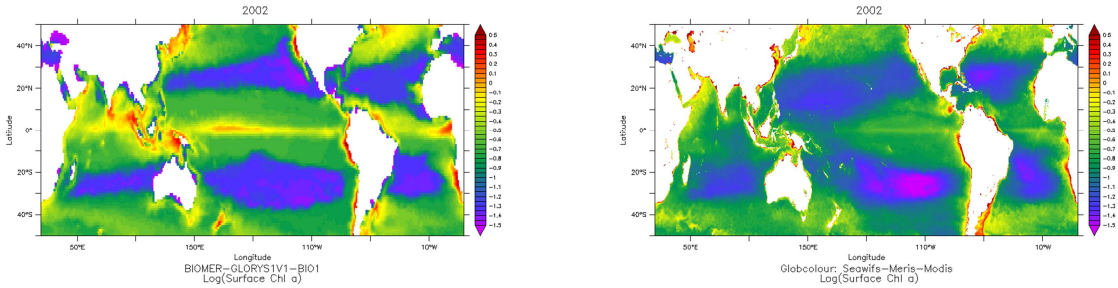

(a) (b)

Figure 54: Log10 of the chl-a annual mean in year 2002 at sea surface(mg Chl.m-3); (a) BIOMER_GLORYS1V1_BIO1; (b) Chl-a data from Seawifs – Meris – Modis sensors (Globcolour)

Coming back to the overestimation of chlorophyll-a levels simulated by BIOMER_GLORYS1V1_BIO1 at the equator, two potential underlying causes can be identified. (1) The model data misfit can be at least partly attributed to the "CLIO" aerodynamic bulk formulae. The later is at the origin of a cool bias in surface temperature leading to an overestimation of upwelling and hence nutrient input at the equator. (2) In BIOMER_GLORYS1V1_BIO1, there is moreover a bias introduced by the assimilation scheme. Preliminary outputs of gravimetric GOCE mission suggest that there are significant errors in the mean sea surface height (MSSH) used to assimilate the satellite altimetry. Regional biases in MSSH are typically of 100km and 5cm (resp. horizontal and vertical scales). The system response to the bias in MSSH is a bias in vertical velocity near the equator, thus introducing anomalous level of nitrate and in chlorophyll.

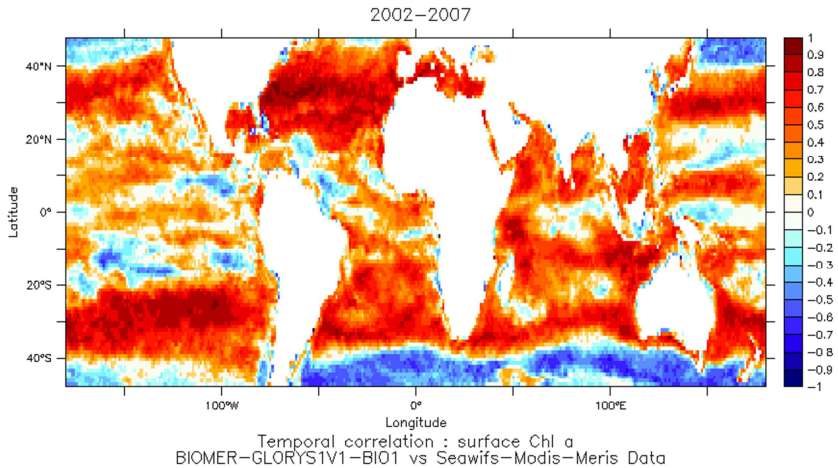

Figure 55: Temporal correlation between model and data

Figure 55 presents the temporal correlation of surface chlorophyll-a between model and data. It gives an assessment of the model capacity to represent the chlorophyll seasonal cycles. We can see that our model is doing a good job at mid-latitudes. At high latitudes, the low correlations reflect that the model does not manage to capture the timing of the bloom, there is a time-lag of about 2 months between model and data. At low latitudes, in the equatorial band, the seasonal cycle is not very marked so we expect lower correlations. Moreover, the low values in the low latitudes also reflect the too high chlorophyll concentrations predicted by the model.

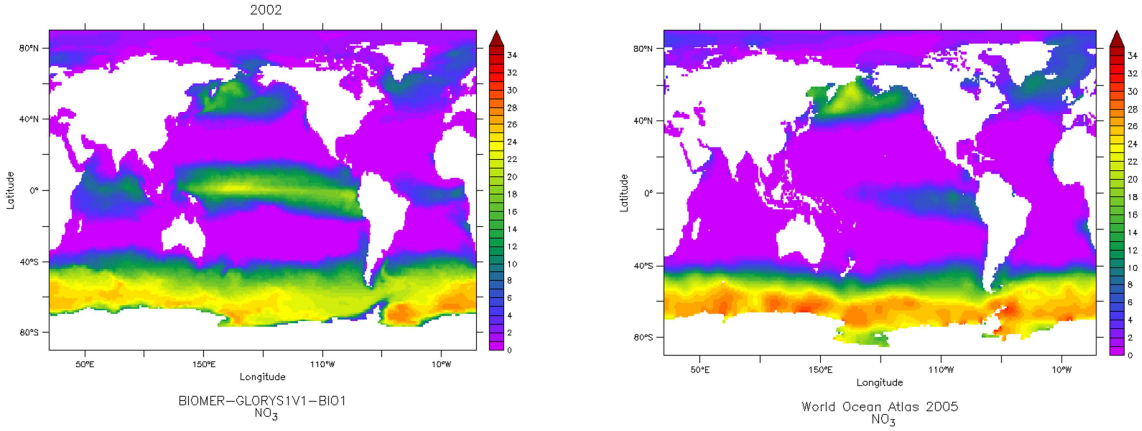

(a) (b)

Figure 56: Concentrations of nitrate in a 10 m deep layer (µmol N.L-1); (a) BIOMER_GLORYS1V1_BIO1; (b) WOA 2005

Figure 56 shows a global comparison of the nitrate concentration derived from data (WOA 2005) and predicted by the model. Globally, there is a good accordance between them except at the equator where the upwelling is too strong.

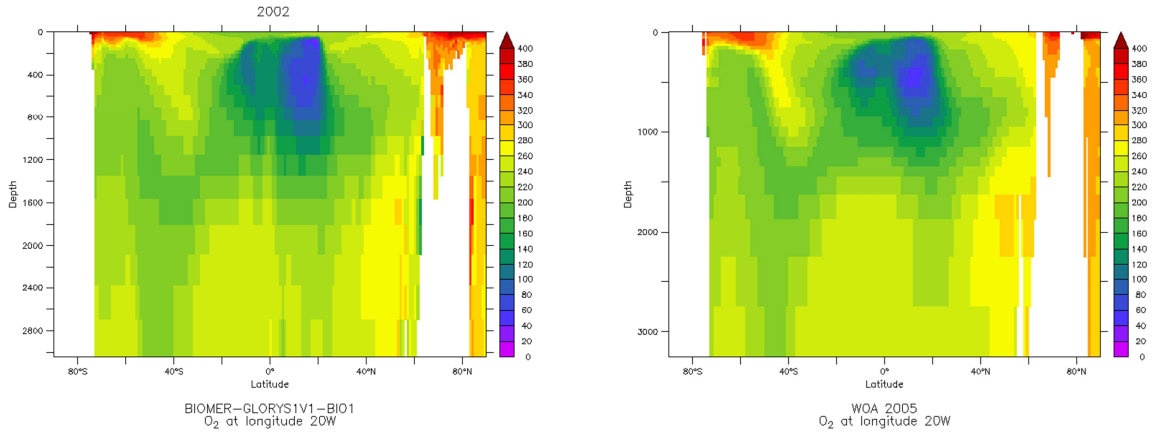

(a) (b)

Figure 57: Annual mean of O2 concentration in sea water in µmol.L-1. Section in the Atlantic Ocean at 20°W; (a) BIOMER_GLORYS1V1_BIO1; (b) WOA 2005

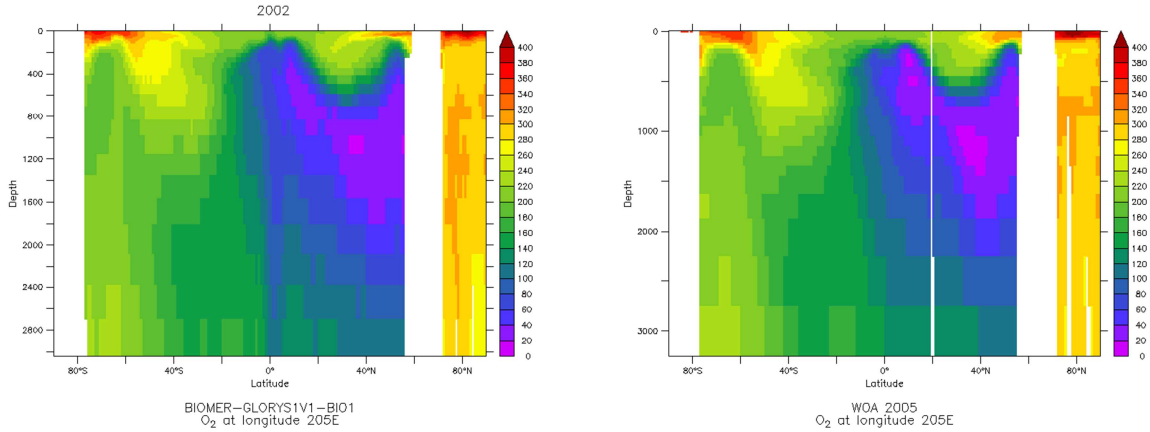

(a) (b)

Figure 58: Annual mean of O2 concentration in sea water in µmol.L-1. Section in the Pacific Ocean at 205°E; (a) BIOMER_GLORYS1V1_BIO1; (b) WOA 2005

Sections of oxygen concentration are presented on Figure 57 and Figure 58, respectively in the Atlantic Ocean and in the Pacific Ocean. They show a good adequacy between model and climatologies (annual mean).

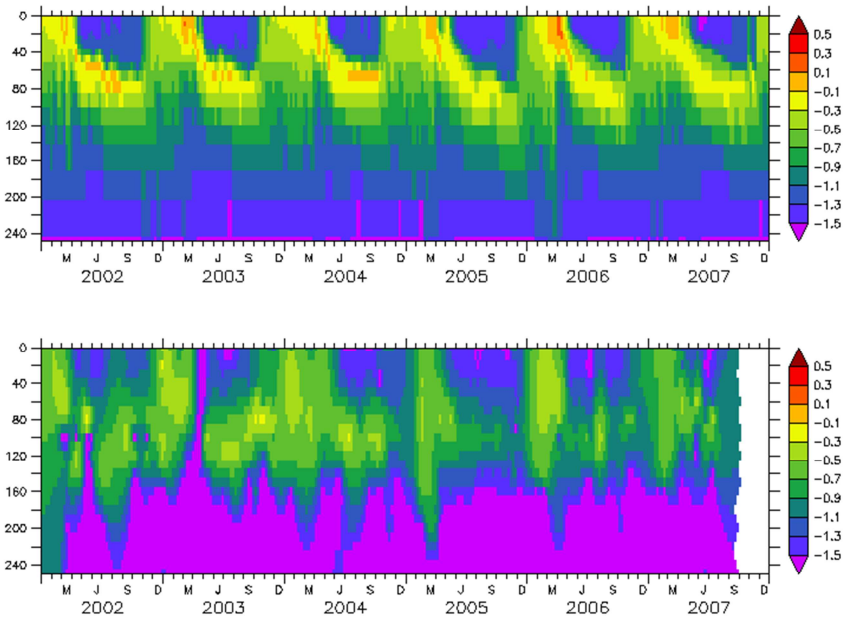

Figure 59: Log10 of the chlorophyll-a (mg Chl.m-3) at the BATS station during 2002-2007 period between 0 and 900 m depth ; (top) BIOMER_GLORYS1V1_BIO1; (bottom) bottle data

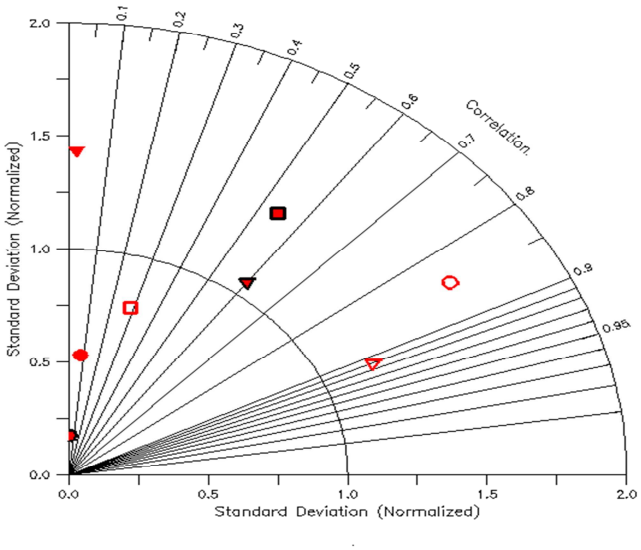

Figure 60: Normalized taylor diagram at the BATS station at sea surface (empty symbols), 100 m (filled symbols) and 200 m (filled symbols with black contour) depth for chlorophyll-a (circles), nitrates (squares) and oxygen (triangles) parameters.

The comparison between model output and biogeochemical data from eulerian observatories provides another way to assess the quality of our simulations. In complement with climatologies (e.g. nitrates), observed data time series constitute independent data against which the model can be validated. The BATS (Bermuda Atlantic Time-series Study) station is one of them. It is situated in the Sargasso Sea (31° 40'N, 64° 10'W). At this station, an exhaustive set of biogeochemical, along with physical variables are measured through bottle samples all year round (Steinberg et al. 2001). This sustained data collections are carried out monthly or even twice a month during bloom events. These data open the possibility for assessing the ability of the biogeochemical model to reproduce the seasonal and interannual variability of the ecosystem. Moreover, they give a valuable insight of the ocean biogeochemical state at a given location characteristic of a particular large-scale biogeographic region (Longhurst, 1998).

BATS is situated in the western North Atlantic subtropical gyre, in a highly-turbulent region, between the Gulf Stream (north) and the North Atlantic equatorial current (Steinberg et al. 2001). BATS is characterized by a deep mixed-layer in winter in which nutrients are injected by entrainment and immediately consumed by phytoplankton. In summer, after spring restratification, nutrients are rapidly depleted and phytoplankton declines in the shallow mixed-layer. A subsurface chlorophyll maximum develops at the base of the mixed layer.

Figure 59 (bottom) presents the concentration of chlorophyll-a as a function of depth and time measured at the BATS station between 2002-2007. It illustrates the seasonal cycle of phytoplankton. Figure 59 (top) shows the results of BIOMER_GLORYS1V1_BIO1. The seasonal cycle is in general well reproduced by the models. BIOMER_GLORYS1V1_BIO1 succeeds well in capturing the interannual variability as demonstrated by the deepening of the mixed-layer in summer 2005. However, the model predicts spring blooms that are not present in the observations. This is due to the nutricline that is too shallow (valid for nitrates, silicates, phosphates) in our simulations.

Variable	Observations	BIOMER	Error (%)
Chlorophyll	Mean = 0.323 mg/m^3 Std = 0.516 mg/m^3	Mean = 0.389 mg/m^3 Std = 0.451 mg/m^3	+20%
Dissolved oxygen	Mean = 277.52 µmol/L Std = 65.794 µmol/L	Mean = 281.35 µmol/L Std = 65.127 µmol/L	+1%
Nitrates	Mean = 6.841 µmol/L Std = 9.179 µmol/L	Mean = 7.091 µmol/L Std = 8.303 µmol/L	+4%
Phosphates	Mean = 0.675 µmol/L Std = 0.596 µmol/L	Mean = 0.721 µmol/L Std = 0.553 µmol/L	+7%

Table 5: Mean and standard deviation values over the whole GLO domain in 2002 at sea surface computed for model and observations on a 1° regular grid.

Figure 60 is a Taylor diagram, allowing to sum up a few basic statistics (standard deviation, error RMS and temporal correlation) performed on the model and data, here for three key-variables of the system: chlorophyll-a, nitrate and oxygen at three different depth of the water column: surface, 100 m and 200 m. It shows a good data – model correlation at sea surface for oxygen and chlorophyll-a. For nitrates, at sea surface, the correlation is not good, but it is not surprising because nitrates are quasi-exhausted during all year at surface. The concentrations are almost negligible. However, the corresponding standard deviation is close to data. It shows that their magnitudes of variations are similar. The statistical scores are lower at 100 m and 200 m depth, because there is a shift between model and observed nitracline.

This first calibration phase revealed a good accordance at large scale between annual mean fields from our model and from observations. The large scale structures corresponding to specific biogeographic regions (double-gyres, ACC, etc) are well reproduced. However, there are serious discrepancies in the tropical band. This problem has been thoroughly studied and is attributed to a bias in the Mean Dynamic Topography which is combined to Sea Level Anomalies in the assimilation process. This induces overestimated vertical velocities which are the source of anomalous levels of nitrates in equatorial shallow waters.Table 5 shows a comparison of the global mean and the global standard deviation for the main variables: Chl-a, O2, NO3, PO4 (computed for year 2002 at sea surface). It illustrates the global overestimation of our model and especially of the chlorophyll. This reflects both the problem of equator where there is a too strong biogeochemical activity and a global tendency of our model to overestimate the chlorophyll. O2, however, is very close to climatological estimation. This is due to the intrinsic link of O2 concentration with temperature and salinity (and especially at sea surface), which are constrained to be as close as possible from observations via the assimilation process.
Concerning the temporal monitoring, our model manages well to reproduce the seasonal cycle in most part of the ocean (spring bloom at mid-latitudes, two monsoon blooms in the Indian Ocean etc.). However, the timing of the blooms is not yet in phase with observations (a one or two-month lag). It will need more work and in particular we will have to improve the photo-adaptive model of Geider et al. (1996, 1998). We also detected a shift in the depth of the nutricline between model and observations, which induces a too strong spring bloom (between 30° and 40°N in the west part of the Atlantic Ocean).

In conclusion, the model displays a good behavior considering the present state-of-the-art of biogeochemical modeling at the global scale (Yool et al., 2011, Ford et al., in prep). In the near future, we will improve the physical part, with a focus on the MDT bias at the equator and we will work on the biogeochemical parameterization to improve the timing of the bloom and the magnitude of chlorophyll concentrations.

IV Annex A

IV.1. References

Grodsky S. A., Lumpkin R., Carton J. A. (2011) Spurious trends in global surface drifter currents Geophysical Research Letters, 38(L10606) doi:10.1029/2011GL047393

Poulain, P. M., R. Gerin, E. Mauri, and R. Pennel (2009), wind effects on drogued and undrogued drifters in the eastern Mediterranean, J. Atmos. Oceanic Technol., 26, 1144-1156, doi:10.1175/2008JTECHO618.1

Antoine D., Morel A. 2006: Oceanic primary production: 1. Adaptation of a spectral light-photosynthesis model in view of application to satellite chlorophyll observations. Global Biogeochemical Cycles. 10 (1): 43-55

Aumont O. 2005: PISCES biogeochemical model. Unpublished report.

Aumont O., Orr, J.C., Jamous, D., Monfray, P., Marti, O., and Madec, G. 1998: A degradation approach to accelerate simulationsto steady-state in a 3-D tracer transport model of the global ocean. Climate Dynamics. 14: 101-116.

Aumont, O. and Bopp, L. 2006: Globalizing results from ocean in situ iron fertilization studies. Global Biogeochem. Cycles. 20 (2):10–1029.
Behrenfeld M., Falkowski P. 1997: Photosynthetic rates derived from satellite-based chlorophyll concentration. Limnol. Oceanogr. 42 (1):1-20

Bloom, S.C., Takacs, L.L., Da Silva, A.M. and Ledvina, D. 1996 : Data assimilation using incremental analysis updates. MonthlyWeather Review. 1265-1271.

Bopp L., Aumont, O., Cadule, P., Alvain, S. and Gehlen, M. 2005: Response of diatoms distribution to global warming andpotential implications: A global model study. Geophys. Res. Lett.. 32, L19606, doi:10.1029/2005GL023653.

Brasseur, P. and Verron, J. 2006 : The SEEK filter method for data assimilation in oceanography: a synthesis. Ocean Dynamics.56 (5): 650-661

Conkright, M.E., Locarnini, R.A., Garcia, H.E., O'Brien, T.D., Boyer, T.P., Stephens, C. and Antonov, J.I. 2002: WorldOcean Atlas2001: Objective Analyses, Data Statistics, and Figures, CD-ROM Documentation. National Oceanographic DataCenter, SilverSpring, MD, 17 pp.

Elmoussaoui A., Perruche C., Greiner E., Ethé C. and Gehlen M. 2011 : Integration of biogeochemistry into MercatorOcean system. Mercator Ocean Newsletter #40, January 2011, http://www.mercator-ocean.fr/fre/actualites-agenda/newsletter/newsletter-Newsletter-40-Les-modeles-numeriques-des-ecosystemes-MyOcean

Ferry, N., , L. Parent, G. Garric, B. Barnier, N. C. Jourdain and the Mercator Ocean team, 2010: Mercator Global Eddy PermittingOcean Reanalysis GLORYS1V1: Description and

Results, Mercator Ocean Newsletter #36, January 2010, http://www.mercator.eu.org/documents/lettre/lettre_36_en.pdf

Ford DA, Edwards KP, Lea D, Barciela RM, Mertin MJ, Demaria J. 2011: Assimilating GlobColour ocean colour data into a pre-operational model. in prep.

Foreman, M.G.G., "Manual for tidal heights analysis and prediction," Institute of Ocean Sciences, Pacific Marine Science Report 77-10, Patricia Bay, Sidney, B.C., 1977.

Gehlen, M., Bopp, L., Emprin, N., Aumont, O., Heinze, C. and Ragueneau, O. 2006: Reconciling surface ocean productivity,export fluxes and sediment composition in a global biogeochemical ocean model. Biogeosciences. 1726-4189/bg/2006-3-521,521-537.

Gehlen, M., Gangstø, R., Schneider, B., Bopp, L., Aumont, O. and Ethé, C. 2007: The fate of pelagic CaCO3 production in a highCO2 ocean: A model study. Biogeoscience., 4: 505-519.

Geider M.J., MacIntyre H.L., Kana T.M. 1996: A dynamic model of photoadaptation in phytoplankton. Limnol. Oceanogr. 41: 1-15

Geider M.J., MacIntyre H.L., Kana T.M. 1998: A dynamic regulatory model of phytoplanktonic acclimation to light, nutrients, and temperature. Limnol. Oceanogr. 43, 679-694

Grodsky S. A., Lumpkin R., Carton J. A. (2011) Spurious trends in global surface drifter currents Geophysical Research Letters, 38(L10606) doi:10.1029/2011GL047393
Karl D., Lukas R. 1996: The Hawaii Ocean Time-series (HOT) program: Background, rationale and field implementation. Deep-Sea Research II. 43 (2-3): 129-156

Key, R. M., Kozyr, A., Sabine, C.L., Lee, K., Wanninkhof, R., Bullister, J.L., Feely, R.A., Millero, F.J., Mordy, C., and Peng, T.-H.2004: A global ocean carbon climatology: Results from Global Data Analysis Project (GLODAP). Global Biogeochem. Cycles. 18.GB4031, doi:10.1029/2004GB002247.

Longhurst, A. 1998: Ecological geography in the sea. Academic Press.

Ourmières Y., Brankart J.M., Berline L., Brasseur P. and Verron J. 2006: Incremental Analysis Update implementation into asequential ocean data assimilation system. Journal of Atmospheric and Oceanic Technology, vol 23: 1729-1744.

Schneider, B., Bopp, L., Gehlen, M., Segschneider, J., Frölicher, T.L., Cadule, P., Friedlingstein, P., Doney, S.C., Behrenfeld M.J.and Joos, F. 2008: Climate-induced interannual variability of marine primary and export production in three global coupled climatecarbon cycle models. Biogeosciences. 5: 597-614

Steinacher, M., Joos, F., Frölicher, T.L., Bopp, L., Cadule, P., Cocco, V., Doney, S.C., Gehlen, M., Lindsay, K., Moore, J.K.,Schneider, B., and Segschneider, J. 2010: Projected 21st century decrease in marine productivity: a multi-model analysis.Biogeoscience. 7: 979-1005.

Steinberg, D.K., Carlson, C.A., Bates, N.R., Johnson, R.J., Michaels, A.F. and Knapp, A.H. 2001: Overview of the US JGOFS Bermuda Atlantic Time-series Study (BATS): a decade-scale look at ocean biology and biogeochemistry. Deep-Sea Research II 48:1405-1447

Tagliabue, A., Bopp, L., Dutay, J.-C., Bowie, A.R., Chever, F., Jean-Baptiste, Ph., Bucciarelli, E., Lannuzel, Remenyi, D.T.,Sarthou, G., Aumont, O., Gehlen, M. and Jeandel, C. 2010: On the importance of hydrothermalism to the oceanic dissolved ironinventory. Nature Geoscience. 3: 252 – 256, doi:10.1038/ngeo818.

Yool A., Popova E.E., Anderson T.R. 2011: MEDUSA-1.0: a new intermediate complexity plankton ecosystem model for the global domain

IV.2. Table of figures

V Annex B

V.1. Maps of regions for data assimilation statistics

V.1.1. Tropical and North Atlantic

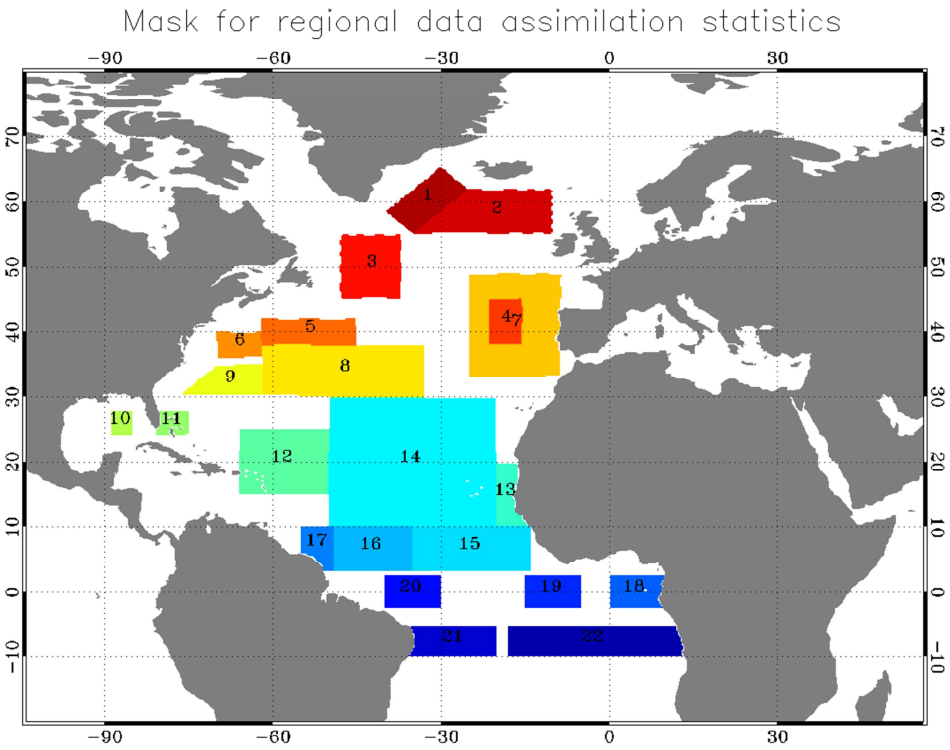

1	Irminger Sea
2	Iceland Basin
3	Newfoundland-Iceland
4	Yoyo Pomme
5	Gulf Stream2
6	Gulf Stream1 XBT
7	North Medeira XBT
8	Charleston tide
9	Bermuda tide
10	Gulf of Mexico
11	Florida Straits XBT
12	Puerto Rico XBT
13	Dakar
14	Cape Verde XBT
15	Rio-La Coruna Woce
16	Belem XBT
17	Cayenne tide
18	Sao Tome tide
19	XBT - central SEC
20	Pirata
21	Rio-La Coruna
22	Ascension tide

V.1.2. Mediterranean Sea

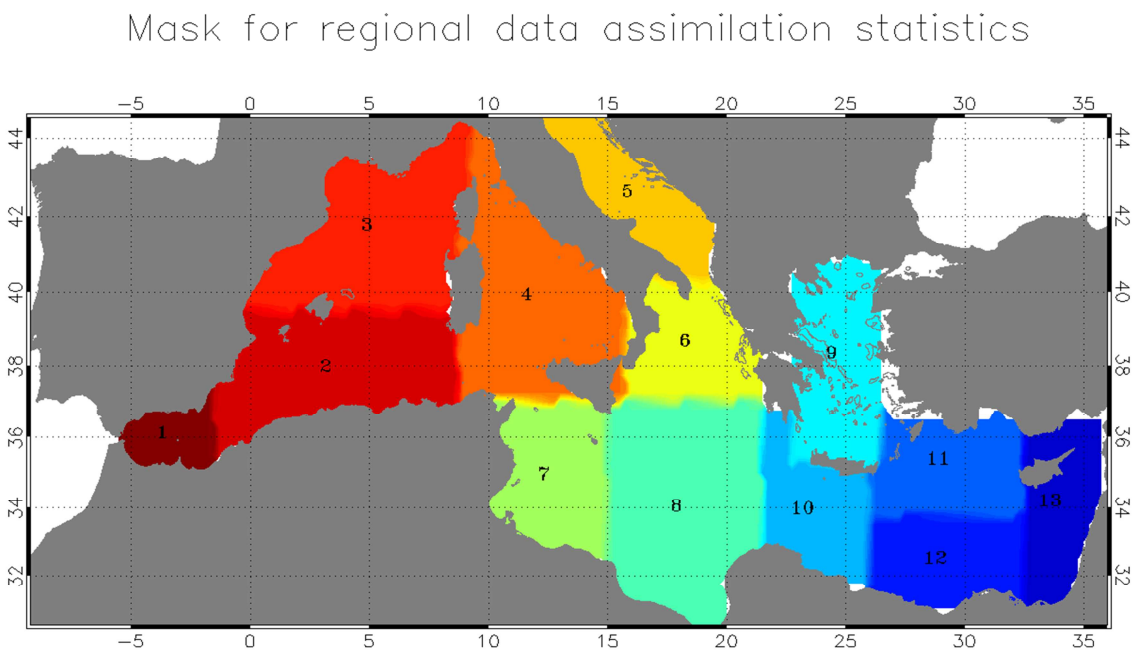

1	Alboran
2	Algerian
3	Lion
4	Thyrrhenian
5	Adriatic
6	Otranto
7	Sicily
8	Ionian
9	Egee
10	Ierepetra
11	Rhodes
12	MersaMatruh
13	Asia Minor

V.1.3. Global ocean

Mask for regional data assimilation statistics

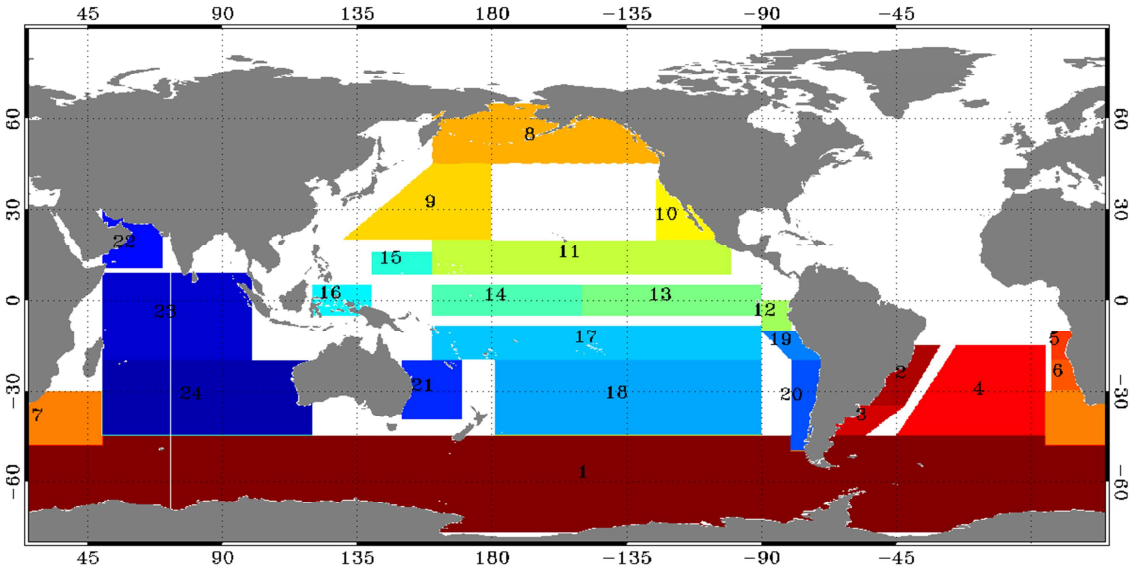

1	Antarctic Circumpolar Current
2	South Atlantic
3	Falkland current
4	South Atl. gyre
5	Angola
6	Benguela current
7	Aghulas region
8	Pacific Region
9	North Pacific gyre
10	California current
11	North Tropical Pacific
12	Nino1+2
13	Nino3
14	Nino4
15	Nino6
16	Nino5
17	South tropical Pacific
18	South Pacific Gyre
19	Peru coast
20	Chile coast
21	Eastern Australia
22	Indian Ocean
23	Tropical indian ocean
24	South indian ocean

VI Annex C

VI.1. Quality control algorithm for the Mercator Océan drifter data correction (Eric Greiner)

Before estimating the bias, it is essential to conduct a quality control. We must consider an individual monitoring of buoys, and a comparison with the geostrophy and windage. In real time, this is not possible, and I propose below a simple test developed by position (date by date) which involves only the mean wind (2 days) and the buoy drift. Basically, we found drifters where drift is close to argue between 0.2 and 3% of the wind (almost the same direction with a drag corresponding to a loss of drogue). For these buoys, if the contamination is real, then the error due to the wind is important with respect to current real at 15m depth. We test different values of windage (wind effect for a fraction of a given wind between 0.2% and 3%). If a questionable observation is found for a given windage, we estimate a correction. We apply at the end an average correction QC (windage among all acceptable). We although increase the error of observation. Note that in delayed time, we could correct all the data from the buoy, at least in a 10-day window. **Note however that a buoy that has lost its drogue can give a good measure if the wind is low**

- **No anomaly : slippage correction of 0.07% of the 10m wind speed**
- **Windage > 0.2% or < 3% correction of 1% of windage**

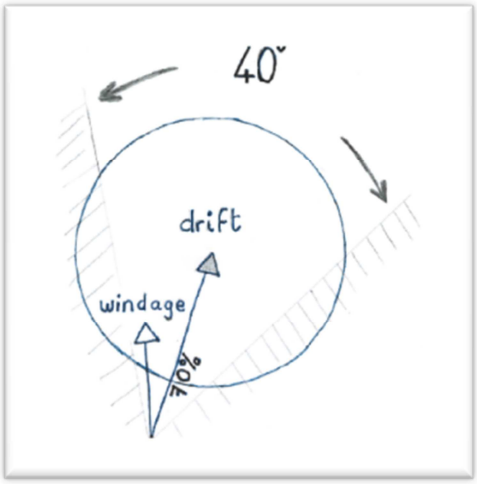

Figure 61 : illustration of QC: Quality test example chosen for windage (eg. 1%) we reject or correct a drift that differs little from the windage (less than 70% of the drift angle <40 °)

Note that a correction of more than 3% is not normally possible (construction of the buoy). This may correspond to breaking waves and swell. Between 2% and 3%, there is ambiguity between Stokes and windage. In other words, it is likely that beyond 2%, we eliminate all or part of the effect of waves and swell. If waves and swell are not aligned with the mean wind (swell remote for example), then the correction will be approximate. Ideally, you should use the Stokes drift from a wave model like Wavewatch3.

When calculating the equivalent models with AOML positions, which were filtered to remove 36h gravity waves and reduce positioning errors, we must :

- **add 0.07% wind averaged over 48h 10m : slippage correction**
- **windage correction and modify the error**